

UNCLASSIFIED

AD NUMBER

AD857627

LIMITATION CHANGES

TO:

Approved for public release; distribution is unlimited.

FROM:

Distribution authorized to U.S. Gov't. agencies and their contractors; Specific Authority; MAY 1969. Other requests shall be referred to Army Aviation Materiel Labs., Fort Eustis, VA.

AUTHORITY

USAAMRDL ltr, 23 Jun 1971

THIS PAGE IS UNCLASSIFIED

Disclaimers

The findings in this report are not to be construed as an official Department of the Army position unless so designated by other authorized documents.

When Government drawings, specifications, or other data are used for any purpose other than in connection with a definitely related Government procurement operation, the United States Government thereby incurs no responsibility nor any obligation whatsoever; and the fact that the Government may have formulated, furnished, or in any way supplied the said drawings, specifications, or other data is not to be regarded by implication or otherwise as in any manner licensing the holder or any other person or corporation, or conveying any rights or permission, to manufacture, use, or sell any patented invention that may in any way be related thereto.

Trade names cited in this report do not constitute an official endorsement or approval of the use of such commercial hardware or software.

Disposition Instructions

Destroy this report when no longer needed. Do not return it to the originator.

ACCESSION FOR		
ORST	WHITE SECTION	<input type="checkbox"/>
DOG	OFF SECTION	<input checked="" type="checkbox"/>
UNANNOUNCED		<input type="checkbox"/>
JUSTIFICATION		
.....		
BY		
DISTRIBUTION/AVAILABILITY CODES		
DIST.	AVAIL. and/or	SPECIAL
2		



DEPARTMENT OF THE ARMY
U. S. ARMY AVIATION MATERIEL LABORATORIES
FORT EUST. 3, VIRGINIA 23604

Appropriate technical personnel of this Command have reviewed this report and concur with the conclusions contained herein.

The findings and recommendations outlined herein were taken into account in planning the subsequent phases of the program.

Task 1G162203D14413
Contract DA 44-177-AMC-392(T)
USAAVLABS Technical Report 68-90B
May 1969

SINGLE-STAGE AXIAL COMPRESSOR COMPONENT DEVELOPMENT
FOR
SMALL GAS TURBINE ENGINES

Volume II
Rotor Development

by

C. Muller
L. Cox

Prepared by

Curtiss-Wright Corporation
Wood-Ridge, New Jersey

for

U.S. ARMY AVIATION MATERIEL LABORATORIES
FORT EUSTIS, VIRGINIA

This document is subject to special export controls
and each transmittal to foreign governments or foreign
nationals may be made only with prior approval of US Army
Aviation Materiel Laboratories, Fort Eustis, Virginia 23604.

SUMMARY

The objectives of this program are to advance and demonstrate high pressure ratio axial compressor technology to the point where an engine designer has sufficient data to incorporate the axial compressor in a small gas turbine engine.

The design and analysis of a single-stage axial supersonic compressor were conducted under Phase I of this contract (Volume I of this report). The rotor for this compressor design was developed and evaluated through experimental testing under Phase II of the contract, and the results are presented in this report.

The compressor performance goals are:

	<u>Rotor with Inlet Guide Vanes</u>	<u>Overall Stage</u>
Pressure Ratio	2.89:1	2.8:1
Adiabatic Efficiency (Percent)	85.2	82.2
Corrected Airflow (Pounds Per Second)	4.0	4.0
Corrected Design Speed (Revolutions Per Minute)	50,700	50,700

The average performance demonstrated by the rotor with the inlet guide vanes was 2.77:1 pressure ratio at 82.5 percent efficiency and 4.0 pounds per second airflow.

Data analysis indicates that the final blade configuration tested can meet the rotor performance goals. A nonuniform circumferential compressor back pressure (throttling condition), together with the inability to obtain complete traverse data in the near sonic flow at the rotor exit, prevented a demonstration of the full rotor performance potential.

Final performance optimization will be accomplished in the Phase III stage development testing. The axial direction and low Mach number (approximately 0.3) of the exit stator discharge flow are expected to result in a relatively uniform back-pressure level and therefore provide more favorable conditions for demonstrating the optimum rotor performance.

FOREWORD

Work is being performed under United States Army Contract DA 44-177-AMC-392(T) (Task 1G162203D14413) by Curtiss-Wright Corporation to advance and demonstrate high pressure ratio axial compressor technology for small gas turbines. This contract is administered by the Aeronautical Propulsion Division of the U. S. Army Aviation Materiel Laboratories. The Phase I effort for this program consisted of the design of a single-stage supersonic axial compressor and test rig and an analytical evaluation of the compressor's potential as a boost stage for small gas turbine engine compressors. The rotor performance of this compressor has been investigated experimentally and developed under Phase II. The experimental investigation of the total stage performance is scheduled for Phase III.

The manager of the Small Gas Turbine Engine Program is T. Schober, and the manager of this Compressor Technology Contract is C. H. Muller. Principal contributing engineers are L. Cox, W. Litke, H. Weiser, A. Schmitter, and F. Spindler. The overall guidance and technical direction provided by Mr. A. Sabatiuk, and the direction of Mr. S. Lombardo, are gratefully acknowledged. The guidance of Mr. J. White, Mr. E. Johnson, and Mr. D. Cale of the U. S. Army Aviation Materiel Laboratories is also gratefully acknowledged.

CONTENTS

	<u>Page</u>
SUMMARY	iii
FOREWORD	v
LIST OF ILLUSTRATIONS	viii
LIST OF TABLES	xi
LIST OF SYMBOLS	xii
INTRODUCTION	1
COMPRESSOR FABRICATION	3
ROTOR TEST WITH INLET GUIDE VANES	18
MODIFICATION OF ROTOR DESIGN AND RETEST	32
CONCLUSIONS	72
APPENDIXES	
I. PHASE II TEST PLAN	73
II. PHASE III TEST PLAN	90
DISTRIBUTION	102

LIST OF ILLUSTRATIONS

<u>Figure</u>		<u>Page</u>
1	Layout of 2.8:1 Supersonic Compressor and Test Rig	5
2	Exploded View of 2.8:1 Supersonic Compressor and Test Rig Components	7
3	2.8:1 Supersonic Compressor Rig Assembled - Front View . . .	8
4	2.8:1 Supersonic Compressor Rig Assembled - Side View . . .	9
5	Compressor Test Rig Installed on Test Stand	10
6	2.8:1 Supersonic Compressor Inlet Guide Vanes	11
7	2.8:1 Supersonic Compressor Rotor - Integral Blade and Disc - Side View	12
8	2.8:1 Supersonic Compressor Rotor - Integral Blade and Disc - Front View	13
9	2.8:1 Supersonic Compressor Rotor Assembly - Front View . . .	14
10	2.8:1 Supersonic Compressor Rotor Assembly - Rear View . . .	15
11	Leading-Edge Angle Criteria	17
12	Tip Clearance Geometry for Rotor Test Builds 1 and 2	19
13	Build 1 Rotor Test Data Compared to Predicted Stage Performance Map	21
14	Rotor Incidence for Build 1 Compared to Design Conditions . .	25
15	Build 1 Total Pressure and Temperature Profiles at Rotor Exit	26
16	2.8:1 Supersonic Compressor Design Point Vector Diagrams . .	27
17	Build 1 Vector Diagrams for 90 Percent Speed Data	28
18	Rotor Passage Pressure Recovery for Build 1 - Data Point 9	30
19	Rotor Passage Pressure Recovery for Build 1 - Data Point 11	31
20	Rotor Redesigned Leading-Edge Expansion Surface Angles . . .	33

<u>Figure</u>	<u>Page</u>
21 Redesigned Rotor Airfoil Typical Section	34
22 Blades of Second Rotor After Test of Build 2	37
23 Blades of Second Rotor After Blending	38
24 Tip Clearance Geometry for Rotor Test Builds 3, 4, and 5 . .	39
25 Performance Map Rotor Test Data, Build 2	43
26 Performance Map Rotor Test Data, Build 3	44
27 Performance Map Rotor Test Data, Build 4	45
28 Performance Map Rotor Test Data, Build 5	46
29 Effect of Inlet Guide Vane Setting for Builds 3, 4, and 5 . .	48
30 Circumferential Variation in Rotor Exit Conditions	50
31 Comparison of 90 Percent Speed Peak Pressure Ratio Data for Builds 1, 2, and 3	51
32 Rotor Inlet Relative Air Angle at 100 Percent Speed, Build 3	53
33 Modified Rotor Incidence Angle at 100 Percent Speed, Build 3	54
34 Rotor Relative Inlet Mach Number, Build 3	55
35 Modified Rotor Incidence Angle Versus Radius, Build 3	56
36 Variation of Modified Rotor Incidence With Speed	58
37 Build 3 Total Pressure and Temperature Profiles at Rotor Exit	59
38 Build 3 Rotor Exit Absolute Flow Angles	60
39 Build 3 Rotor Exit Deviation Angles	61
40 Effects of Speed and Build Configuration on Relative Exit Angle	62
41 Build 2 Vector Diagrams for 90 Percent Speed	63
42 Build 3 Vector Diagrams for 100 Percent Speed	64
43 Build 3 Vector Diagrams for 95 Percent Speed	65

<u>Figure</u>		<u>Page</u>
44	Build 3 Vector Diagrams for 90 Percent Speed	66
45	Build 4 Vector Diagrams for 100 Percent Speed	68
46	Build 4 Vector Diagrams for 90 Percent Speed	69
47	Build 5 Vector Diagrams for 90 Percent Speed	70
48	Rotor Passage Total Pressure Recovery	71
49	Compressor Test Rig Installation	75
50	Schematic of Rotor Test Pressure and Temperature Instrumentation	77
51	2.8:1 Supersonic Compressor Predicted Stage Map	87
52	Schematic of Stage Test Pressure and Temperature Instrumentation	92

LIST OF TABLES

<u>Table</u>		<u>Page</u>
I	2.8:1 Supersonic Compressor, Build No. 1, Rotor Test Data, Design IGV Setting	22
II	Summary of Rotor Test Data for Builds 1 Through 5	49
III	Rotor Test Instrumentation	80
IV	Scheduled Test Points for Rotor Test	84
V	Stage Test Instrumentation	95
VI	Scheduled Stage Test Points	98

SYMBOLS

A/A^*	isentropic area ratio - dimensionless
A^*	area at which sonic flow would occur - square inches
A_{ann}	annular area - square inches
A_{flow}	flow area - square inches
a	acoustic velocity (based on static temperature) - feet per second
a_t	acoustic velocity (based on total temperature) - feet per second
C_p	specific heat for a constant pressure process - BTU per pound per degree Rankine
D	diameter - inches
D_m	mean diameter - inches
g	acceleration of gravity - feet per second squared
h	hub streamtube
IC	iron-constantan thermocouple
ID	inside diameter - inches
i	incidence angle - degrees
i'	modified incidence angle - degrees
J	work constant (778 foot-pounds per BTU)
K	continuity equation constant (0.26048 pound square root of degree Rankine per second per square inch per inch of mercury)
k	spring rate - pounds per inch
M	Mach number - dimensionless
m	mean streamtube
N	rotational speed - revolutions per minute
OD	outside diameter - inches
P_s	static pressure - inches of mercury

P_T	total pressure - inches of mercury
R	radius of curvature in meridional plane - inches; (or gas constant, 53.4 foot-pounds per pound per degree Rankine, when occurs in the expression $\sqrt{KgPT_s}$)
REC	total pressure recovery - ratio of total pressure remaining after losses through blade row passage to initial total pressure at blade row inlet - dimensionless
r	radius from compressor axis - inches
T_s	static temperature - degrees Rankine
T_T	total temperature - degrees Rankine
t	tip streamtube
t_c	ratio of maximum blade thickness to the chord length
U	rotor blade section speed - feet per second
V	velocity - feet per second
V_{ax}	axial velocity component - feet per second
V_{tan}	tangential velocity component - feet per second
W	airflow - pounds per second
α	tangential airflow angle relative to the compressor axis - degrees
β	tangential angle to blade camber line - degrees
β'	tangential angle to blade suction surface - degrees
δ	deviation angle - degrees (or ratio of local total pressure to a reference pressure, when it occurs in $(W\sqrt{\theta})/\delta$ - dimensionless)
Δ	change of a quantity across a blade row - dimensionless
ξ	airflow slope angle in meridional plane - degrees
η_{ad}	adiabatic efficiency - dimensionless
γ	ratio of specific heats - dimensionless

- ϕ blade camber angle - degrees
- ρ density - pounds per cubic foot
- θ air turning angle through a blade row - degrees (or ratio of local total temperature to a reference temperature, when it occurs in either $N/\sqrt{\theta}$ or $(W\sqrt{\theta})/g$ - dimensionless)

Subscripts

- amb ambient conditions
- o station at entrance to inlet guide vanes
- 1 absolute conditions (relative to nonrotating reference) at a station representing exit of inlet guide vanes and inlet to rotor
- 2 entrance conditions to rotor relative to the rotating rotor blade
- 3 exit conditions from the rotor relative to the rotating rotor blade
- 4 absolute conditions (relative to non-rotating reference) at a station representing the rotor exit and inlet to the exit stator
- 5 absolute conditions at a station representing the exit of the exit stator and interconnecting duct

INTRODUCTION

The objective of the U. S. Army Aviation Materiel Laboratories in the field of small gas turbine engines is to advance the technology in the major component areas to the point where a small gas turbine engine can be designed to provide a nonregenerated engine with a specific fuel consumption of less than 0.460 pound per horsepower per hour. The compressor component required to make this performance goal possible must be capable of high pressure ratio (16:1 range) at good component efficiencies and, in addition, must be designed for simplicity, ruggedness, durability, and minimum cost.

The objectives of this program are to advance and demonstrate high pressure ratio axial compressor technology to the level that, when matched analytically with the advanced centrifugal compressor technology supplied by USAAVLABS, will provide a 16:1 compressor which offers the desired engine performance. Specifically, this program is to develop a supersonic axial compressor to serve as the boost or supercharging stage. Since the part-power performance of small gas turbine engines is also critical, several study tasks have been included in the program to gain some insight into the important off-design parameters and trade-offs which should influence the axial compressor development when considered in the overall compressor and engine operation.

The program is scheduled in three phases. Phase I involved (1) the design of the supersonic axial stage compressor and test rig, (2) an analytical study to evaluate the performance potential and characteristics of various compressor and engine configurations, and (3) the preliminary design of an advanced 16:1 axial/centrifugal compressor, an advanced gas generator incorporating this compressor, and a variable-geometry compressor rotor. In Phase II the inlet guide vanes and compressor rotor were procured and developed through experimental testing. In Phase III the design of the exit stator and interconnecting duct for the supersonic axial stage was finalized and this hardware was procured and developed through experimental testing. An advanced inlet guide vane was designed and procured, and its improvement of stage performance was experimentally evaluated.

The supersonic axial compressor selected and designed under Phase I of the program is a single-stage shock-in-rotor type of compressor with stage performance goals of 2.8:1 pressure ratio, 82.2 percent adiabatic efficiency, and 4.0 pounds per second corrected airflow. The performance goals for the rotor with inlet guide vanes, but without exit stators or interconnecting duct, are 2.89:1 pressure ratio, 85.2 percent adiabatic efficiency, and 4.0 pounds per second corrected airflow.

Phase I was completed in September 1966. The compressor design procedures, criteria, predicted performance, and results of various analytical studies performed are presented in Volume I of this report.*

*Single-Stage Axial Compressor Component Development for Small Gas Turbine Engines (U), USAAVLABS Technical Report 68-90A, U. S. Army Aviation Materiel Laboratories, Fort Eustis, Virginia, March 1969.

Phase II was completed in May 1967. The purposes of this phase were to evaluate the compressor rotor performance, when tested with the inlet guide vanes but without exit stators, and to develop the rotor to an acceptable performance level prior to finalizing the exit stator design. In this manner the performance capability of each blade row can be established and design deficiencies can be pinpointed more readily. The results of the experimental testing and data analysis performed under the tasks of this phase are presented in this report. These data formed the basis for finalizing the exit stator design and for analyzing the experimental stage performance of Phase III of the program.

COMPRESSOR FABRICATION

The facility and test equipment on which the experimental evaluation of the compressor was performed is described in Appendix I (Phase II Test Plan). The test rig consists of a Rover engine, modified to serve as a steam-driven power turbine, mated to the compressor test rig unit. The Rover engine was an existing unit and required only minor modifications. The compressor test rig, inlet guide vanes, and rotor were fabricated during this phase of the program.

TEST RIG - A layout of the compressor rig is presented in Figure 1. Aft of the compressor rotor, the hardware arrangement above the centerline differs from that below the centerline. The arrangement below the centerline depicts the configuration for the rotor development testing and represents the test rig hardware fabricated under this phase of the program. The arrangement above the centerline is the planned configuration for the stage testing under Phase III. The layout also shows an arrangement providing a slip ring assembly within the nose of the rig and an alternate arrangement for a nose assembly without slip rings. The slip rings were planned in the event that strain gaging of the rotor blades was deemed necessary for monitoring blade stresses. The results of the 2:1 supersonic compressor testing indicated that the strain gages were not required; consequently, the alternate nose assembly without slip rings was fabricated for this testing. Figure 2 shows the test rig components. Figures 3 and 4 present the assembled compressor rig, and Figure 5 presents the overall test rig installed on the test stand.

INLET GUIDE VANES AND ROTOR

Inlet Guide Vanes

The inlet guide vanes are an NACA 65 series airfoil and are fabricated as individual blades (Figure 6). A source inspection of these blades indicated that all airfoil coordinates were within the specified tolerance.

Rotor

The compressor rotor blades are developed airfoils and are machined from a forging as an integral blade and disc unit. During the design, the blade sections are initially developed along streamline paths and are then transformed to sections in planes perpendicular to the stacking line (mylar planes) for manufacturing. The source inspection data indicated that the airfoil coordinates were within the specified tolerance with respect to the mylar plane blade sections. The compressor rotor is shown in Figures 7 and 8. Figures 9 and 10 present the rotor assembly.

Due to the relatively large circumferential arc between the leading and trailing edges of the blade, and the relatively high streamline slope angles with respect to the axis of rotation, the mylar blade sections diverge considerably from the streamline sections at the leading and trailing edges. Certain key leading-edge criteria could be readily measured

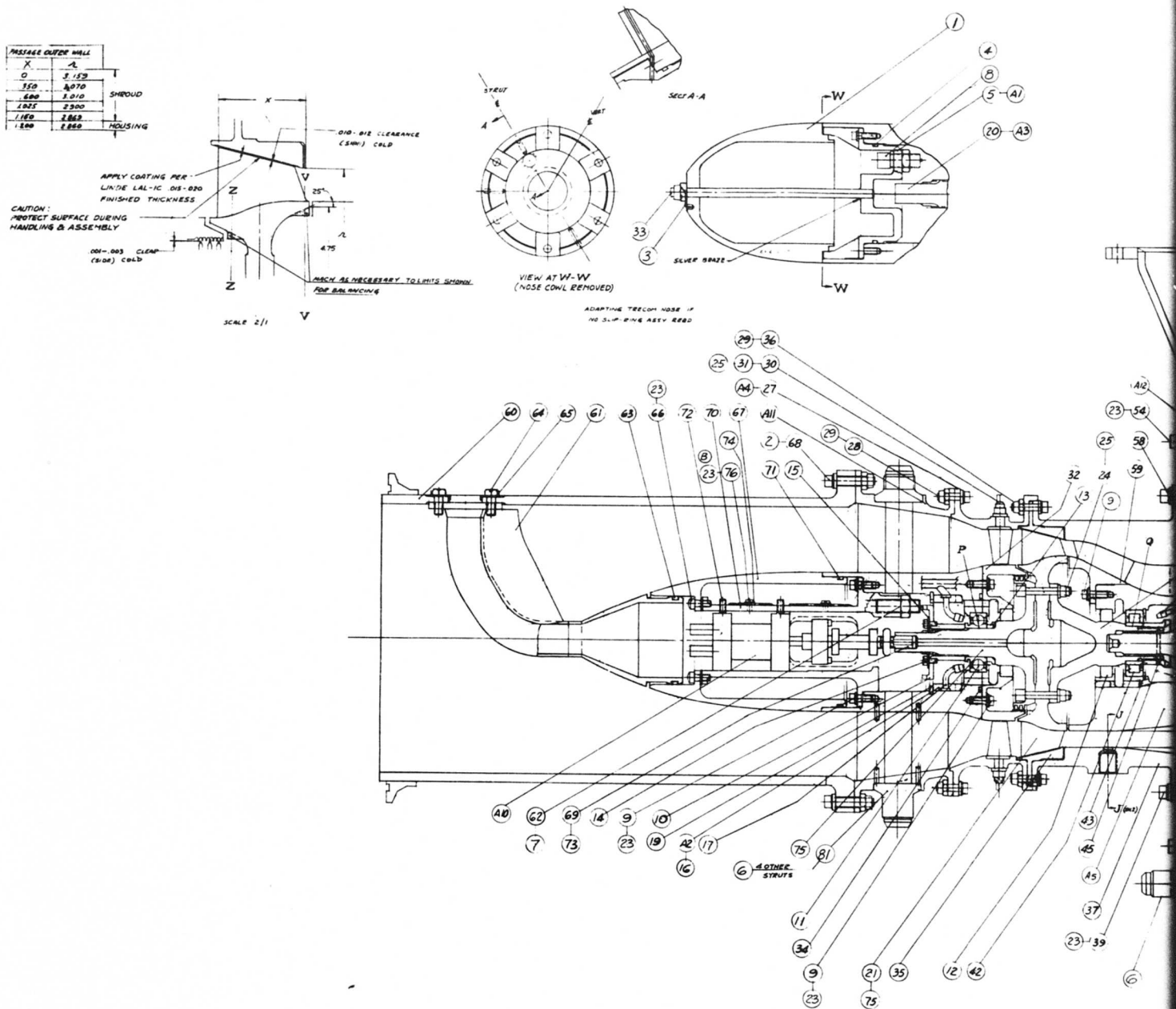


Figure 1. Layout of 2.8:1 Supersonic Compressor and Test Rig.

BLANK PAGE

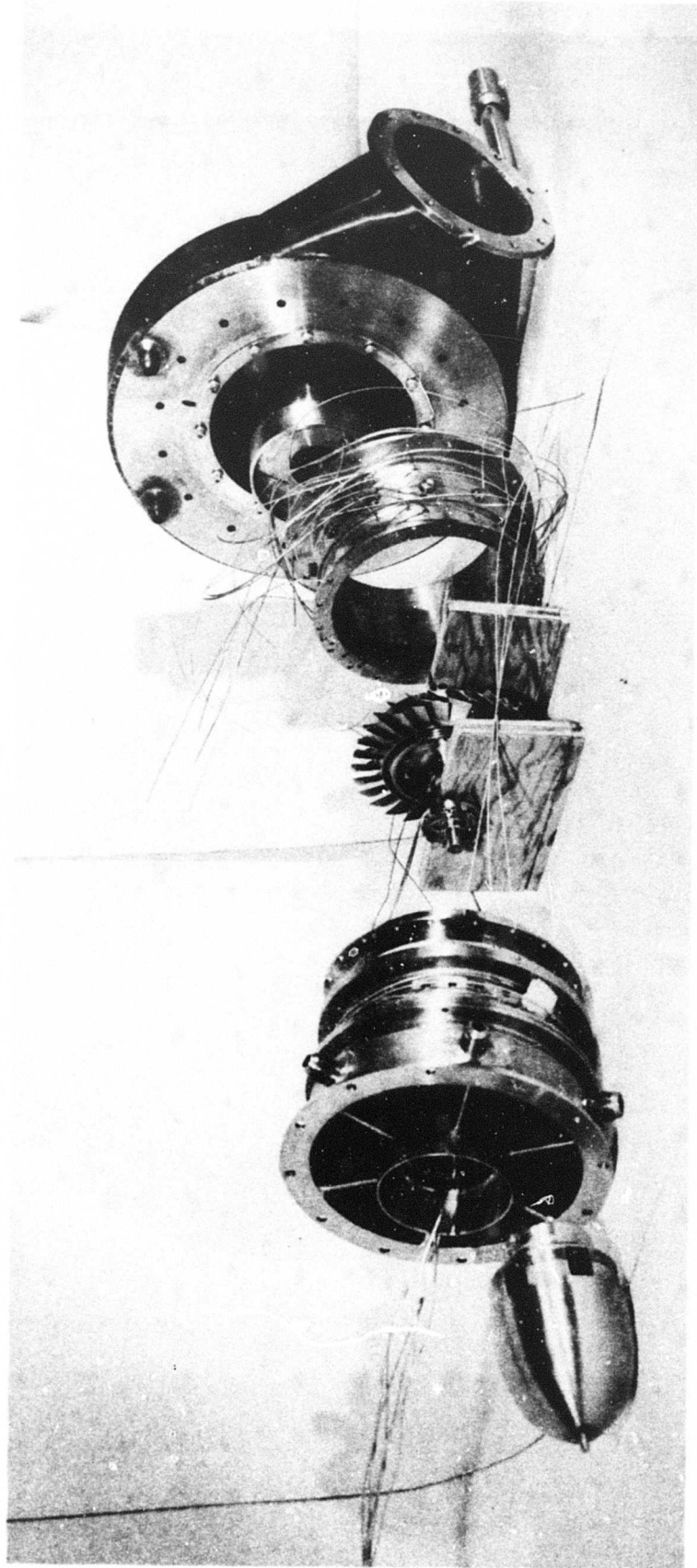


Figure 2. Exploded View of 2.8:1 Supersonic Compressor and Test Rig Components.

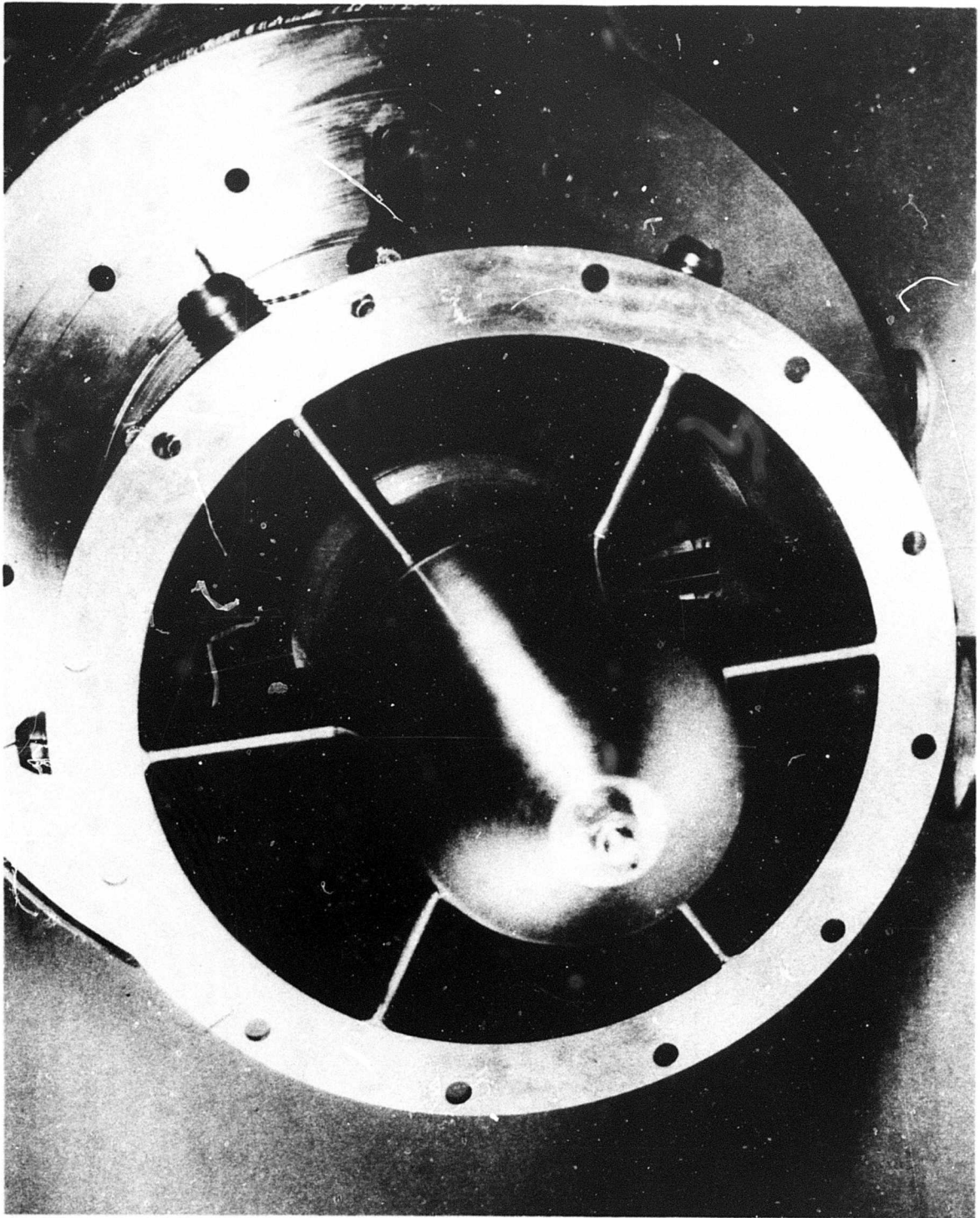


Figure 3. 2.8:1 Supersonic Compressor Rig Assembled - Front View.

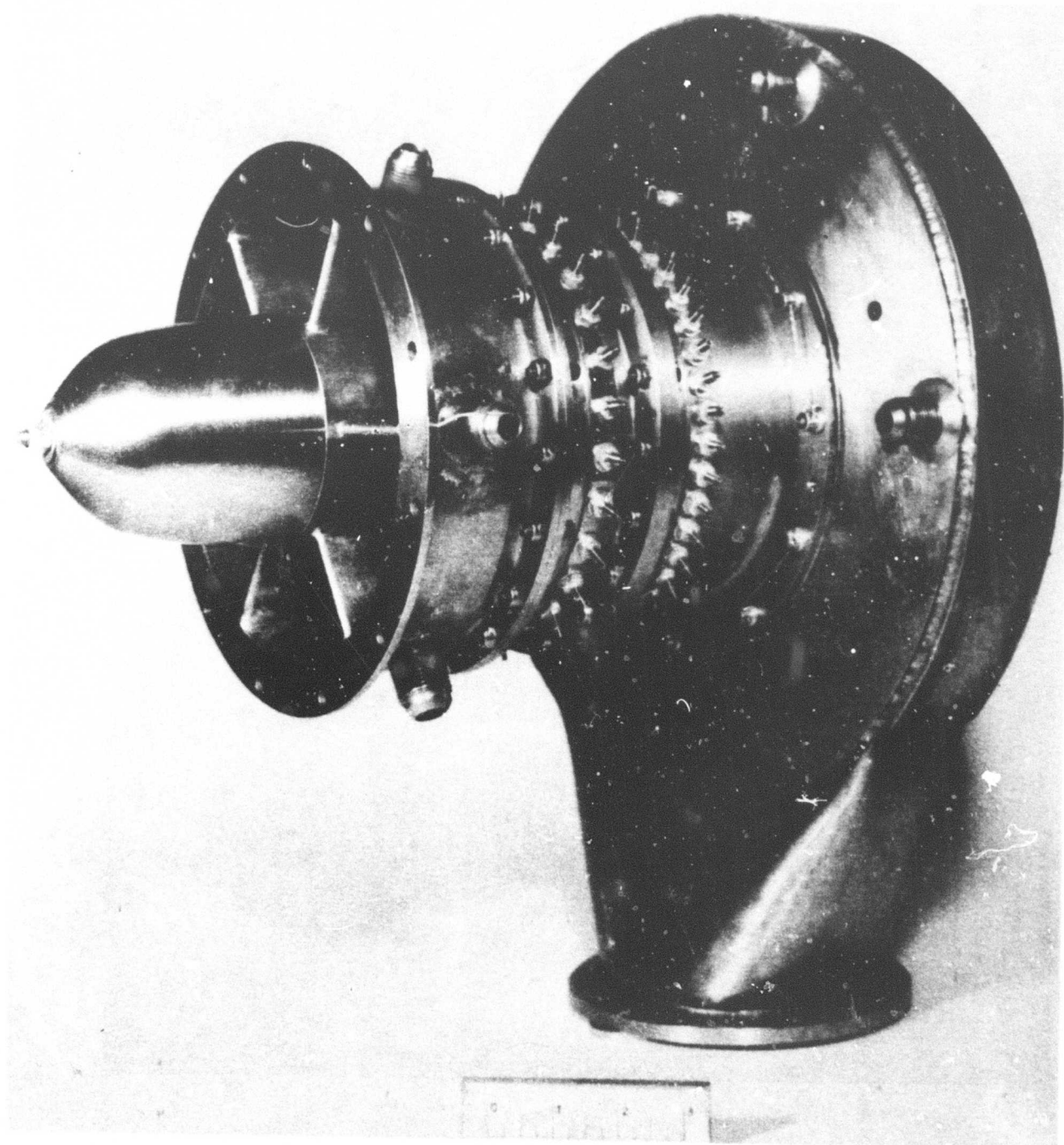


Figure 4. 2.8:1 Supersonic Compressor Rig Assembled - Side View

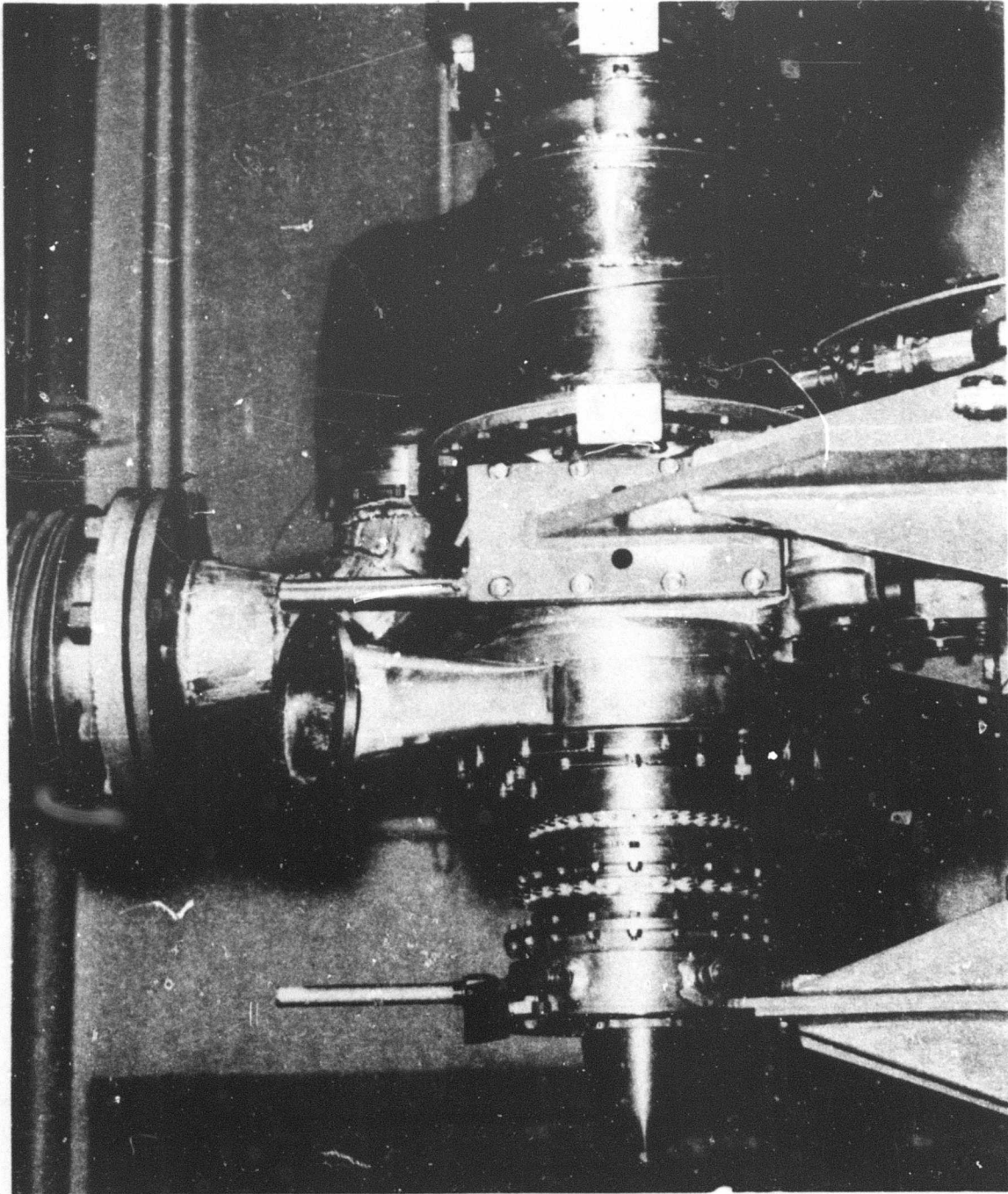


Figure 5. Compressor Test Rig Installed on Stand.

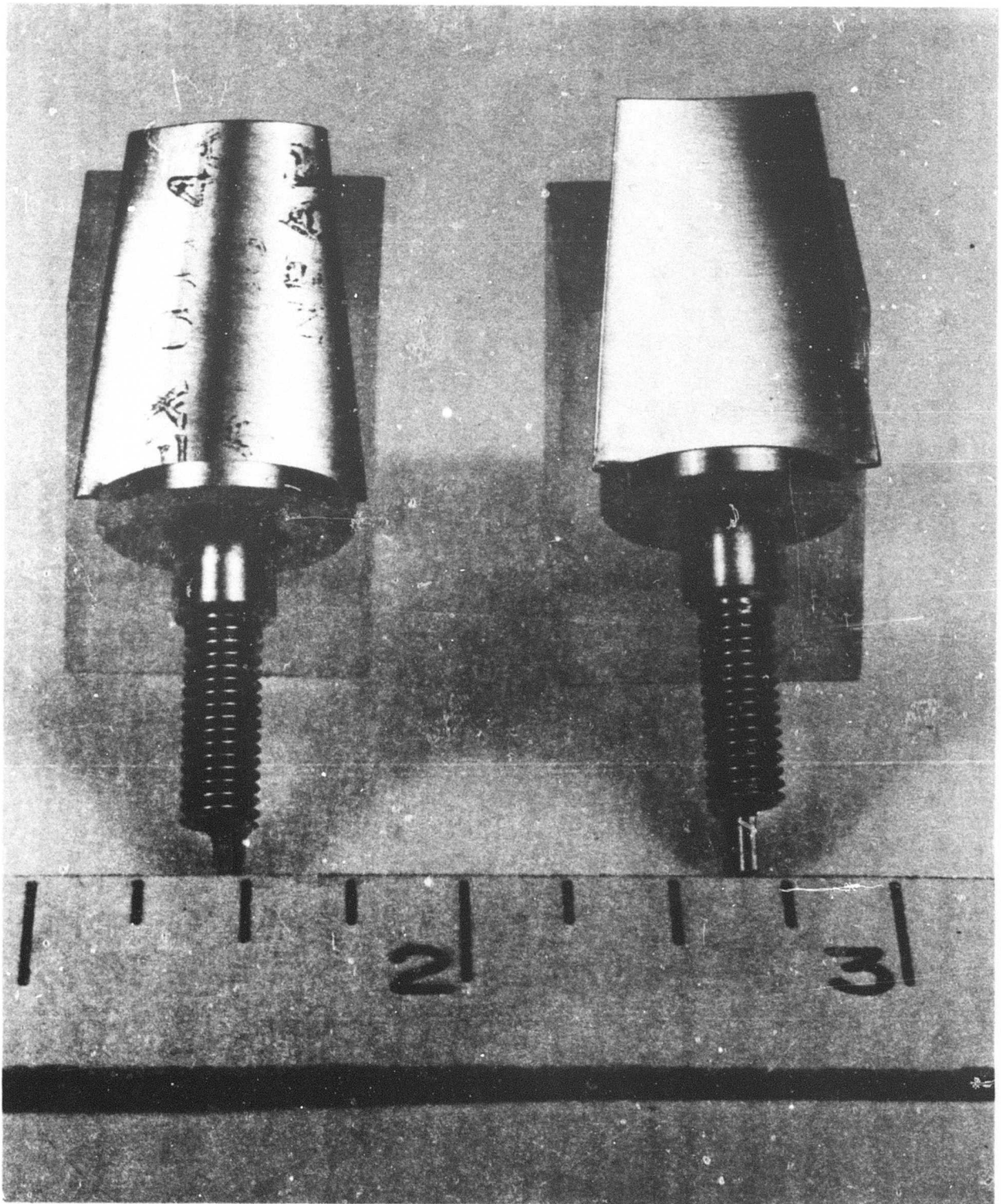


Figure 6. 2.8:1 Supersonic Compressor Inlet Guide Vanes.



Figure 7. 2.8:1 Supersonic Compressor Rotor Integral Blade and Disc - Side View.

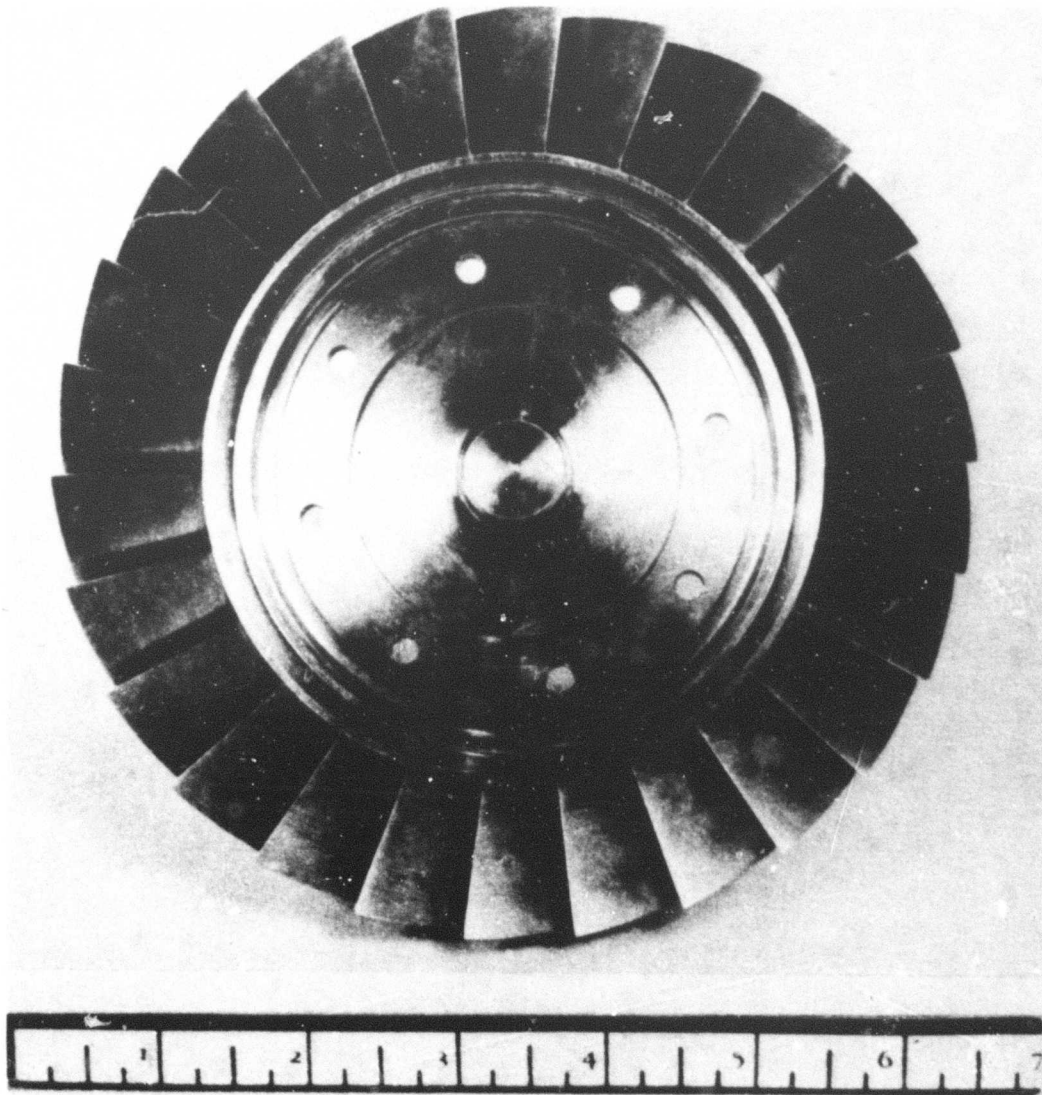


Figure 8. 2.8:1 Supersonic Compressor Rotor Integral Blade and Disc - Front View.

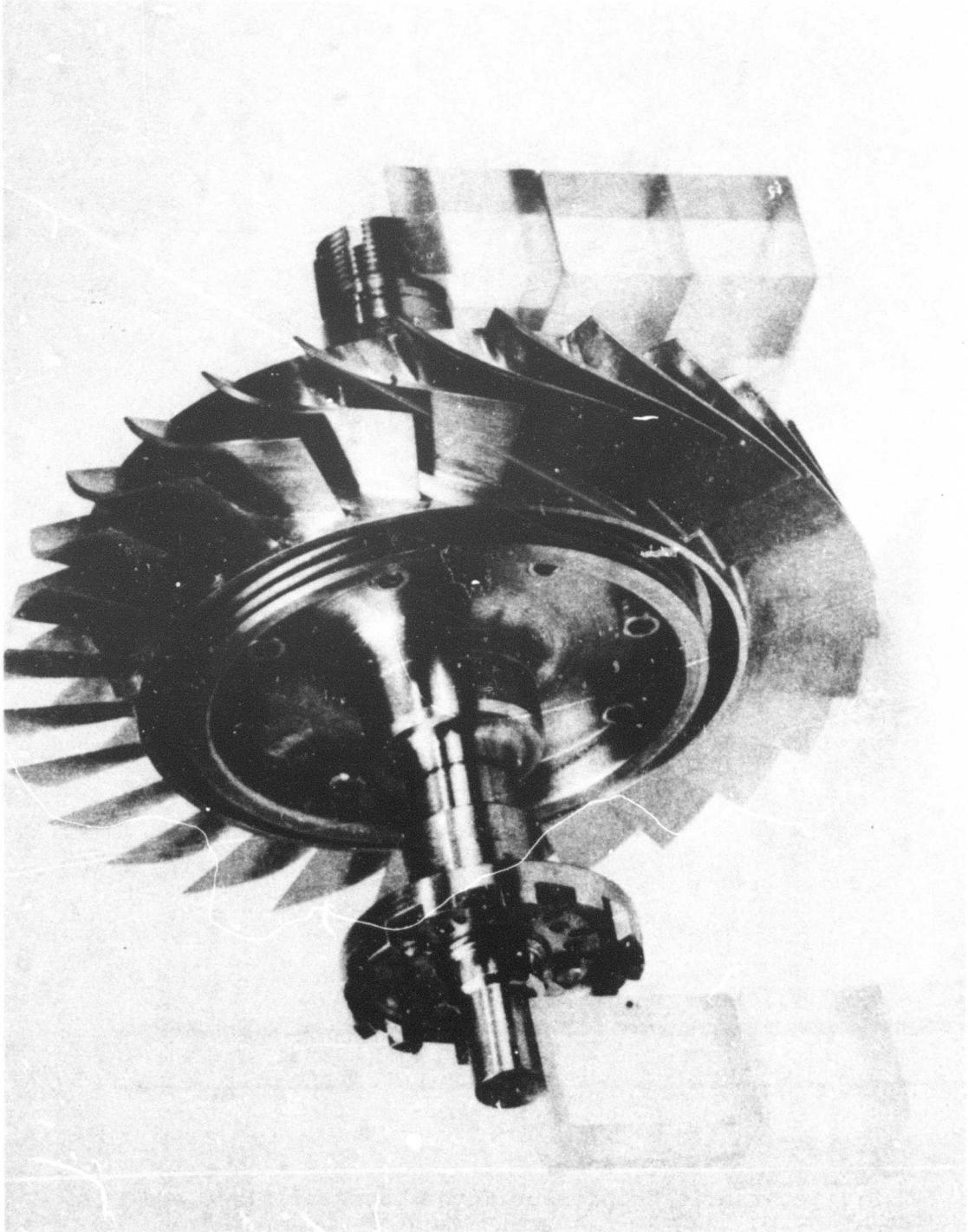


Figure 9. 2.8:1 Supersonic Compressor Rotor Assembly - Front View.

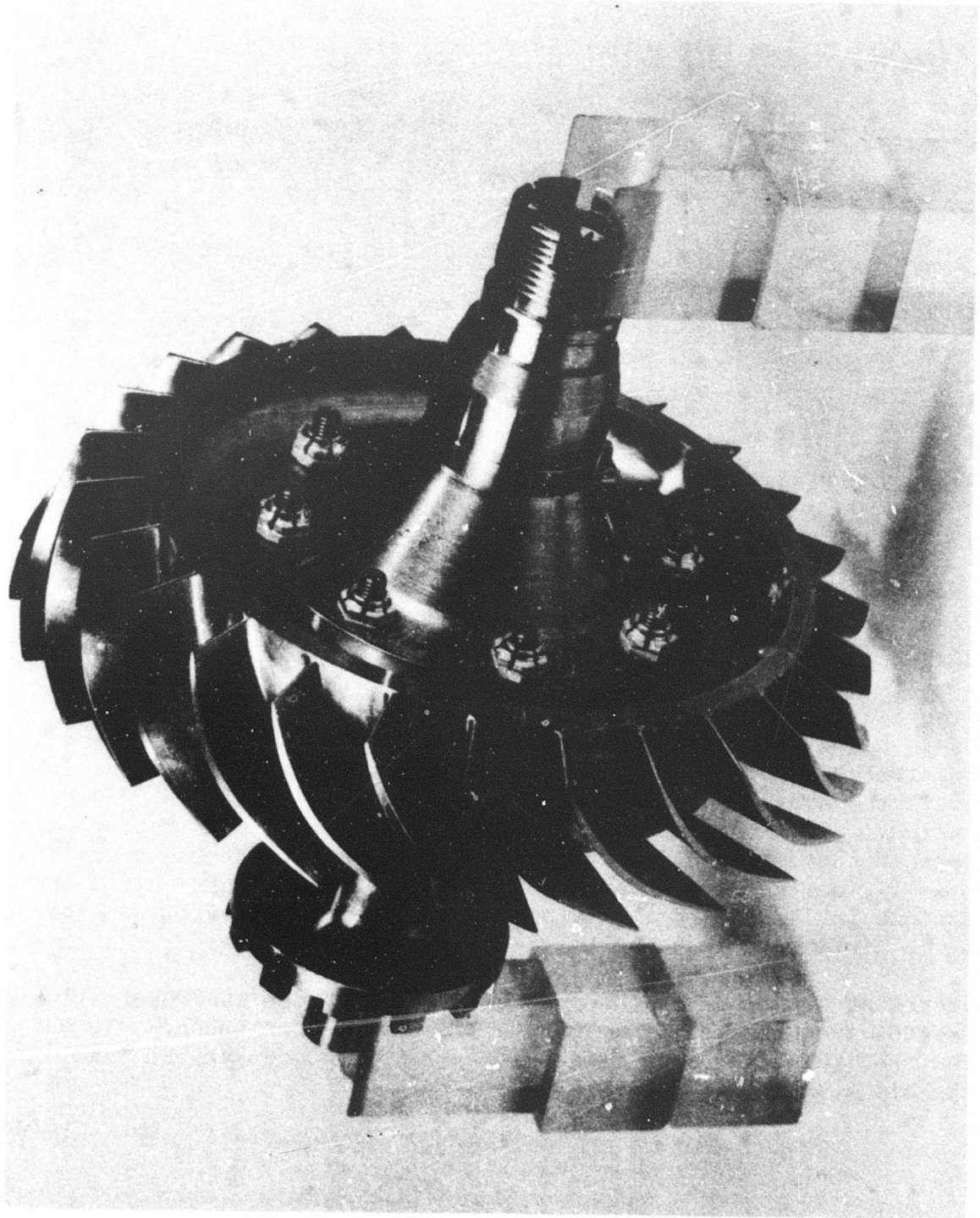


Figure 10. 2.8:1 Supersonic Compressor Rotor Assembly - Rear View.

along streamline sections and, therefore, were obtained in inspection after completion of fabrication. These measurements included (1) the angle which the leading-edge expansion surface forms with an axial direction, (2) the leading-edge wedge angle formed by the expansion surface and the compression surface, and (3) the blade thickness at the leading edge. Figure 11 defines these criteria.

The inspection results for the first rotor are as follows:

	<u>Design Specifications</u>	<u>Measurements of First Rotor</u>	
		<u>Range</u>	<u>Weighted Average</u>
Expansion Surface Leading-Edge Angle			
Hub	67°41'	68°02'-69°10'	68°15'
Mean	68°50'	69°10'-69°55'	69°21'
Tip	70°11'	70°40'-71°50'	70°55'
Leading-Edge Wedge Angle			
Hub	4°00'	3°35'-6°40'	5°00'
Mean	4°00'	4°17'-5°50'	4°54'
Tip	4°00'	3°45'-7°00'	5°01'
Leading-Edge Thickness	.004-.010"	.007-.015"	.011"

The range of measured leading-edge angles indicates the extremes of the blade-to-blade variation. The weighted average is computed by considering the distribution of the measured angles for the number of blades inspected. The weighted average represents the reference value which should be used for aerodynamic data analysis. The results indicate that the weighted average of the leading-edge expansion surface angle for the overall blade span is 1/2 degree higher than the design specifications. Based on the deviations in leading-edge expansion angle and thickness, it was projected that the airflow would be on the order of 5 percent low.

A natural static blade frequency check was made, and the results indicated a resonant frequency of from 3455 to 3560 cycles per second. It was concluded that this frequency represents a flapping mode at the leading edge of the blade.

Convention Incidence: $\alpha - \beta$

Modified Incidence: $\alpha - \beta'$

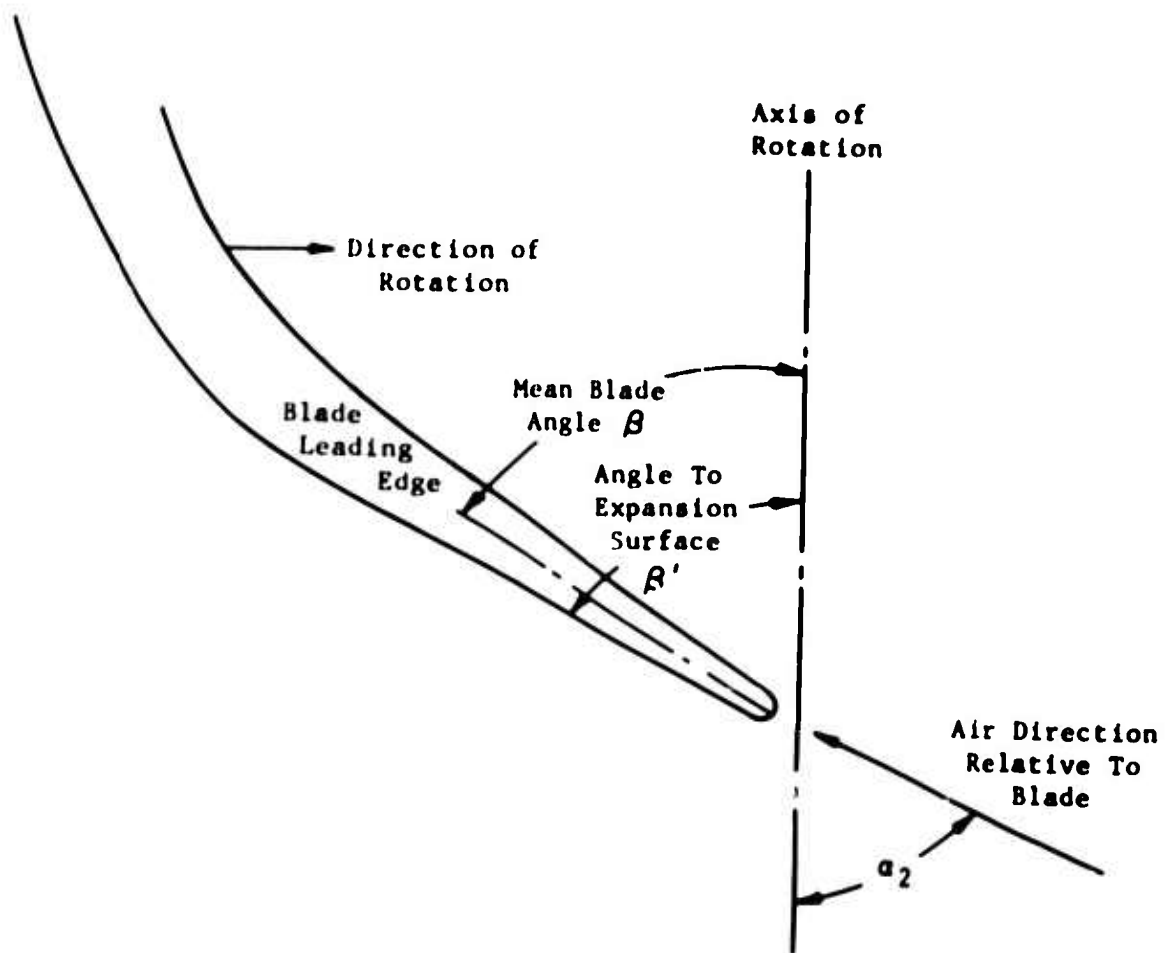


Figure 11. Leading-Edge Angle Criteria.

ROTOR TEST WITH INLET GUIDE VANES

Build 1 of the compressor and test rig with the first 2.8:1 compressor rotor (rotor configuration 1) was tested under this task.

TEST CONFIGURATION

The compressor configuration for this test consisted of the inlet guide vanes, the compressor rotor and shroud, and an annular exit duct without vanes (see Figure 1 arrangement below centerline).

Inlet Guide Vanes

The inlet guide vanes are of the NACA 65 airfoil series and were positioned at the design angle setting.

Rotor

The rotor was the first 2.8:1 supersonic compressor rotor (configuration 1).

Shroud

An uncoated (no abradable coating) steel shroud was used in this build.

Tip Clearance

Figure 12 presents the nominal static rotor to shroud tip clearance configuration. The tip clearance variation with circumferential position was within ± 0.0015 inch.

INSTRUMENTATION

The test instrumentation is described in Appendix I. The traversing probe was not installed for the initial test period. The plan was to install the traversing probe after obtaining preliminary data through 100 percent speed.

DESCRIPTION OF TEST

Data points were obtained along the 50, 70, 80, and 90 percent speed lines during the test of build 1. No attempt was made to establish the surge line within this test period. The data results are discussed in the following section.

Testing was terminated while setting a 95 percent speed point because the compressor thrust bearing failed. Disassembly and posttest inspection revealed that fibers from a Teflon tape material had plugged the oil jet to the thrust bearing; thus loss of oil flow caused the bearing failure. The accumulated testing time on the rig was 3 hours 30 minutes.

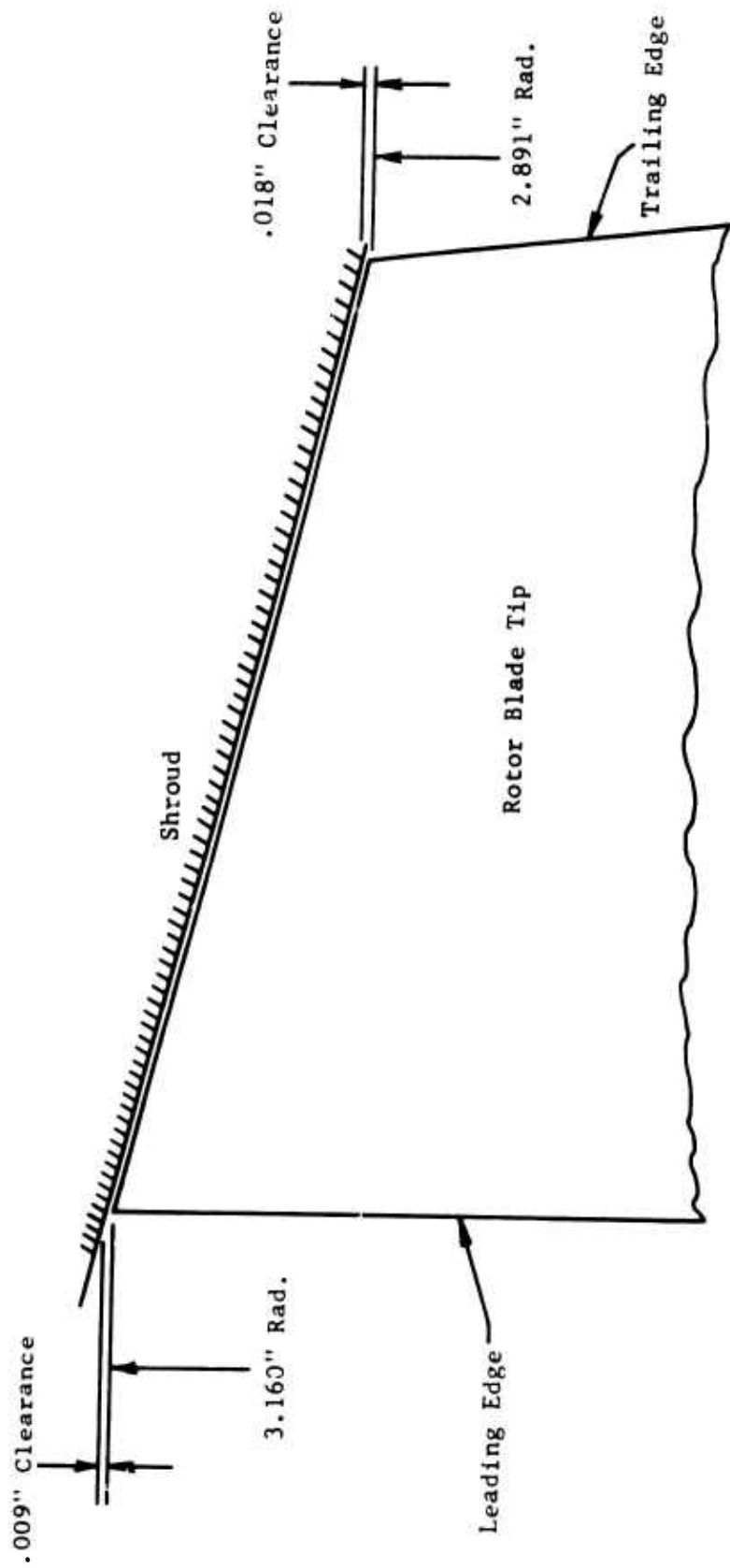


Figure 12. Tip Clearance Geometry for Rotor Test Builds 1 and 2.

Aside from the damage which was directly attributable to the bearing failure, there was no other evidence of rotor blade deterioration or a rotor tip rub.

TEST RESULTS

The performance data obtained during the testing of this build included the fixed probe total pressures and temperatures from the five-element rakes at the compressor inlet and from the single-element probes for each of three streamtube locations at the rotor exit, the wall static pressures along the flow path, the compressor airflow, and the speed. No traverse data were obtained. Comparison of the experimental data to predicted performance is made where possible, but comparison to design point conditions cannot be made since 100 percent speed was not attained.

The data analysis computer program is used to determine the vector diagrams, Mach number profiles, rotor exit flow angles, and streamline paths as a function of radius. The program input data are the inlet total temperature and pressure profiles, airflow, absolute flow angle leaving the inlet guide vane, guide vane loss coefficient, flow path geometry, rotor speed, rotor exit total temperature and pressure profiles, and exit blockage factor. The program calculates the aerodynamic solution between each blade row which satisfied continuity and energy along streamlines and radial equilibrium for both the tangential velocities and meridional streamline curvature. The exit blockage factor is adjusted to establish a solution which matches the experimental exit static pressure. The absolute leaving flow angle and loss coefficient for the inlet guide vanes as a function of radius are input as established by the inlet guide vane tests.* The remaining input data are as measured during the rotor test.

Performance Map

The experimental rotor test data points for build 1 are shown plotted on a map of predicted stage performance in Figure 13. Table I presents the performance for the data points in terms of the tip, mean, and hub streamtubes; it also presents the overall average.

Rotor Pressure Ratio

The rotor pressure ratio is computed as the ratio of the average total pressure at the rotor exit to that in the inlet duct. The data presented are based on a numerical average of the rotor exit data for each of the three streamtube locations. The data analysis computer program determines a pressure ratio based on mass weighted exit conditions. The mass weighted pressure ratios from the computer runs agreed with the numerical averages within the accuracy represented by the three-point exit profiles.

*Single-Stage Axial Compressor Component Development for Small Gas Turbine Engines (U), USAAVLABS Technical Report 68-90A, U. S. Army Aviation Materiel Laboratories, Fort Eustis, Virginia, March 1969.

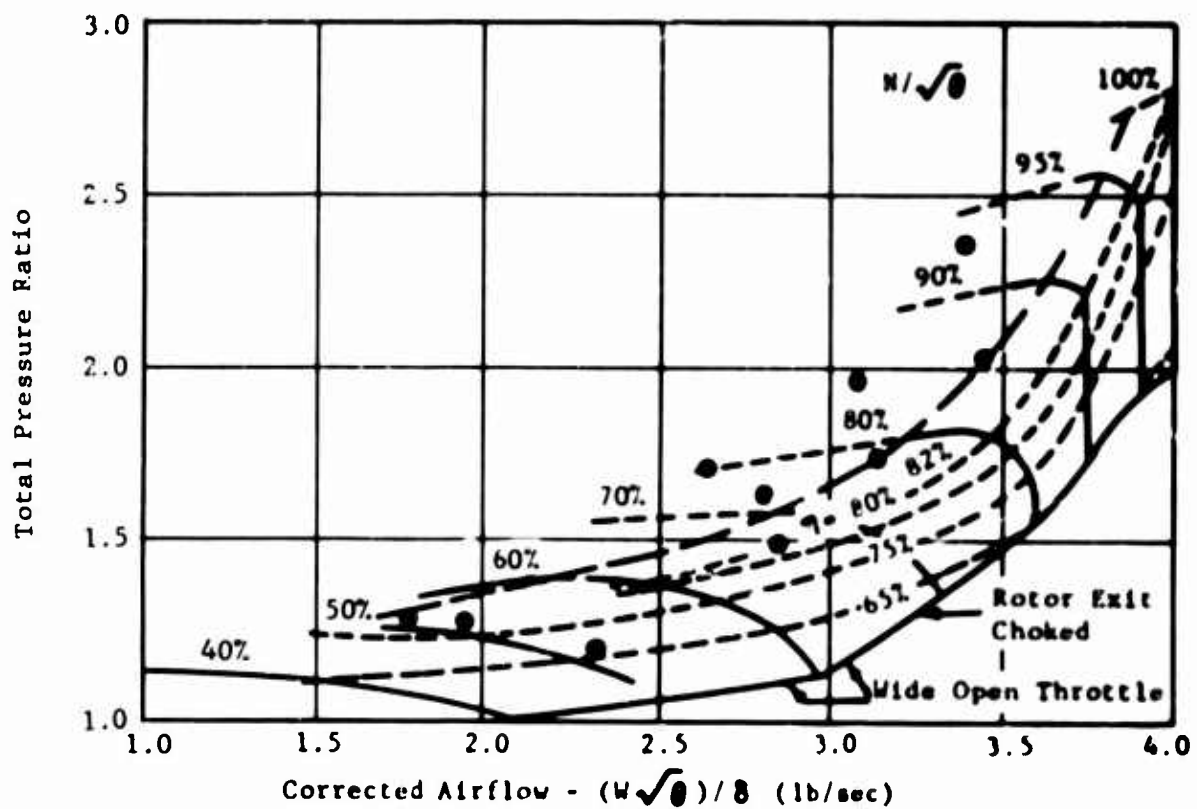
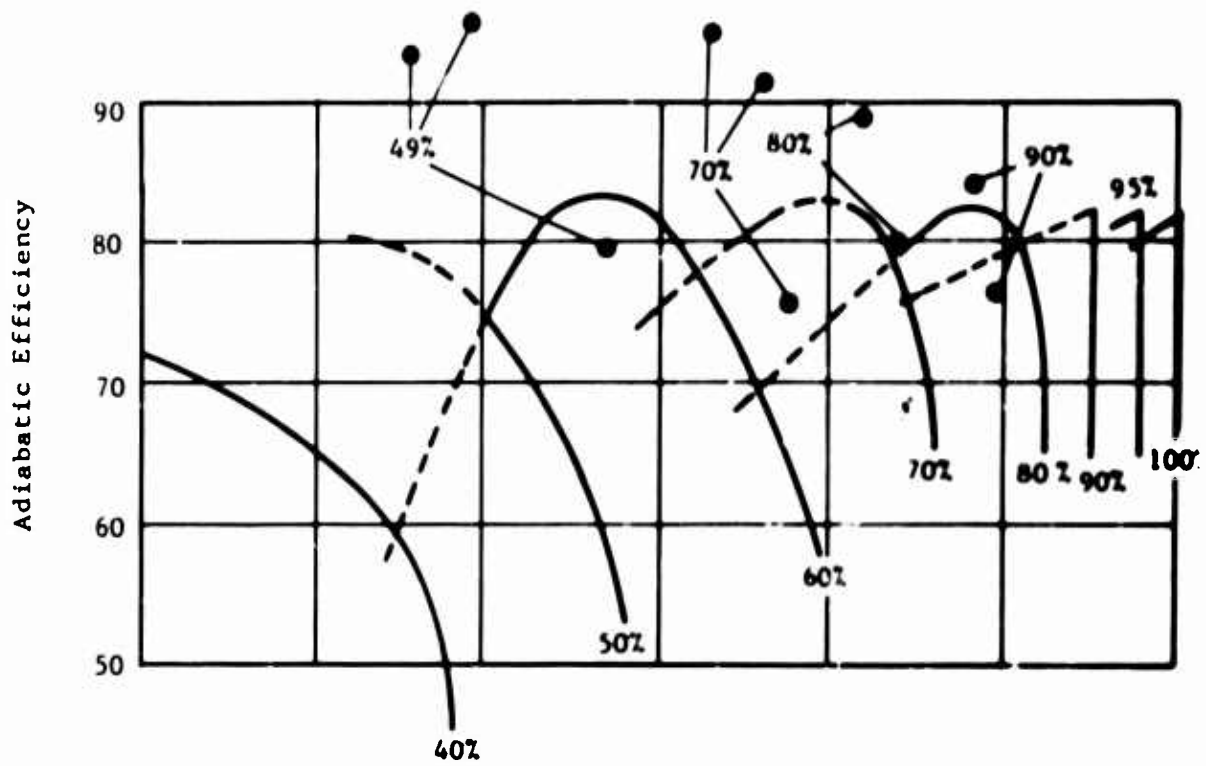


Figure 13. Build 1 Rotor Test Data Compared to Predicted Stage Performance Map.

TABLE I. 2.8:1 SUPERSONIC COMPRESSOR BUILD 1 ROTOR TEST DATA - DESIGN IGV SETTING

Point No.	$\%N/\sqrt{\theta}$	Pressure Ratio			Adiabatic Efficiency - %			Corrected Airflow lb/sec			
		Hub	Mean	Tip	Hub	Mean	Tip				
1	49	1.22	1.22	1.18	1.21	83.8	88.4	66.8	79.7	2.352	
2	49	1.30	1.29	1.28	1.29	99.0	98.5	90.0	95.8	1.962	
3	49	1.32	1.30	1.28	1.30	91.8	95.9	93.0	93.6	1.764	
4	62	1.37	1.39	1.29	1.35	76.9	83.4	57.7	72.7	2.643	
5	70	1.54	1.58	1.41	1.51	80.8	83.4	62.5	75.5	2.875	
6	70	1.63	1.70	1.65	1.66	94.7	97.1	82.4	91.4	2.801	
7	70	1.74	1.73	1.72	1.73	99.0	98.5	87.5	95.0	2.648	
8	80	1.77	1.83	1.69	1.76	87.4	81.7	69.8	79.6	3.188	
9	80	2.00	2.01	1.94	1.98	96.1	91.3	79.2	88.9	3.119	
10	90	2.10	2.14	1.91	2.05	84.4	77.8	66.6	76.2	3.491	
11	90	2.41	2.39	2.32	2.37	89.3	84.8	78.8	84.3	3.432	
12	95	--	--	--	--	--	--	--	--	3.636	
Design Point for Stage		100	2.77	2.82	2.81	2.80	84.5	82.2	79.7	82.2	4.00

The rotor data indicate higher peak pressure ratios than those predicted for each of the speed lines. The following tabulation of data for 90 percent speed illustrates this.

	<u>Percent Speed</u>	<u>Pressure Ratio</u>	<u>Adiabatic Efficiency-%</u>	<u>Corrected Airflow lb/sec</u>
Predicted Stage	90	2.265 (Peak)	81.2	3.64
Predicted Stage	90	2.240	82.5 (Peak)	3.76
Predicted Rotor	90	2.340 (Peak)	84.7	3.64
Predicted Rotor	90	2.310	86.2 (Peak)	3.76
Test Data Point	90	2.37	84.3	3.43

Adiabatic Efficiency

The adiabatic efficiency is computed as the ratio of the ideal enthalpy rise for the measured total pressure ratio to the actual enthalpy rise from the inlet duct to the rotor exit (see Appendix I, page 73). The results presented are based on a numerical average of the exit temperatures for the three streamtubes. As in the case of the pressure ratio, the mass average data from the computer runs agree within the accuracy represented by the three-point exit profiles. The data tabulated in the previous section (Rotor Pressure Ratio) indicate that the actual compressor work is slightly higher than predicted, based on the slightly higher pressure ratio at slightly lower efficiency than predicted. Since the data points obtained were not sufficient to establish the peak pressure ratio and peak efficiency, final conclusions with respect to the optimum performance cannot be drawn. In general, however, the demonstrated efficiencies are close enough to the predicted values to support the feasibility of the predicted goals.

Corrected Airflow and Rotor Incidence

As discussed under the section on compressor fabrication, the measured angle of the rotor blade leading-edge expansion surface was 1/2 degree higher and the leading edge was thicker than design specification; this was expected to result in a corrected airflow approximately 5 percent short of the design goal.

The test data of 90 percent speed for build 1 indicated a wide-open throttle corrected airflow 8.5 percent lower than predicted. Prior to the bearing failure, the wide-open throttle corrected airflow at 95 percent speed was noted to be 3.636 pounds per second, which is 7 percent below the predicted value. The data from the 2:1 supersonic compressor tested previously under a Curtiss-Wright program established a linear relationship between the wide-open throttle corrected airflow and corrected speed over the speed range from 93 to 100 percent.* In addition, the corrected air-flow

*Single-Stage Axial Compressor Component Development for Small Gas Turbine Engines (U), USAAVLABS Technical Report 68-90A, U. S. Army Aviation Materiel Laboratories, Fort Eustis, Virginia, March 1969.

at 100 percent speed was expected to remain constant between wide-open throttle and the design point. Based on these conditions, an extrapolation to 100 percent speed indicates a corrected airflow of 3.72 pounds per second, which is 7 percent below the design goal of 4.0 pounds per second.

The average rotor inlet relative air angle was computed for the extrapolated 100 percent speed airflow ($W\sqrt{\theta}$)/ $\delta = 3.72$ pounds per second). The calculation was based on the absolute air angle leaving the inlet guide vane and the guide vane total pressure loss as established by the inlet guide vane flow tests.* The resultant relative air angle is 71.6° , which is 1.6° higher than the average design relative air angle of 70.0° .

A modified incidence angle (i') with respect to the rotor in this analysis is defined as the angle between the relative inlet air vector and the leading-edge expansion surface of the blade. This angle is significant in supersonic compressors since the air angle responds primarily to the blade expansion surface angle. An average modified incidence angle of 1.2 degrees was used in the compressor design. The build 1 data indicate an average modified rotor incidence angle of 2.3 degrees, or an increase of 1.1 degrees over the design value. Figure 14 presents these results.

Rotor Exit Conditions

The experimental rotor exit total pressure and total temperature profiles for the absolute vectors are presented as a function of radius for the highest pressure ratio data point (point 11) at 90 percent speed in Figure 15. These data are based on the fixed probe measurements.

Vector Diagrams

Figure 17 presents the vector diagrams for data point 11. The temperature and pressure profiles presented in Figure 15 represent the rotor exit data for the computer inputs. A zero exit blockage factor satisfied the experimental static pressure within 1 inch of mercury for this case. Figure 16 presents the vector diagrams for the design points. A comparison of the results for point 11 with the design case indicates that the rotor is performing within design expectations except for the deficiency in airflow.

Rotor Passage Recoveries

The rotor passage total pressure recovery is calculated along a streamline by the equation

$$\text{Recovery} = \frac{P_{T_4}}{P_{T_2}} \left(\frac{T_{T_1}}{T_{T_4}} \right)^{\gamma/\gamma - 1}$$

*Single-Stage Axial Compressor Component Development for Small Gas Turbine Engines (U), USAAVLABS Technical Report 68-90A, U. S. Army Aviation Materiel Laboratories, Fort Eustis, Virginia, March 1969.

Build 1, Rotor Configuration 1

----- Design Condition
———— Test Data Extrapolated
to 100 Percent Speed

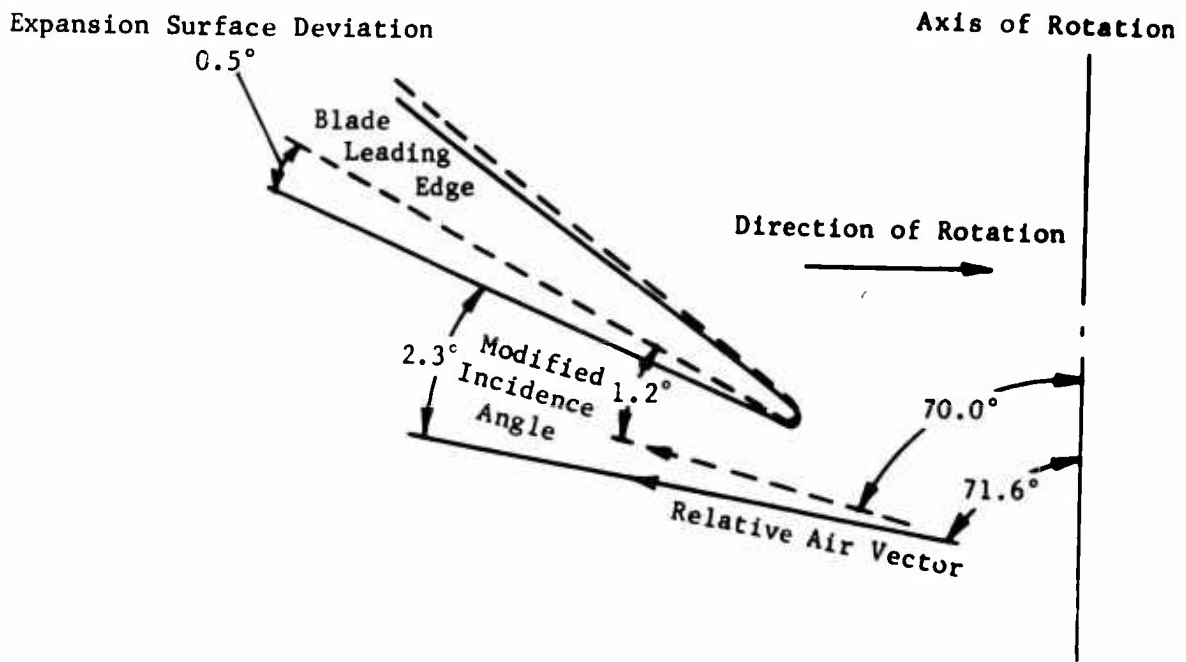


Figure 14. Rotor Incidence for Build 1 Compared to Design Conditions.

$907N/\sqrt{\theta}$

$(W\sqrt{\theta})/S = 3.432 \text{ lb/sec}$

Pressure Ratio = 2.306

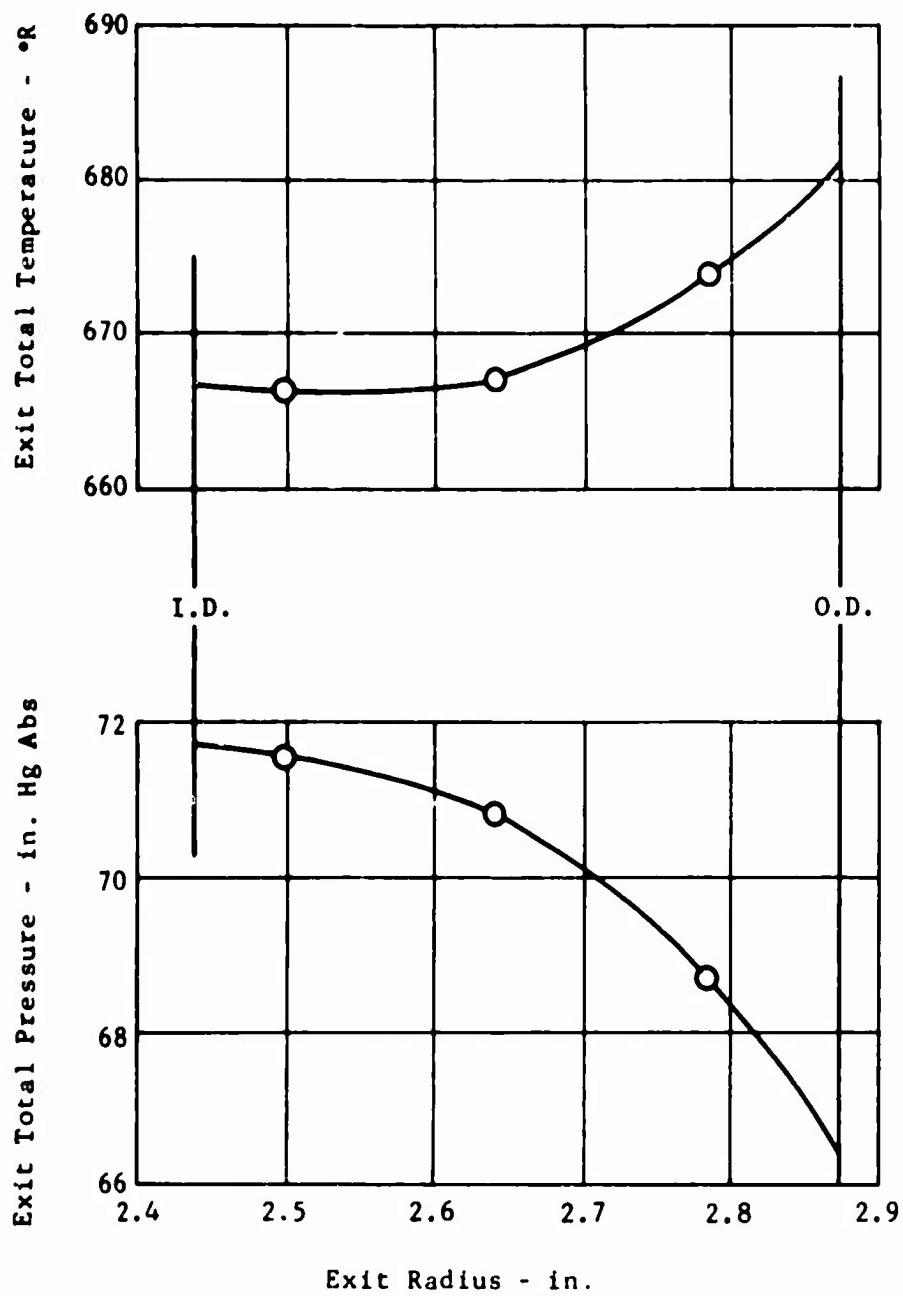


Figure 15. Build 1 Total Pressure and Temperature Profiles at Rotor Exit.

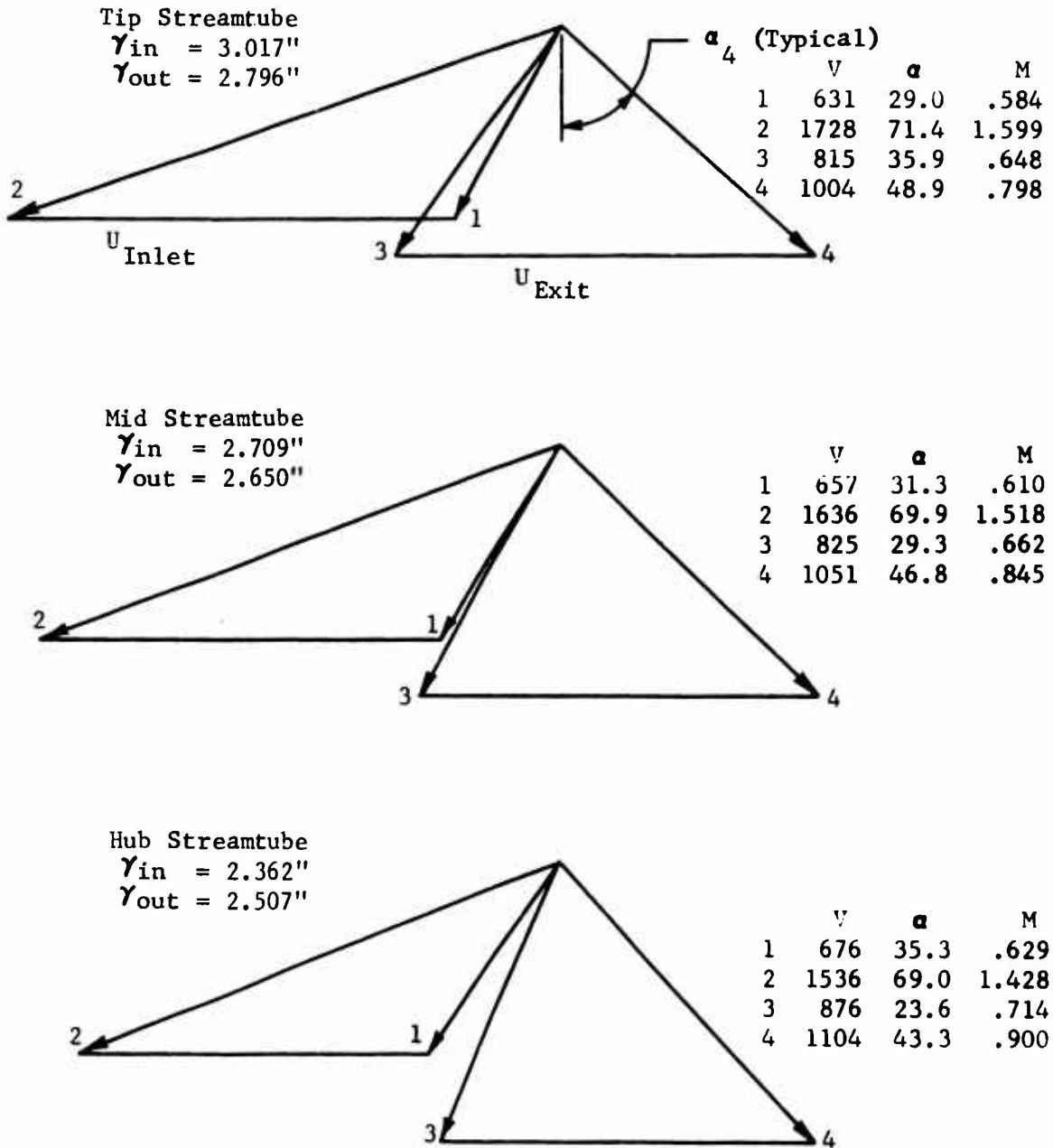


Figure 16. 2.8:1 Supersonic Compressor Design Point Vector Diagrams.

$$90\%N/\sqrt{\theta}$$

Adiabatic Efficiency = 84.3%

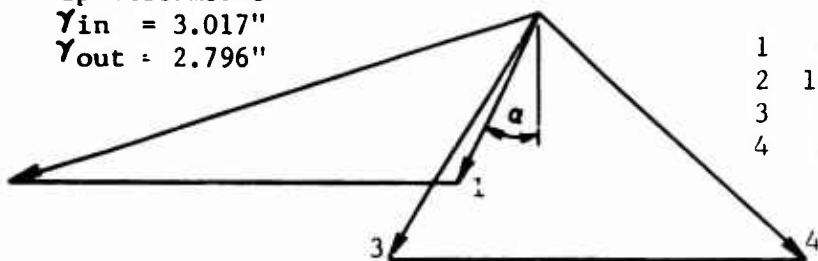
$$(W\sqrt{\theta})/8 = 3.432 \text{ lb/sec}$$

Pressure Ratio = 2.306

Tip Streamtube

$$Y_{in} = 3.017''$$

$$Y_{out} = 2.796''$$

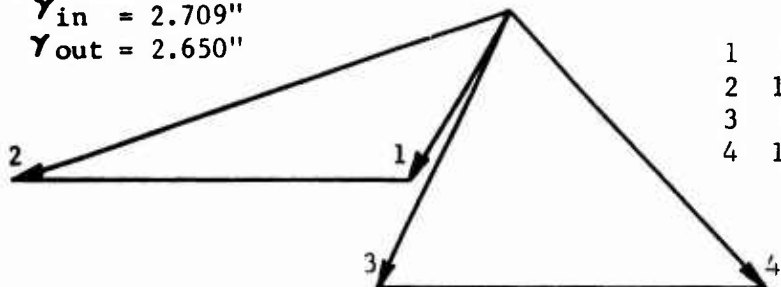


	V	α	M
1	489	26.1	.455
2	1467	72.6	1.365
3	739	31.4	.616
4	953	48.6	.794

Mid Streamtube

$$Y_{in} = 2.709''$$

$$Y_{out} = 2.650''$$

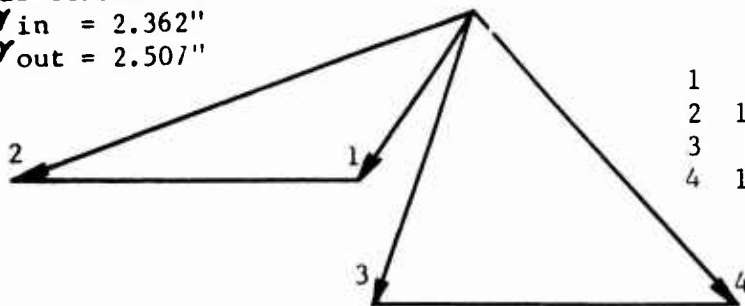


	V	α	M
1	506	29.3	.471
2	1383	71.4	1.288
3	792	25.0	.669
4	1006	44.5	.850

Hub Streamtube

$$Y_{in} = 2.362''$$

$$Y_{out} = 2.507''$$



	V	α	M
1	521	34.1	.486
2	1294	70.5	1.207
3	793	18.6	.675
4	1048	44.2	.892

Figure 17. Build 1 Vector Diagram for 90 Percent Speed Data.

The output data from the data analysis computer runs are used for this calculation.

Figures 18 and 19 present the rotor passage total pressure recoveries for the highest pressure ratio data points at 80 and 90 percent corrected speeds respectively (points 9 and 11). The design recovery curves presented for comparison represent the result of the Mach number recovery adjusted for the hub benefit and tip penalty attributable to the centrifuging of the low-energy boundary layer toward the blade tip. The results indicate that this latter effect is more extreme than anticipated in the design case and probably warrants a revision of the design factors for this condition. The average recovery at the peak pressure ratio for each of the 80 and 90 percent speed lines should exceed that of the design case. The two data points presented do not necessarily represent the peak pressure ratios for the respective speed lines; this is probably why the recovery was somewhat lower than expected.

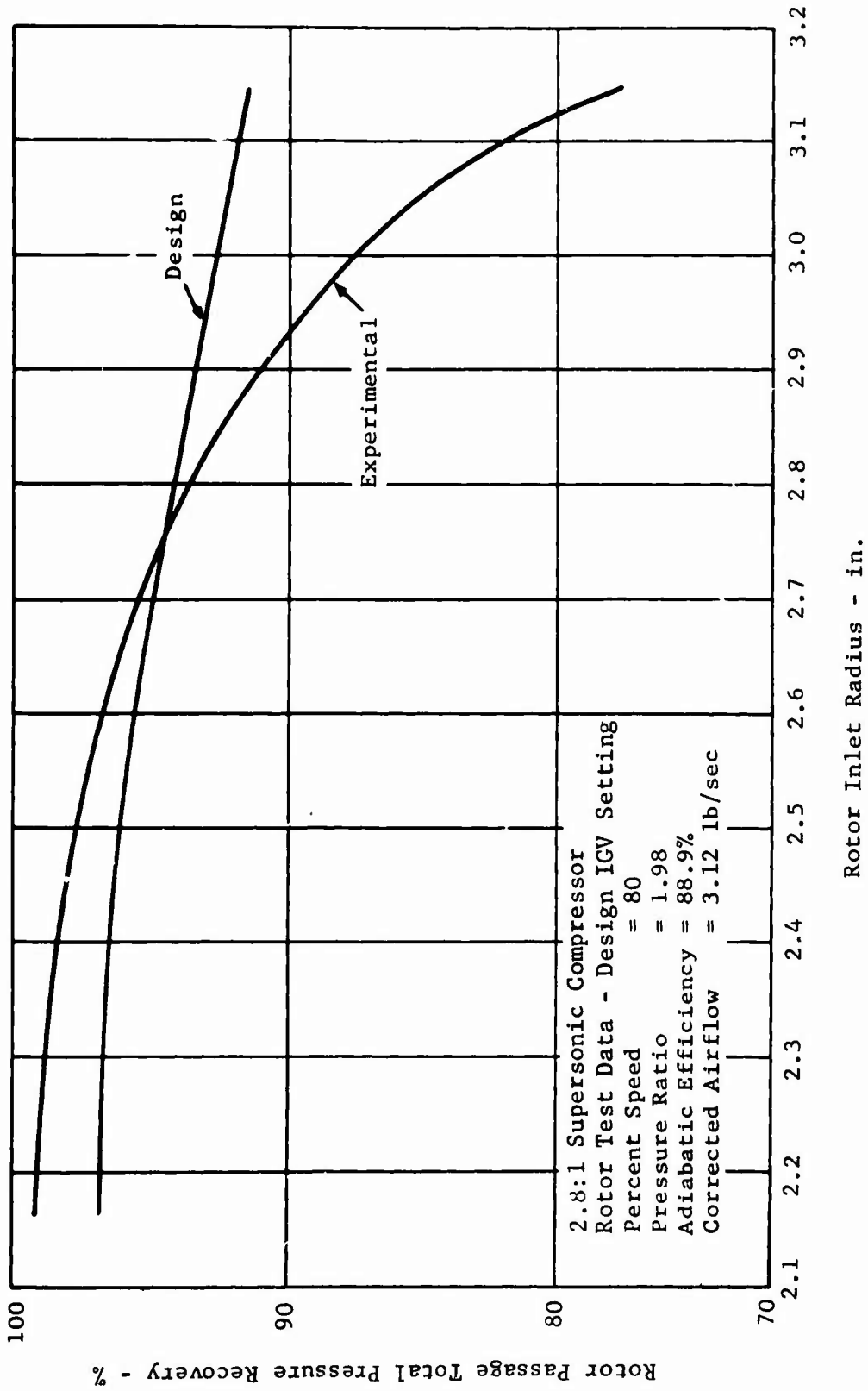
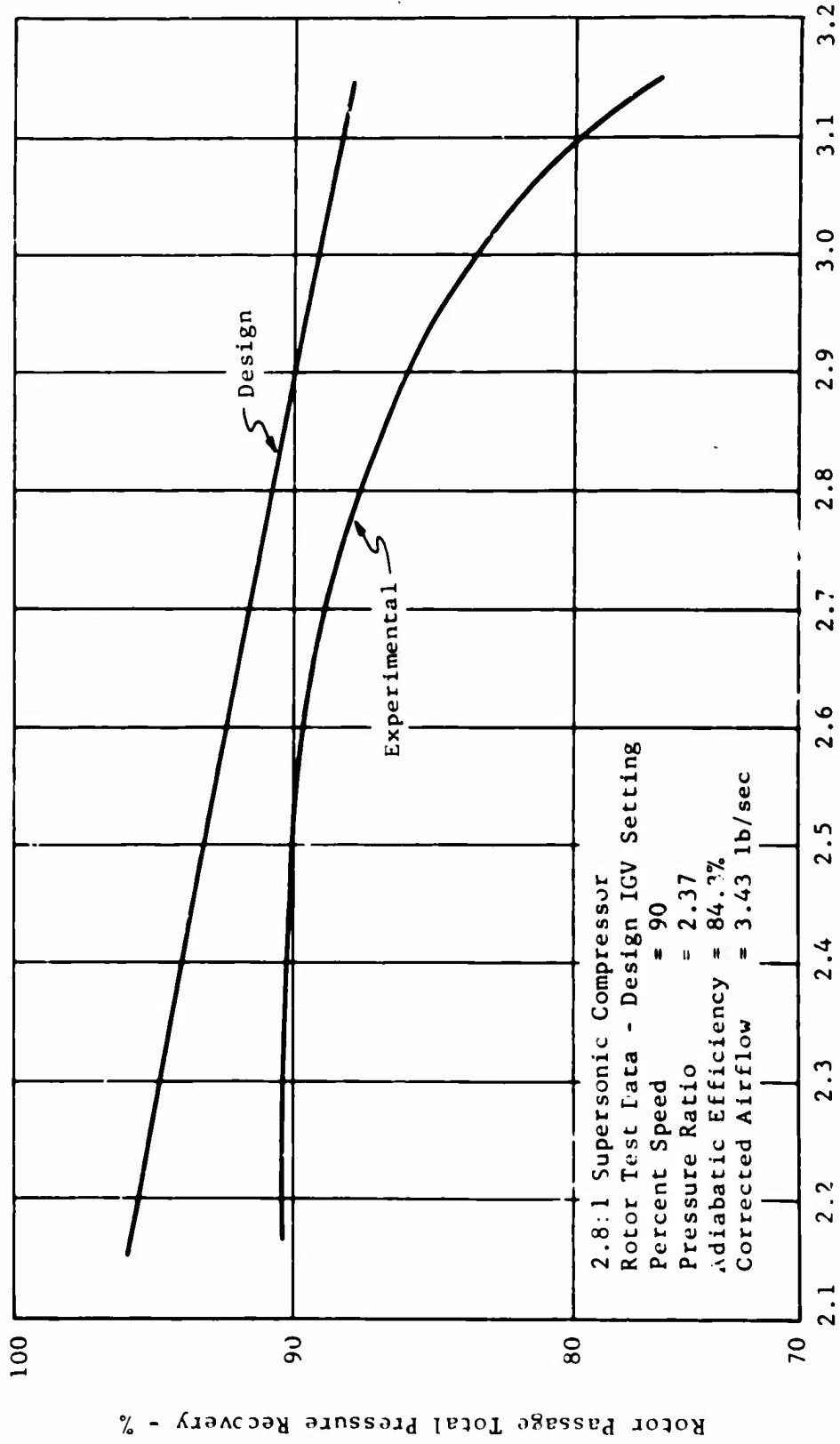


Figure 18. Rotor Passage Pressure Recovery for Build 1 - Data Point 9.



Rotor Inlet Radius - in.

Figure 19. Rotor Passage Pressure Recovery for Build 1 - Data Point 11.

MODIFICATION OF ROTOR DESIGN AND RETEST

Builds 2, 3, 4, and 5 were tested under this task. The tests for these builds were conducted with a second compressor rotor which incorporated the redesigned leading-edge expansion surface angle. Build 2 represented a design inlet guide vane setting. Between builds 2 and 3, the tip clearance configuration was changed and three rotor blades were blended back at the leading edge. Builds 4 and 5 represented changes in the inlet guide vane setting to 6 degrees closed and 8 degrees open, respectively.

ROTOR REDESIGN

The results of the data analysis from the test of build 1 with rotor configuration 1 indicated that a low corrected airflow was the only clear performance deficiency.

The results of the rotor blade inspection for the first rotor indicated that the leading-edge thickness, the leading-edge expansion surface angle, and the leading-edge wedge angle were larger than specified (see Compressor Fabrication, page 3). Correction of the leading-edge thickness involves defining a fabrication procedure which will insure that the specifications are met; this subject is discussed in the following section (Fabrication).

The airflow is primarily a function of the leading-edge expansion surface angle; therefore, this is the only area of the airfoil which required redesign under this task. The average relative rotor inlet air angle required to meet the design corrected airflow of 4.0 pounds per second is 70.0 degrees. The results from the test of build 1 indicate that the modified incidence angle at the design point is 2.3 degrees (Figure 14). The required average leading-edge expansion surface angle for the rotor blade is 67.7 degrees. This represents the angle along streamline sections. The average measured expansion angle for the first rotor was 69.3 degrees, or 1.6 degrees higher than required.

The blade sections are defined along mylar planes for fabrication. A change of 1.6 degrees in a streamline plane will differ by less than 0.1 degree in a mylar plane. On this basis, the expansion surface angle was redefined in the mylar plane as 1.6 degrees lower than the measured mylar plane expansion angles of the first rotor. Figure 20 compares the mylar plane expansion angles for the redesign with those of the first rotor. Figure 21 presents the redesigned portion of the airfoil.

FABRICATION

The method of fabricating the redesigned rotor was thoroughly reviewed in order to meet (1) the redesigned airfoil shape, (2) the leading-edge thickness specifications, (3) the minimum cost, and (4) the shortest schedule.

Two approaches were considered. The first was to produce new tooling for the redesigned airfoil. The second was to fabricate a rotor from the original tooling and then provide special tooling to rework the redesigned area local to the leading-edge expansion surface.

2.8:1 Supersonic Compressor Rotor

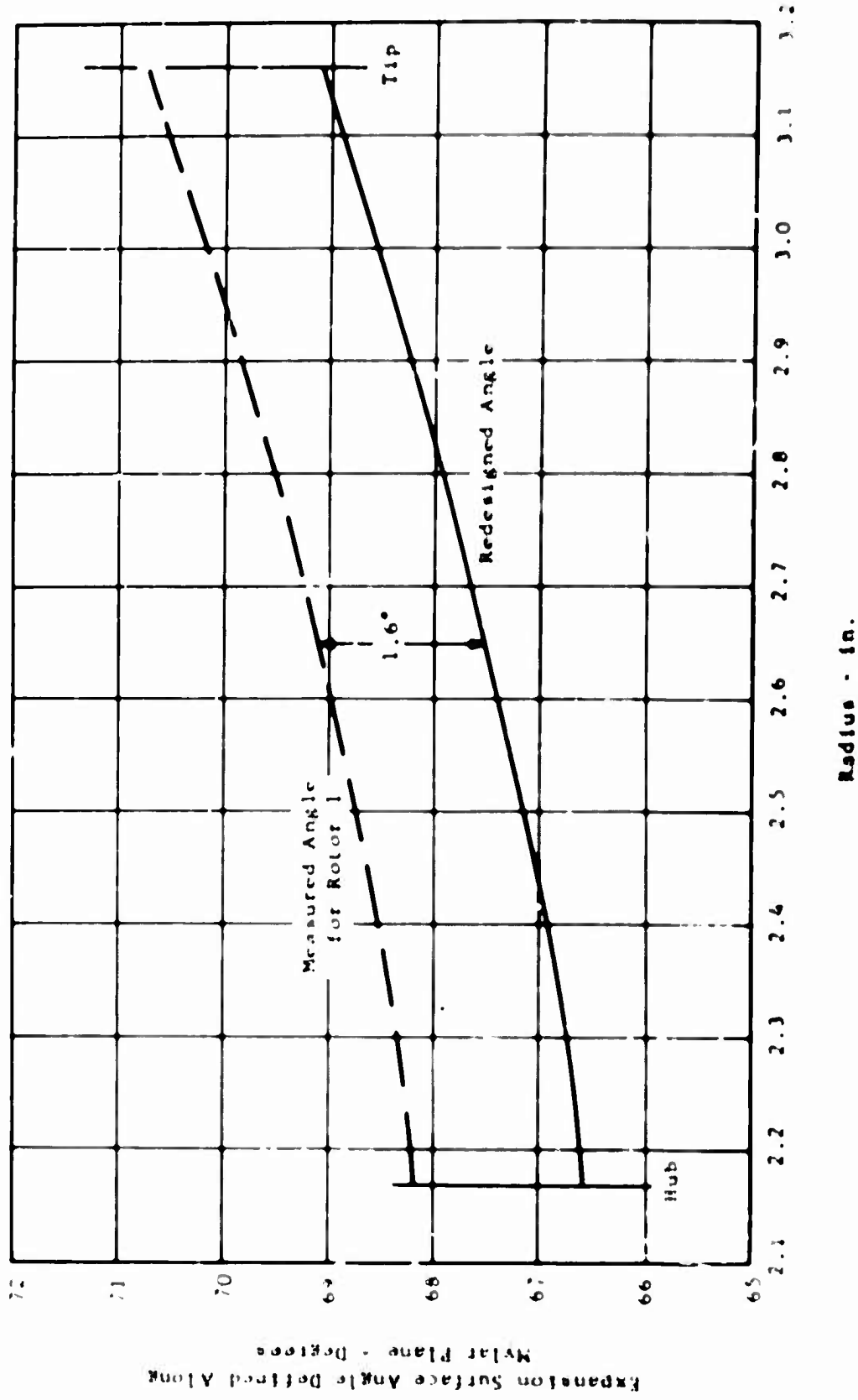


Figure 20. Rotor Redesigned Leading-Edge Expansion Surface Angles.

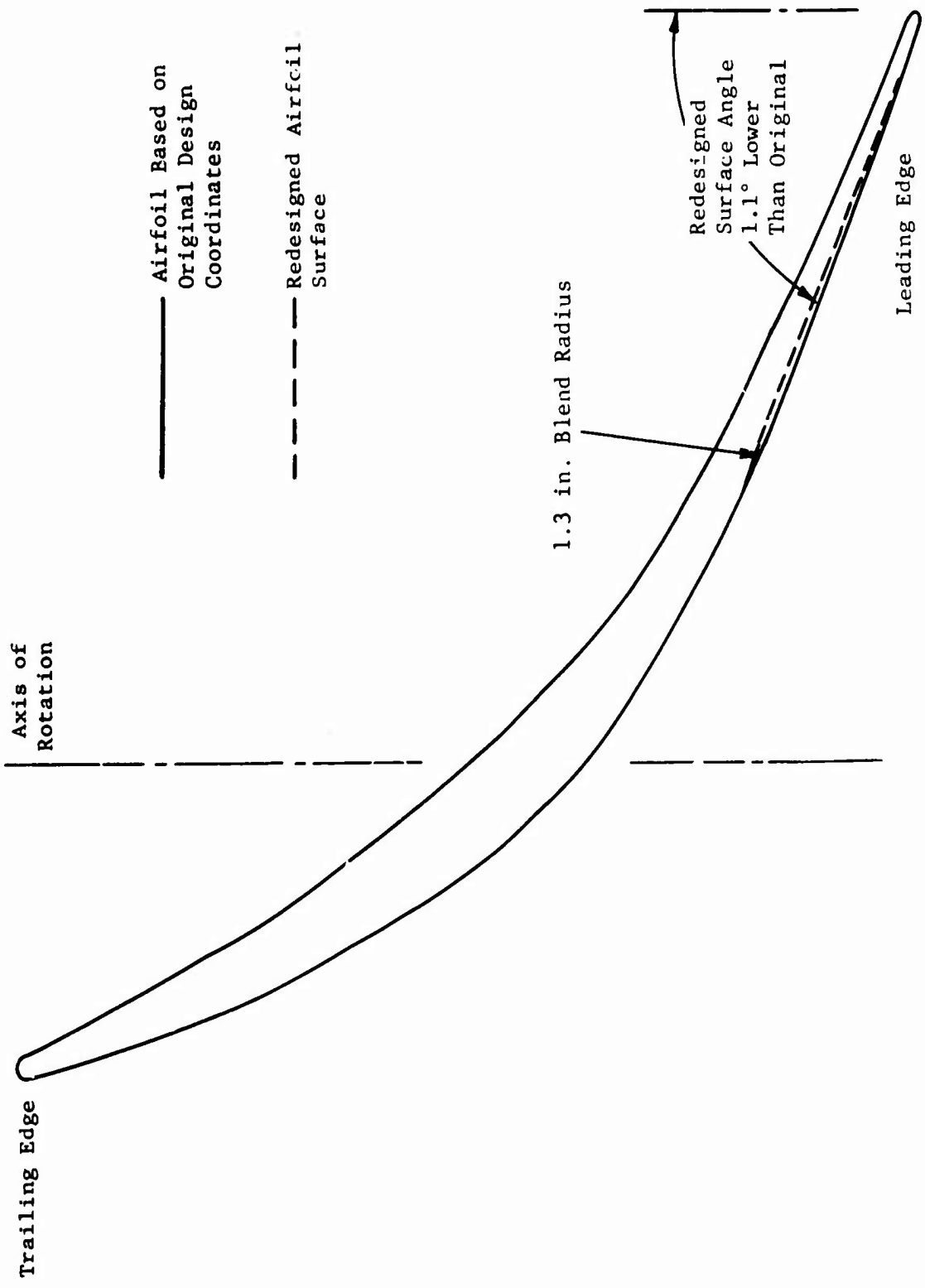


Figure 21. Redesigned Rotor Airfoil Typical Section.

The latter approach was chosen because of the following advantages: there was higher confidence that the unchanged section of the airfoil would be reproduced, the special tooling for a rework provided closer control of the leading-edge thickness and expansion surface angle, the tooling cost was one-tenth that of the alternate approach, and the fabrication period was one-third that of the alternate approach. The disadvantages of this approach were that the leading-edge wedge angle would fall below the desired value of 4 degrees and that the radius of curvature on the blade expansion surface aft of the area which defines the leading-edge angle was limited to values smaller than would have been chosen during a complete redefinition of the airfoil. The radius of curvature achieved was considered adequate, however, and this disadvantage did not represent a real concern. The average leading-edge wedge angle for the first rotor was 5 degrees, or 1 degree higher than the design specification. On the assumption that the original tooling would reproduce the same leading-edge compression surface angle on the new rotor, the resultant wedge angle should have been 1.6 degrees smaller than that of the first rotor, or 3.4 degrees. Although this wedge angle was below the desired design wedge angle of 4 degrees, it was not considered to be low enough to jeopardize the structural integrity of the blade.

The inspection results for the second rotor are tabulated below. Trailing-edge and leading-edge measurements were made on this rotor.

	Redesign Specifications for Rotor No. 2	Measurements of Second Rotor	
		Range	Weighted Average
Expansion Surface Leading-Edge Angle			
Hub	66°39'	66°18'-69°09'	66°42'
Mean	67°45'	67°30'-68°12'	67°54'
Tip	69°19'	68°45'-59°17'	69°06'
Leading-Edge Wedge Angle			
Hub	3°24'	2°20'-3°45'	3°07'
Mean	3°18'	2°45'-3°40'	3°00'
Tip	3°25'	2°10'-3°05'	2°41'
Leading-Edge Thickness	.004-.010	.006-.010	.009
Compression Surface Trailing-Edge Angle			
Hub	23°48'	22°24'-22°36'	22°30'
Mean	28°30'	28°03'-28°08'	28°05'
Tip	34°48'	30°54'-31°06'	31°00'
Trailing-Edge Wedge Angle			
Hub	10°00'	7°30'-7°50'	7°40'
Mean	10°00'	7°57'-8°17'	8°8'
Tip	10°00'	4°40'-4°46'	4°42'

The above data indicate that the specified leading-edge expansion surface angles and leading-edge thickness were basically met. It appears, however, that the leading-edge compression surface did not reproduce exactly and resulted in even lower leading-edge wedge angles than planned. Consequently, the stiffness of the leading edges was somewhat marginal, but the rotor was considered to be capable of being tested without experiencing excessive blade stresses.

TEST CONFIGURATION

Build 2

This build had two changes in test configuration from build 1: (1) the substitution of the second rotor, which represents the redesigned rotor (designated rotor configuration 2), for the first rotor (rotor configuration 1); and (2) the use of a new rotor shroud with an abradable coating.

The nominal tip clearance geometry was the same as that of build 1 (Figure 12). The runout of the abradable surface was somewhat higher than that of the uncoated shroud used in build 1; therefore, a circumferential clearance variation from nominal of $\pm .003$ inch resulted. Although the higher variation tip clearance meant that a rotor tip rub was more likely to occur in this build than in build 1, the purpose of the abradable surface coating on the shroud was to provide a surface which would adjust to a tip rub without damage to the rotor blades. Consequently, a potential tip rub was within the planned operation of this compressor build.

The natural static frequencies (flapping mode) measured for this rotor were 3200-3582 cycles per second.

Build 3

During the testing of build 2, a rotor tip interference occurred which resulted in leading-edge damage to several rotor blades (see Figure 22). This subject is discussed under the section Description of Test, page 40. Rotor blades 13, 16, and 18 were cut back at the leading edges with approximately a 25-degree sweep angle to remove the broken out and cracked areas; their leading edges were resharpener to approximately .010 inch thickness (see Figure 23). The buckling of the blades was considered to be too minor to warrant repair since the operating centrifugal force would tend to restore the blades to their original radial shape. A cylindrical grinding cut has been taken to provide a maximum tip diameter of 6.305 inches in the leading-edge area. This latter operation is a part of a change in tip clearance configuration to prevent a rotor tip rub. The repaired rotor is referred to as rotor configuration 3. Figure 24 presents the new tip clearance geometry for build 3.

The surface of shroud from build 1 has been reworked to meet the new tip clearance configuration. This shroud does not have an abradable coating. The cylindrical cut in the leading-edge area provides .020 inch static clearance with the rotor tip and insures that tip interference will not occur in the leading-edge area even if a flapping mode flutter is

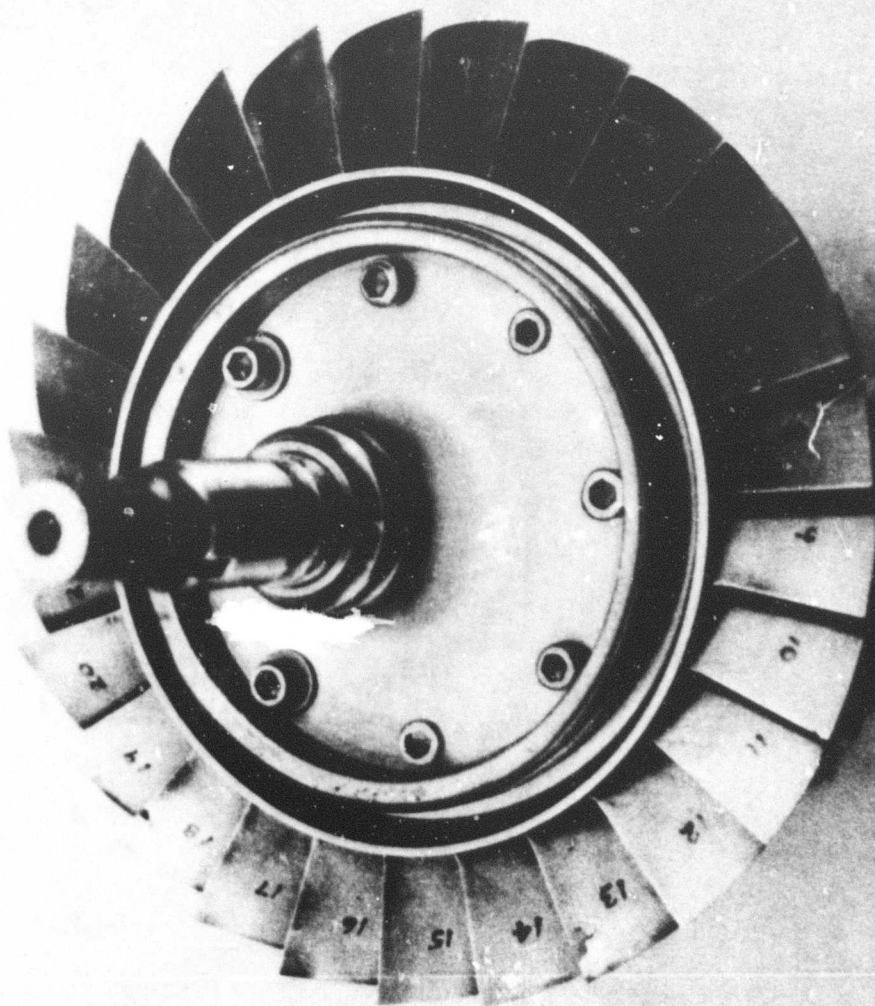


Figure 22. Blades of Second Rotor After Test of Build 2.

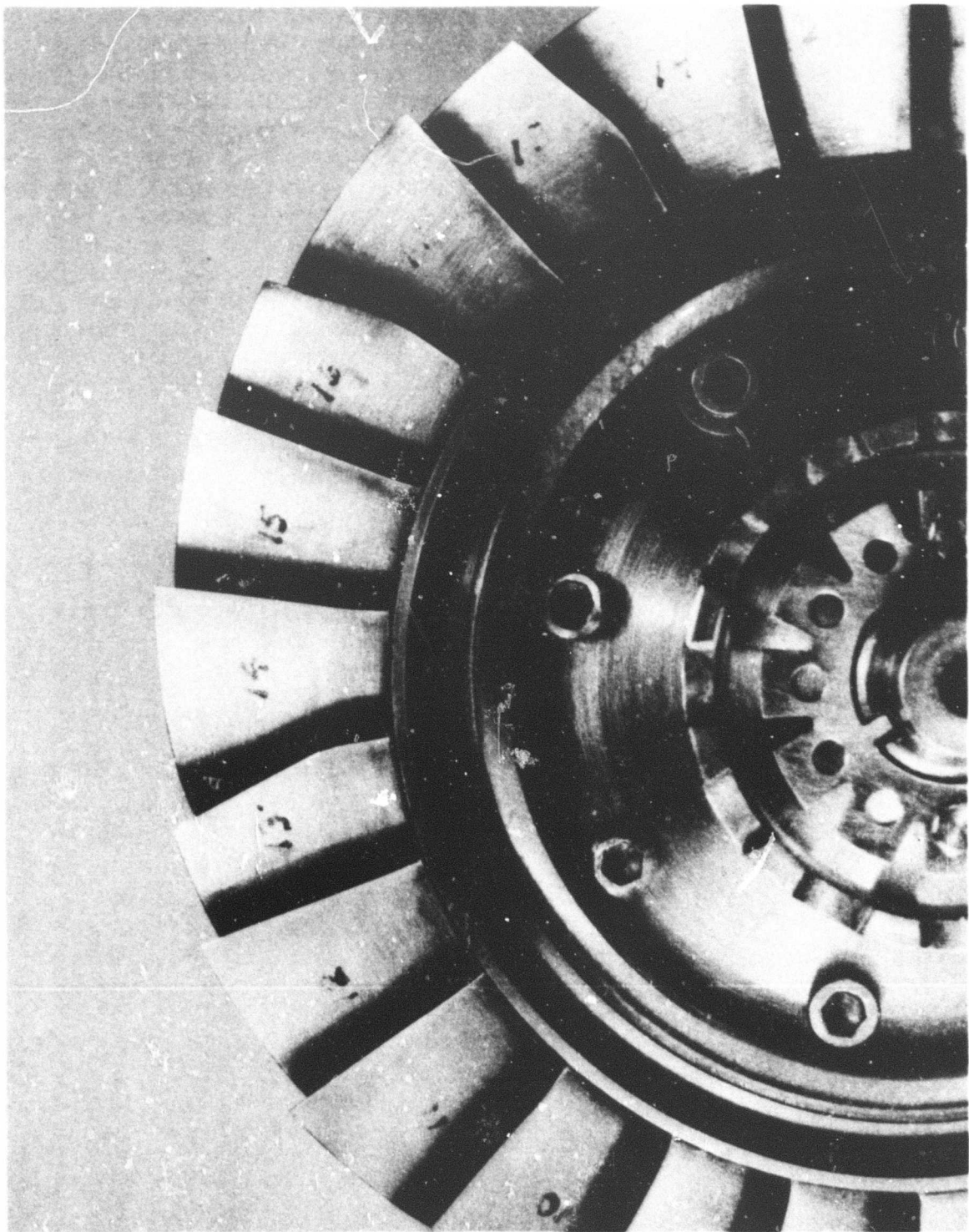


Figure 23. Blades of Second Rotor After Blending.

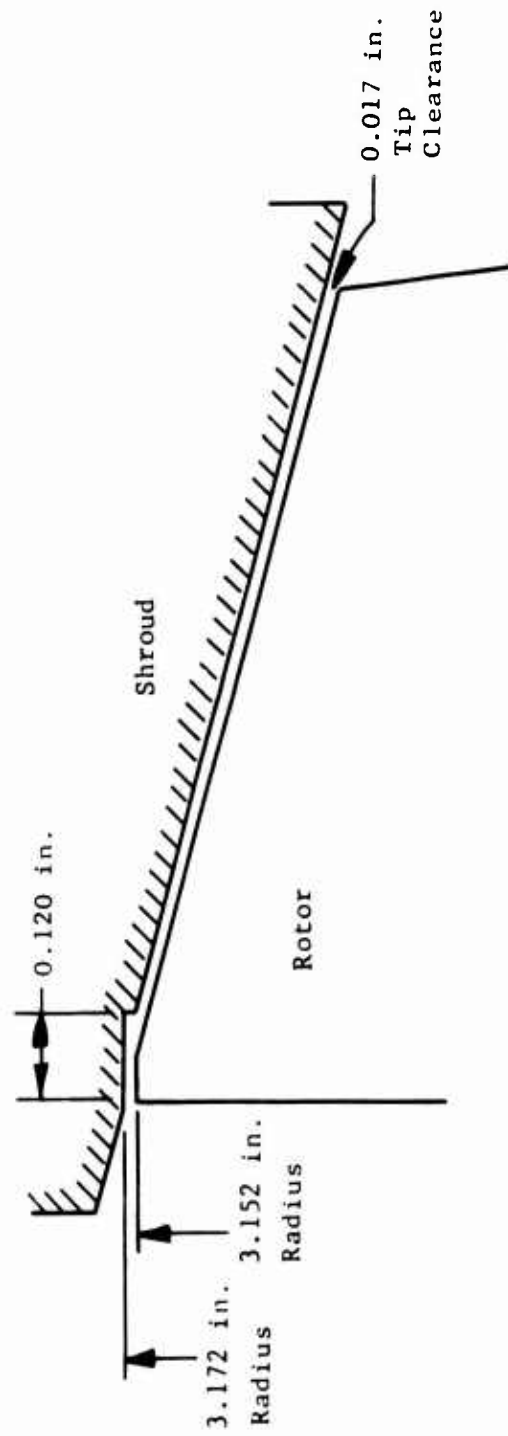


Figure 24. Tip Clearance Geometry for Rotor Test Builds 3, 4, and 5.

encountered. A .017-inch tip clearance was set for the remaining conical surface; this clearance is considered to be sufficient to avoid a tip rub.

An attempt was made to reduce the circumferential variation in back pressure level by installing an annular screen in the test rig exit collector housing. The screen represented a 40 percent open area mesh and was installed during the assembly of build 3. During the initial testing of build 3, the screen did not improve the circumferential effect and was removed.

Except for the changes described, build 3 was the same as build 2.

Build 4

The inlet guide vane setting was adjusted to 6 degrees closed for build 4, but this build was otherwise the same as build 3. At the design setting, the guide vanes prerotate the air opposite to the direction of rotor rotation. A closed setting direction is an increased degree of prerotation, while an open setting direction is a reduced prerotation.

Build 5

The inlet guide vane setting was adjusted to 8 degrees open for build 5, but this build was otherwise the same as builds 3 and 4.

INSTRUMENTATION

Build 2

The instrumentation for build 2 was the same as that for build 1.

Builds 3, 4, and 5

The radial traversing probe was added to builds 3, 4, and 5, but the instrumentation was otherwise the same as for builds 1 and 2.

DESCRIPTION OF TEST

Build 2

Test data were obtained at corrected speeds of 50, 60, 70, 80, and 90 percent of design speed. While approaching a 95-percent speed point, an irregular speed excursion was noted and the rig was shut down. Inspection of the rig revealed that the leading edges of two rotor blades had sustained damage, and the rig was disassembled for further inspection and analysis.

The results of a complete inspection were as follows:

- | a. Compressor rotor | <u>Blade Nos.</u> | <u>Condition</u> |
|---------------------|----------------------|---|
| (see Figure 22) | 11, 18 | Leading edge tips bent, pieces broken out of leading edge at 0.65 to 0.80 inch radial distance from hub |
| | 16 | Leading edge slightly buckled, crack at leading edge 0.65 inch radial distance from hub |
| | 10, 11, 14
17, 13 | Very slightly buckled leading edge |
- b. Compressor rotor shroud (see Figure 3) - Rotor tips had rubbed the abradable coating from a point in line with the rotor leading edge to 0.120 inch downstream of the leading edge. Circumferential grooves up to approximately .025 inch deep were incurred in the abradable coating in this area.
- c. Other parts - No damage.

A review and analysis of this condition led to the following conclusions:

- The blade damage occurred as a result of the localized leading-edge rotor tip interference with the shroud.
- The exact nature and cause of the interference condition which resulted in the damage have not been conclusively established; however, several explanations offer potential solutions. These explanations are discussed below.
- Testing of the rotor could be continued by providing a tip clearance configuration which would ensure no tip rubbing and by removing cracked areas of the damaged blades.
- The reworks indicated under item c are not expected to cause excessive degradation of performance; therefore, useful data will be developed through continued testing of this rotor.

The excessive interference can be explained as follows. Due to the conical shroud, a rearward movement of any point on the rotor blade tip results in a decreasing tip clearance. The shroud surface radius decreases .025 inch in 0.100 inch axial distance. Consequently, under a flapping mode blade flutter, the leading-edge tip section has a higher potential interference with the shroud surface as it moves aft of the leading-edge plane. The blade flutter could be attributed to either normal tip interference, or the natural flutter frequency excited by the compressor strut wakes at sixth engine order, or surge instability. The abradable coating on the shroud was .015-.020 inch thick, and those blades which incurred the most

damage may have hit the steel backing. It should also be noted that the measured wedge angles of 2-1/2 degrees to 3 degrees for the leading-edge sections of this rotor had lower internal damping to flutter than the desired 4-degree wedge angles.

Three possible causes of the blade leading-edge damage are (1) excessive interference of the tip with the shroud surface, (2) normal interference of the tip with the abradable material but an abnormal abrading process, and (3) foreign matter lodged at the tips. There is no evidence which points to the latter two causes and therefore the first is the most likely cause.

Builds 3, 4, and 5

Test points were obtained as follows: for build 3 (design inlet guide vane setting) at 50, 60, 73, 80, 85, 95, and 100 percent corrected speeds; for build 4 (6 degrees closed inlet guide vane setting) at 60, 85, 90, 95, and 100 percent corrected speeds; and for build 5 (8 degrees open inlet guide vane setting) at 60, 85, and 90 percent corrected speeds. The surge line was established for each of these three builds. At the corrected speeds of 90, 95, and 100 percent, increasing the back pressure beyond the last data point resulted in a transient condition under which the compressor speed and airflow could not be stabilized and would drift into the region of audible surge. It was noted that the exit total pressure continued to increase from the last stable point to the point of audible surge.

At 100 and 95 percent speed peak pressure ratio settings, complete traverse data could not be obtained with the traverse probe. The local blockage area presented by the insertion of the probe influences the back-pressure level and initiates a local surge condition before the probe is fully extended to the hub.

The compressor and test rig operated satisfactorily throughout the testing of these three builds. Test points recorded during 23.5 hours of running time accumulated for the three builds totalled 132.

Posttest disassembly and inspection of the test rig revealed no evidence of deterioration. The condition of the rotor blades was unchanged from the pretest condition for build 3, with no evidence of rotor tip rub.

TEST RESULTS

Performance Maps

Figures 25 through 28 present the performance maps for builds 2 through 5, respectively. The map for build 3 (Figure 26), which represents the design inlet guide vane setting, indicates a surge line which provides a wider operating margin than the predicted map.

The compressor maps for guide vane settings of 6 degrees closed and 8 degrees open (Figures 27 and 28) show a definite change in the speed lines between 60 and 95 percent speed. The closed setting results in a higher pressure ratio and airflow for a given speed line, while the open setting

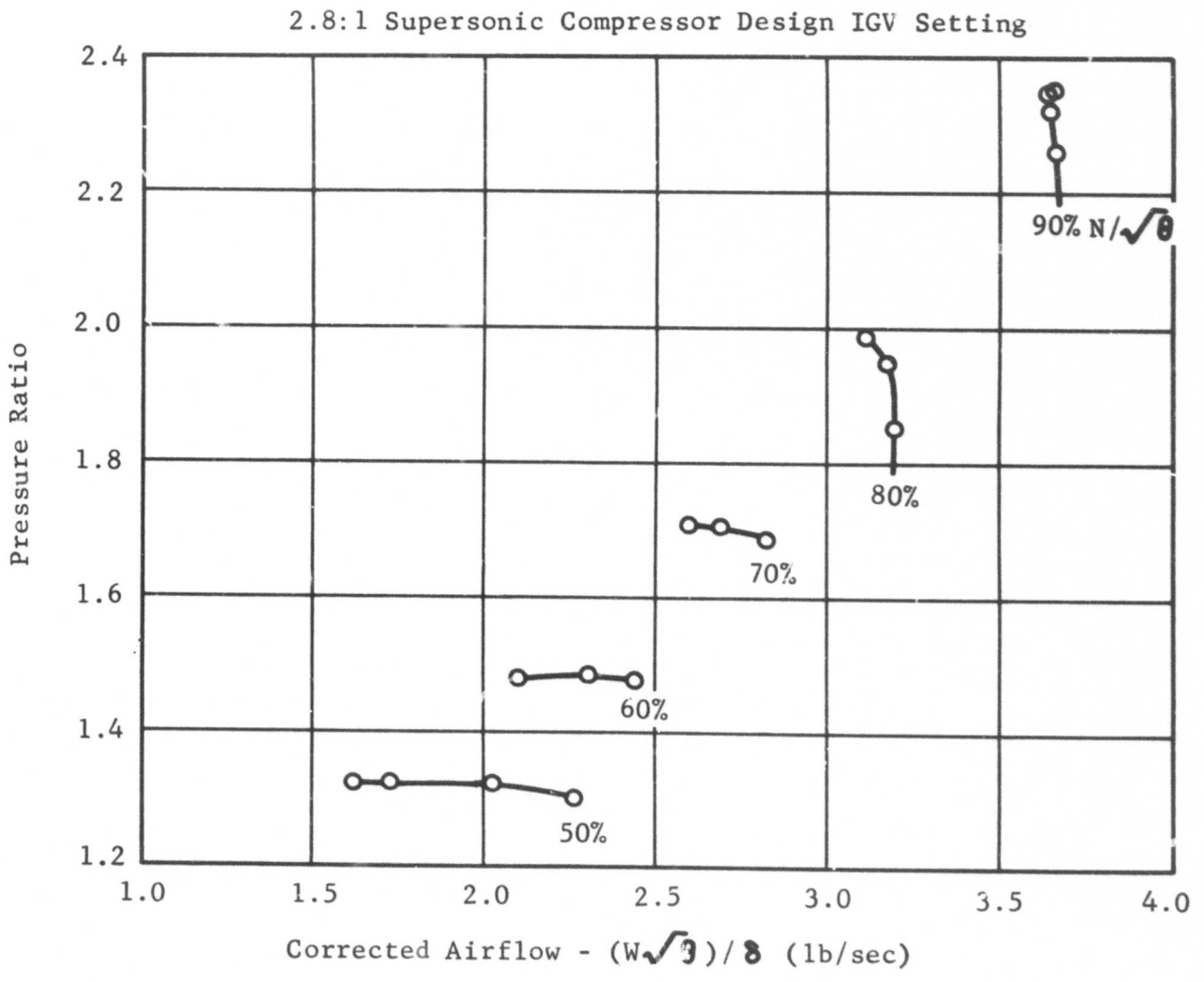
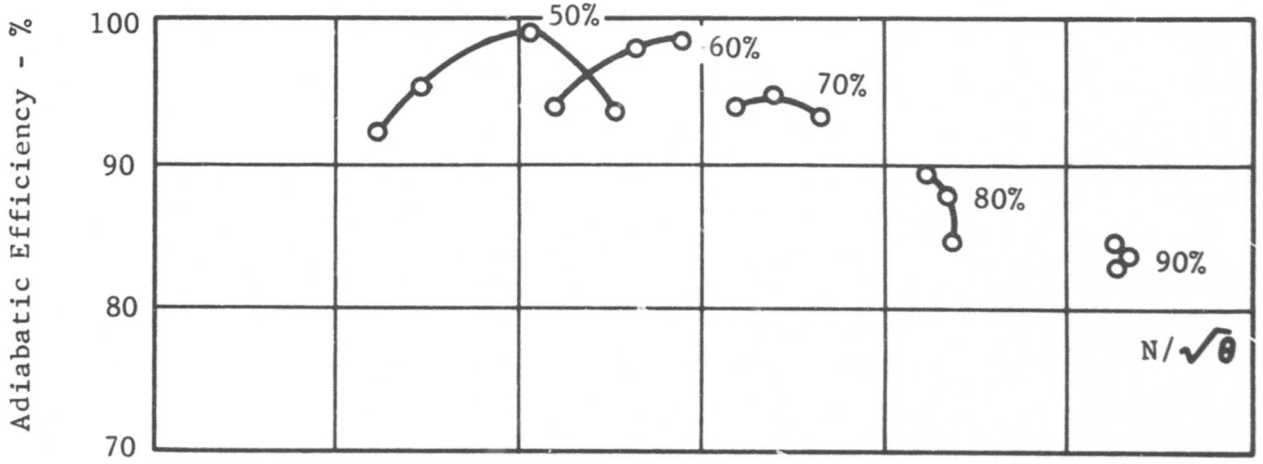
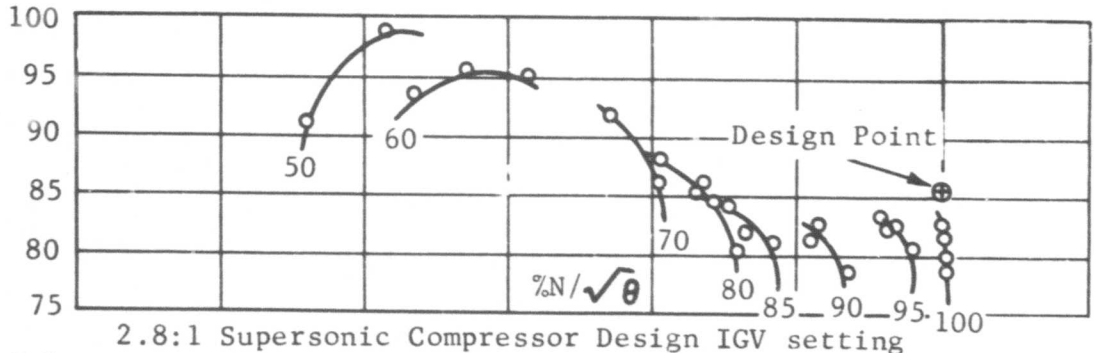


Figure 25. Performance Map Rotor Test Data, Build 2.

Adiabatic Efficiency - %



Pressure Ratio

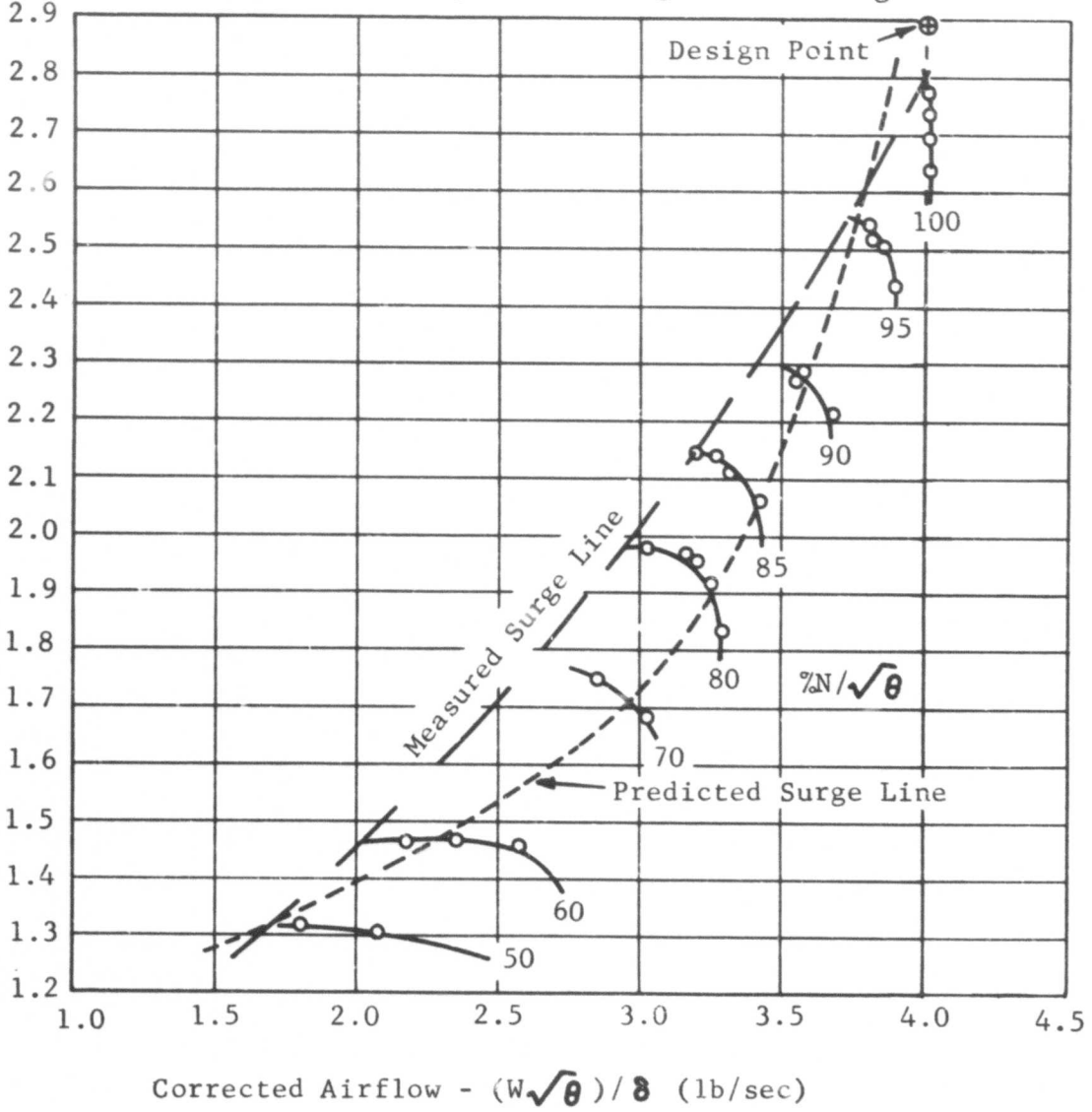
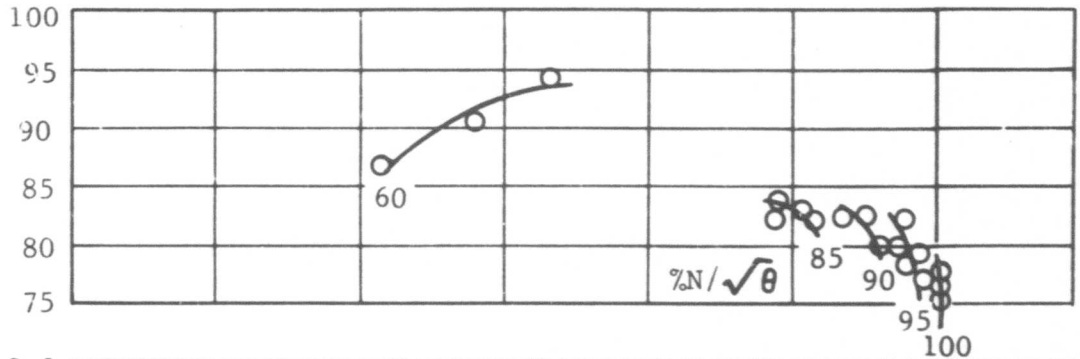


Figure 26. Performance Map Rotor Test Data, Build 3.

Adiabatic Efficiency - %



Pressure Ratio

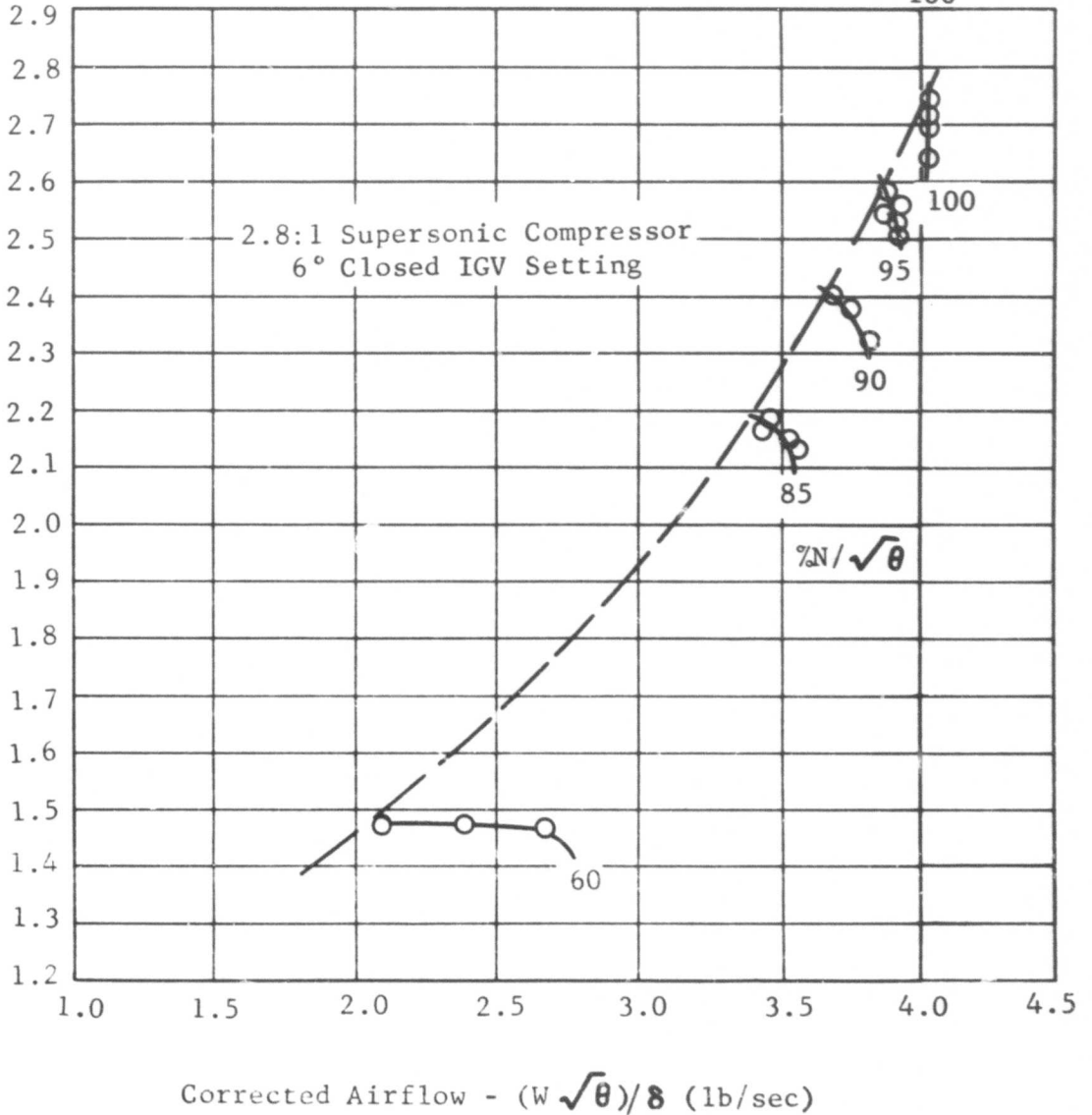
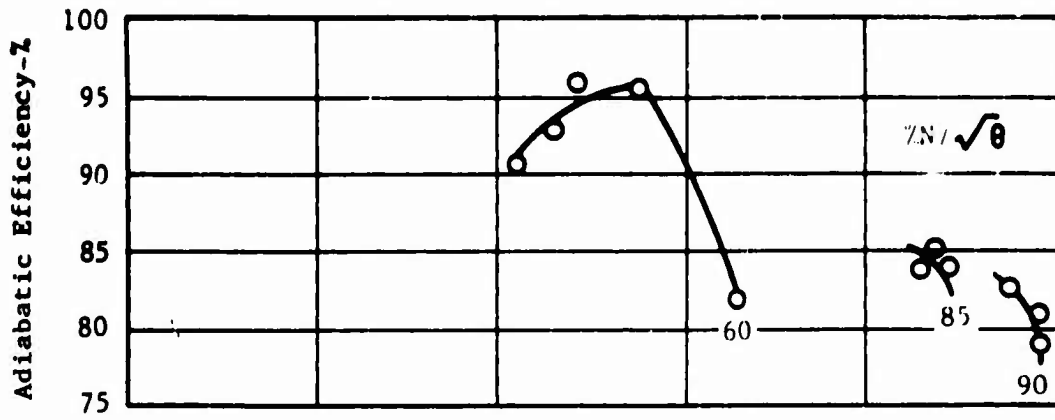


Figure 27. Performance Map Rotor Test Data, Build 4.



2.8:1 Supersonic Compressor 8° Open IGV Setting

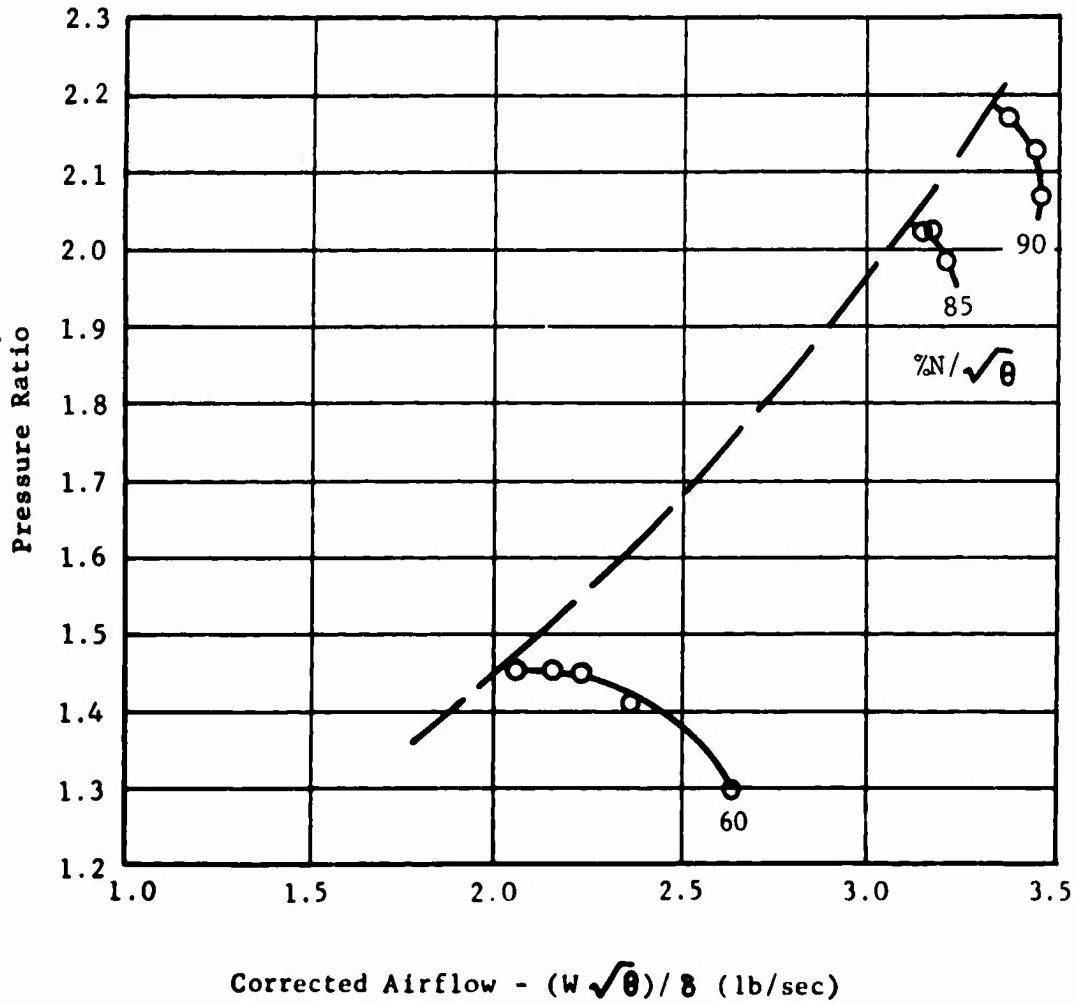


Figure 28. Performance Map Rotor Test Data, Build 5.

results in a lower pressure ratio and lower airflow. These changes are on the order of 3 percent. Figure 29 illustrates this variation.

Rotor Pressure Ratio

The peak pressure ratio achieved at 100 percent corrected speed for build 3 (design inlet guide vane setting) is 2.775 (Figure 26). This represents the last stable test point and is based on the average rotor exit data.

The performance data indicate that at a given setting of the close-coupled valve, used to back pressure the compressor, the back-pressure level varies with circumferential location around the rotor exit. This condition is attributed to the lack of diffusion in the collector housing, from the high Mach number (approximately 0.9) high whirl angle (approximately 45 degrees) rotor exit flow conditions to the low Mach number uniform flow, before entering the single outlet asymmetric exit duct leading to the close-coupled valve. Figure 30 presents the variation in exit total pressure and temperature as a function of circumferential location for the 100 percent speed, build 3, peak pressure ratio data point. The circumferential variation in total pressure is 3 percent; in total temperature, 0.4 percent. At the location of peak circumferential variation a pressure ratio of 2.84:1 is indicated at an 85 percent adiabatic efficiency.

Table II is a summary of the 90 and 100 percent speed peak pressure ratio performance data for the five compressor builds. The 90 percent speed hub, mean, and tip streamtube pressure ratios for build 2 are slightly lower than those of build 1, but they are essentially in the same relationship to each other. The build 1 point may represent a slightly higher back pressure setting. The build 3 data point indicates a close comparison with build 2 for the hub and mean streamtube pressure ratios, but the tip streamtube pressure ratio indicates a significant degradation. This tip performance degradation is attributed to the increased rotor tip clearance and the cut-back rotor blades in build 3. Figure 31 presents a comparison of 90 percent speed peak pressure ratio data for builds 1, 2, and 3.

The data indicate, therefore, that the compressor with the redesigned rotor airfoil (rotor configuration 2) and a static tip clearance of .012 inch can produce a rotor pressure ratio in excess of 2.84:1 when uniformly back pressured, and thus it can meet the design goal of 2.89:1.

The part-speed rotor pressure ratios peak at values equal to or higher than predicted.

Adiabatic Efficiency

The average adiabatic efficiency at the 100 percent speed peak pressure ratio data point is 82.6 percent for build 3 (design inlet guide vane setting).

At the location of the peak circumferential rotor exit pressure, the adiabatic efficiency is 85 percent based on the exit total temperatures at that location (Figure 30).

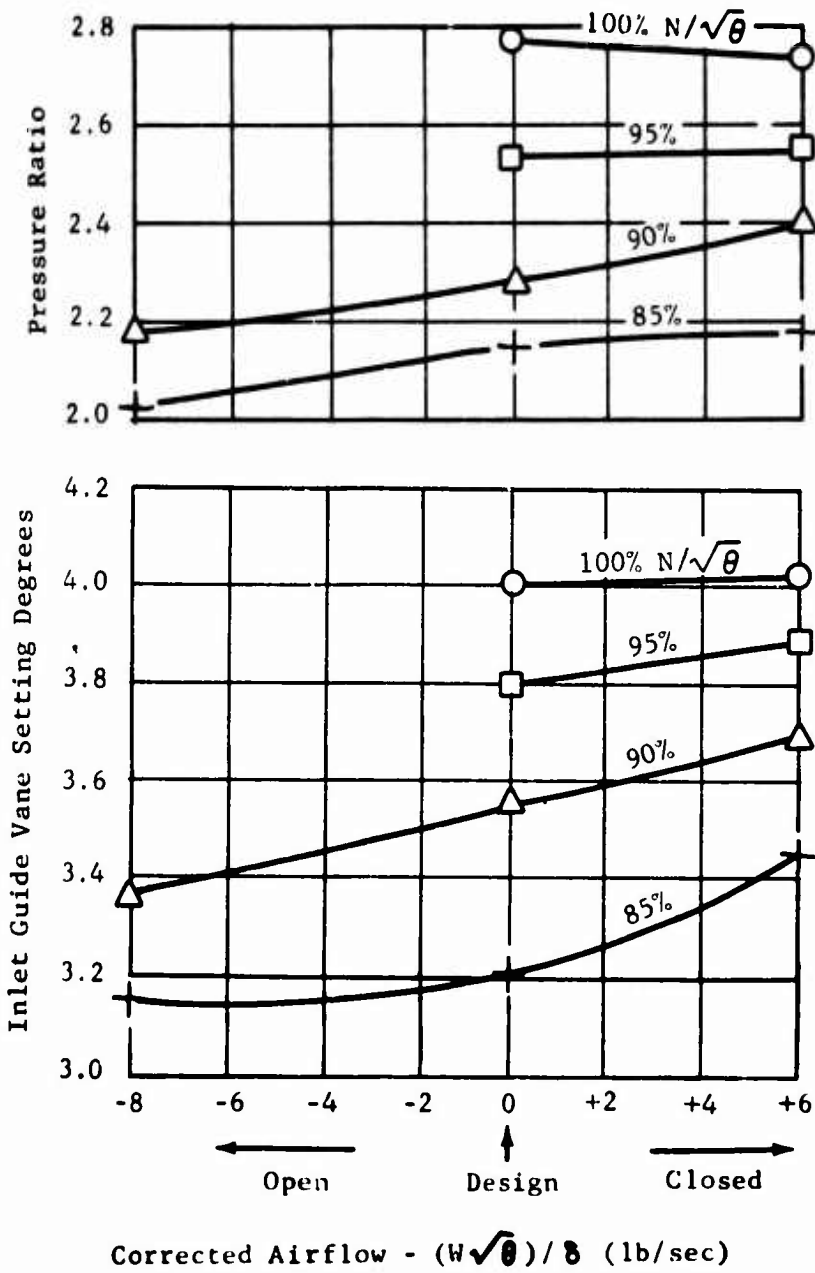
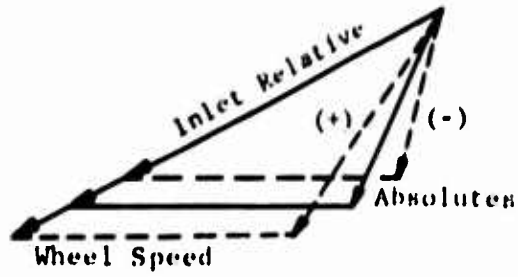


Figure 29. Effect of Inlet Guide Vane Setting for Builds 3, 4 and 5.

Build 3 Design IGV Setting

100% $N/\sqrt{\theta}$
 $(W\sqrt{\theta})/B = 4.006$

Pressure Ratio = 2.775

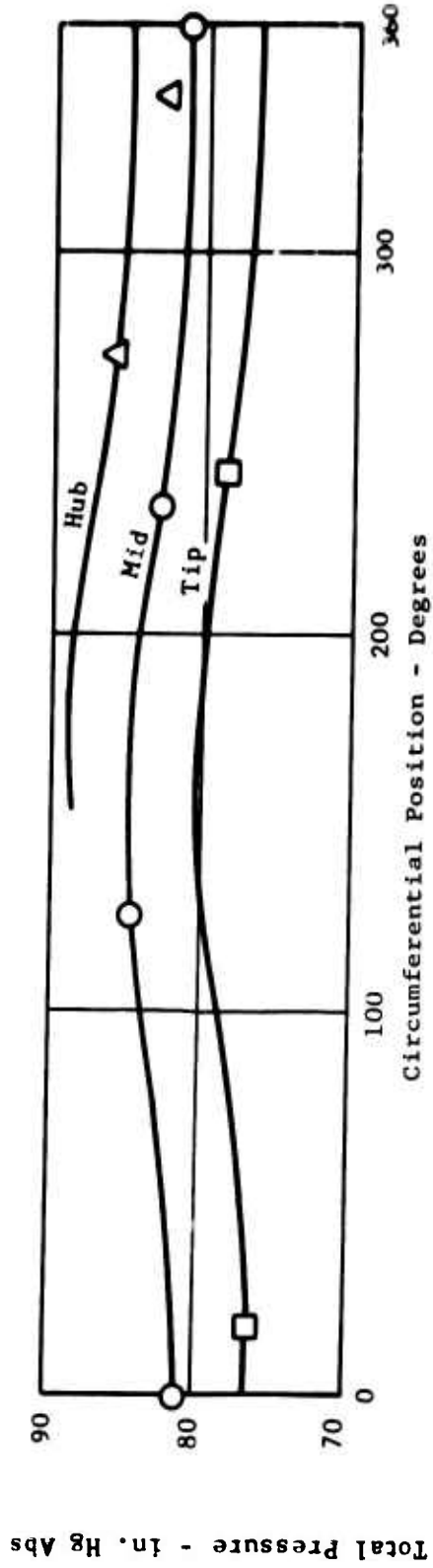
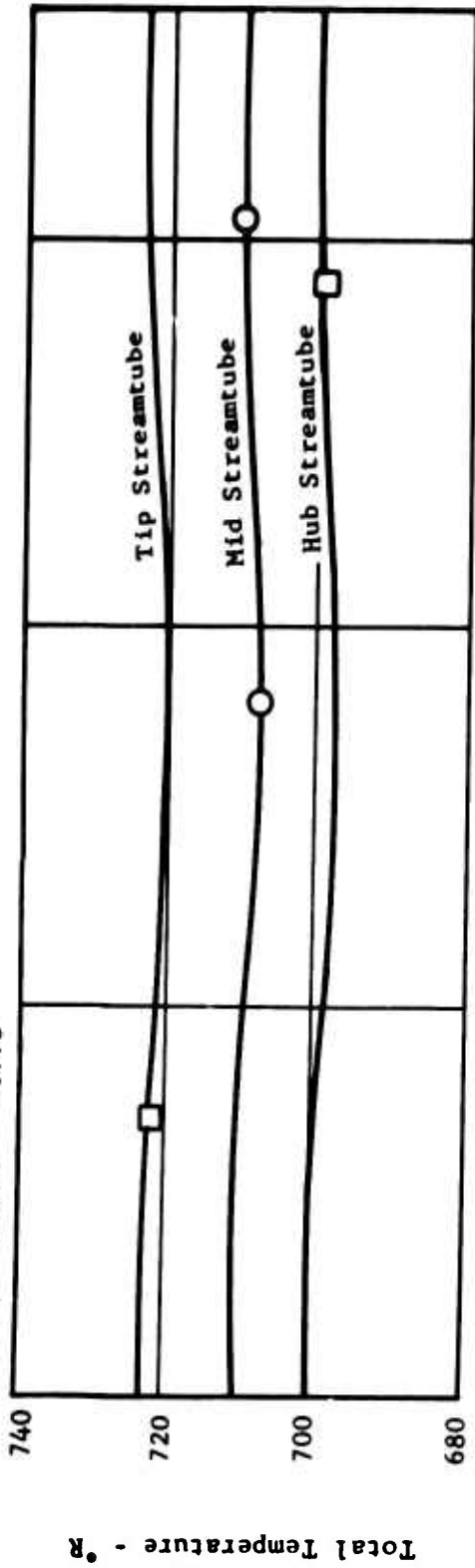


Figure 30. Circumferential Variations in Rotor Exit Conditions.

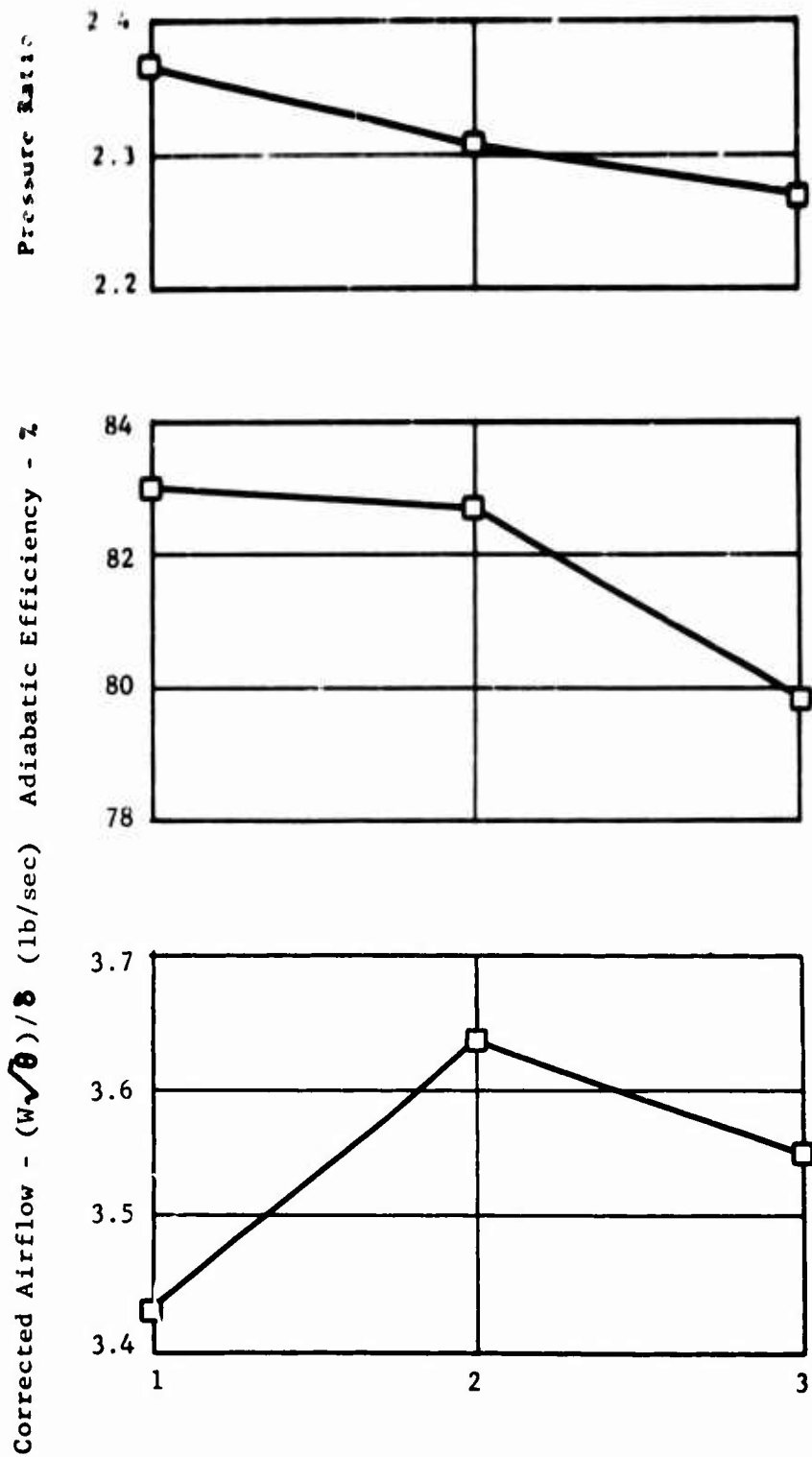


Figure 31. Comparison of 90 Percent Speed Peak Pressure Ratio Data for Builds 1, 2 and 3.

The 90 percent speed efficiency data presented in Table II indicate slightly lower values for each of the hub, mean, and tip streamtubes of build 2 than those of build 1, and may be attributed to a lower back-pressure level for the build 2 data point. The tip efficiency of build 3 is significantly lower than that of builds 1 and 2, and the degradation is attributed to the higher rotor tip clearance and cut-back rotor blades of build 3.

Based on the test data, and rotor adiabatic efficiency goal of 85.7 percent can be met or exceeded with the redesigned airfoil (rotor configuration 2) and a static tip clearance of 0.12 inch when back pressured uniformly.

The part-speed peak rotor efficiencies are higher than predicted.

Corrected Airflow and Rotor Incidence

The measured corrected airflow at the 100 percent speed peak pressure ratio point of build 3 is 4.006 pounds per second, which meets the design goal of 4.0 pounds per second. The 90 percent speed corrected airflow presented in Table II represents the wide-open throttle values. The airflow does not vary significantly as a function of pressure ratio in the region of wide-open throttle for the speed range from 85 to 100 percent; therefore, the measured data at wide-open throttle provide a good basis for comparing the airflow variation between builds. The increase in airflow from build 1 to builds 2 and 3, which resulted from the blade redesign to the leading-edge expansion angle and the thinner leading edges, is 5 percent at 90 percent speed.

The rotor inlet relative air angle for the 100 percent speed peak pressure ratio point of build 3 is compared to the design air angle in Figure 32. The modified incidence angle for this point is 2.3 degrees (Figure 33). The incidence angle varies less than 0.2 degree along the 100 percent speed line. The 100 percent speed conditions represent fully attached supersonic flow over the entire span of the rotor blade leading edge. The fact that the modified incidence angle remains essentially constant between builds 1 and 2 and along the full range of pressure ratios at 100 percent speed confirms the design criterion that the rotor inlet relative air angle for a supersonic compressor with attached flow responds to the leading-edge expansion surface angle plus a fixed allowance for boundary layer growth. The modified incidence angle of 2.3 degrees represents the empirical factor for the fixed boundary layer growth as established in this program.

As the rotor speed decreases, the rotor relative inlet Mach number decreases to a point where it no longer defines attached flow conditions at the leading edge. Below this point, the flow does not respond to the fixed incidence criterion. The effective leading-edge wedge angle is 4.3 to 5.8 degrees (the 2- to 3.5-degree metal angle plus the 2.3-degree boundary layer effect). The two-dimensional detachment Mach number for these wedge angles is 1.22 to 1.27. The 95 percent speed data indicate a hub relative Mach number of 1.24 (Figure 34); therefore, at this speed and below, the fixed incidence is not expected to hold. Figure 35 indicates that the variation of modified rotor incidence at peak pressure ratio from hub to

2.8:1 Supersonic Compressor Rotor Performance Design IGV Setting

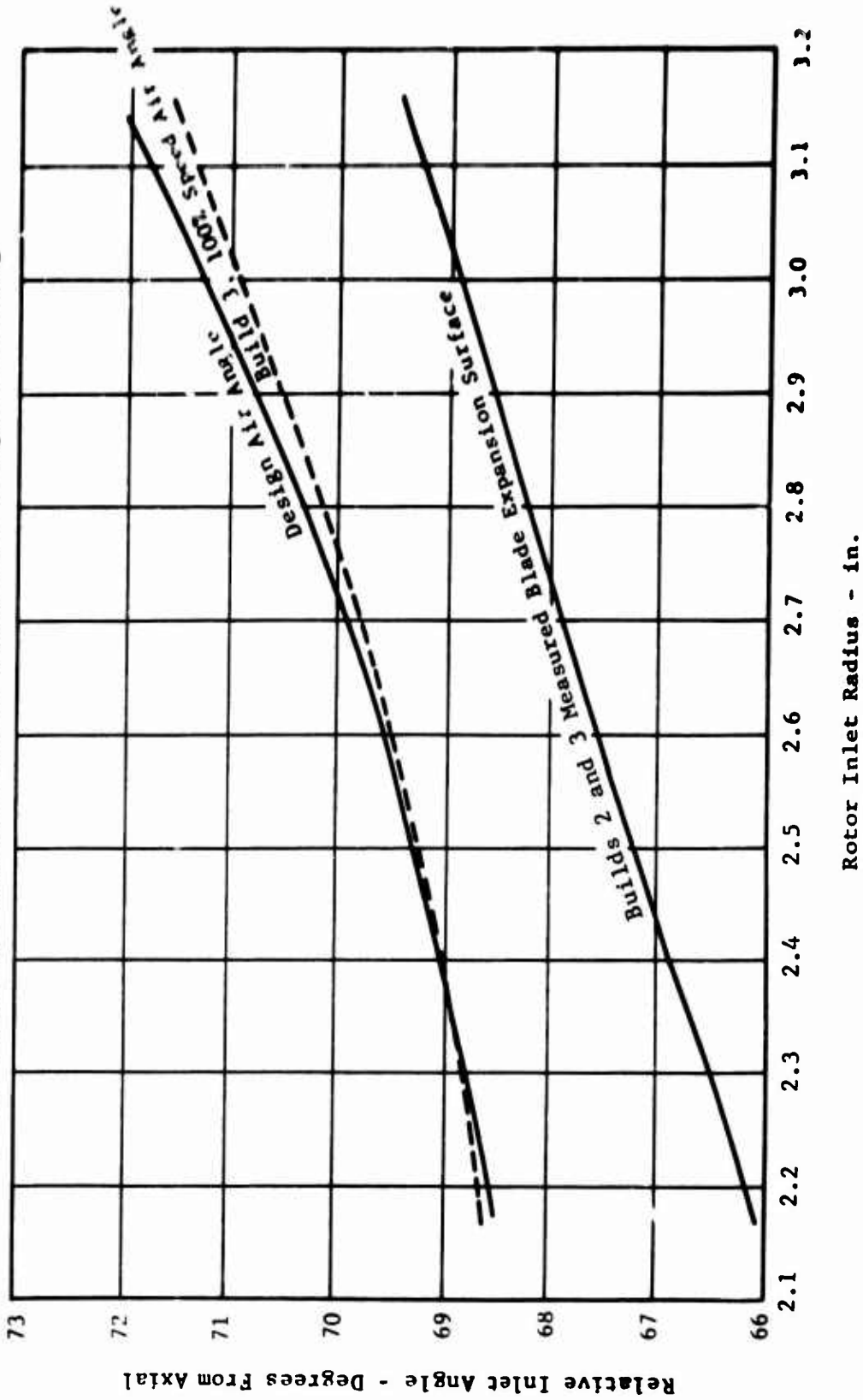


Figure 32. Rotor Inlet Relative Air Angle at 100 Percent Speed, Build 3.

2.8:1 Supersonic Compressor Rotor Test
Design IGV Setting

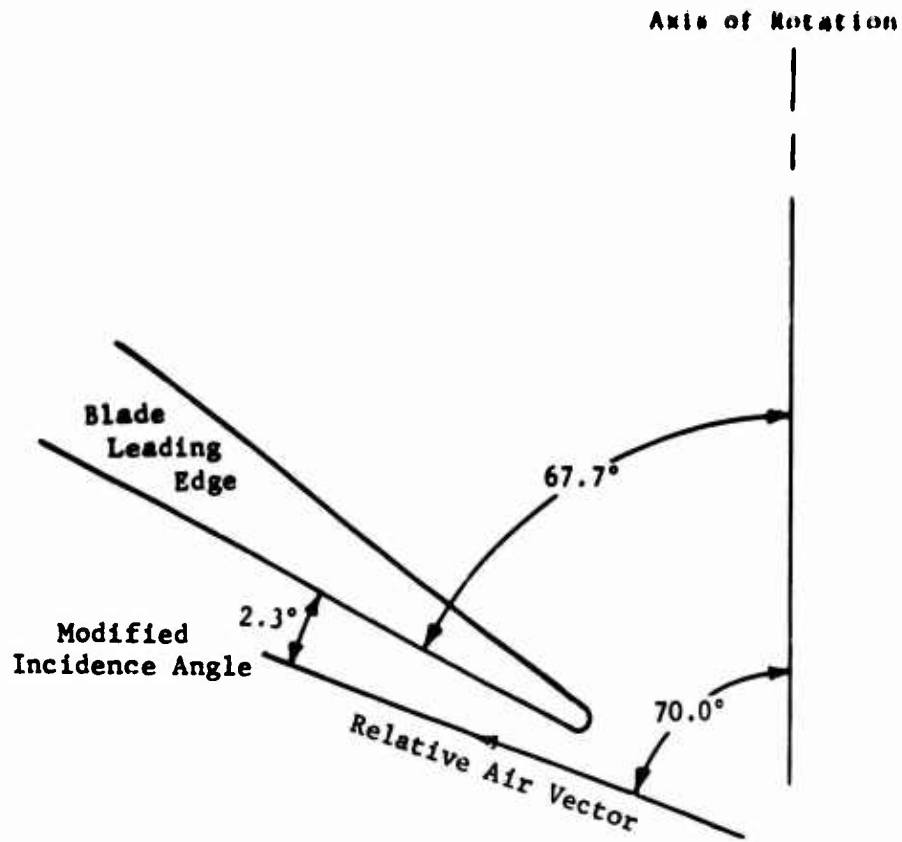


Figure 33. Modified Rotor Incidence Angle at 100 Percent Speed, Build 3.

2.8:1 Supersonic Compressor Design IGV Setting

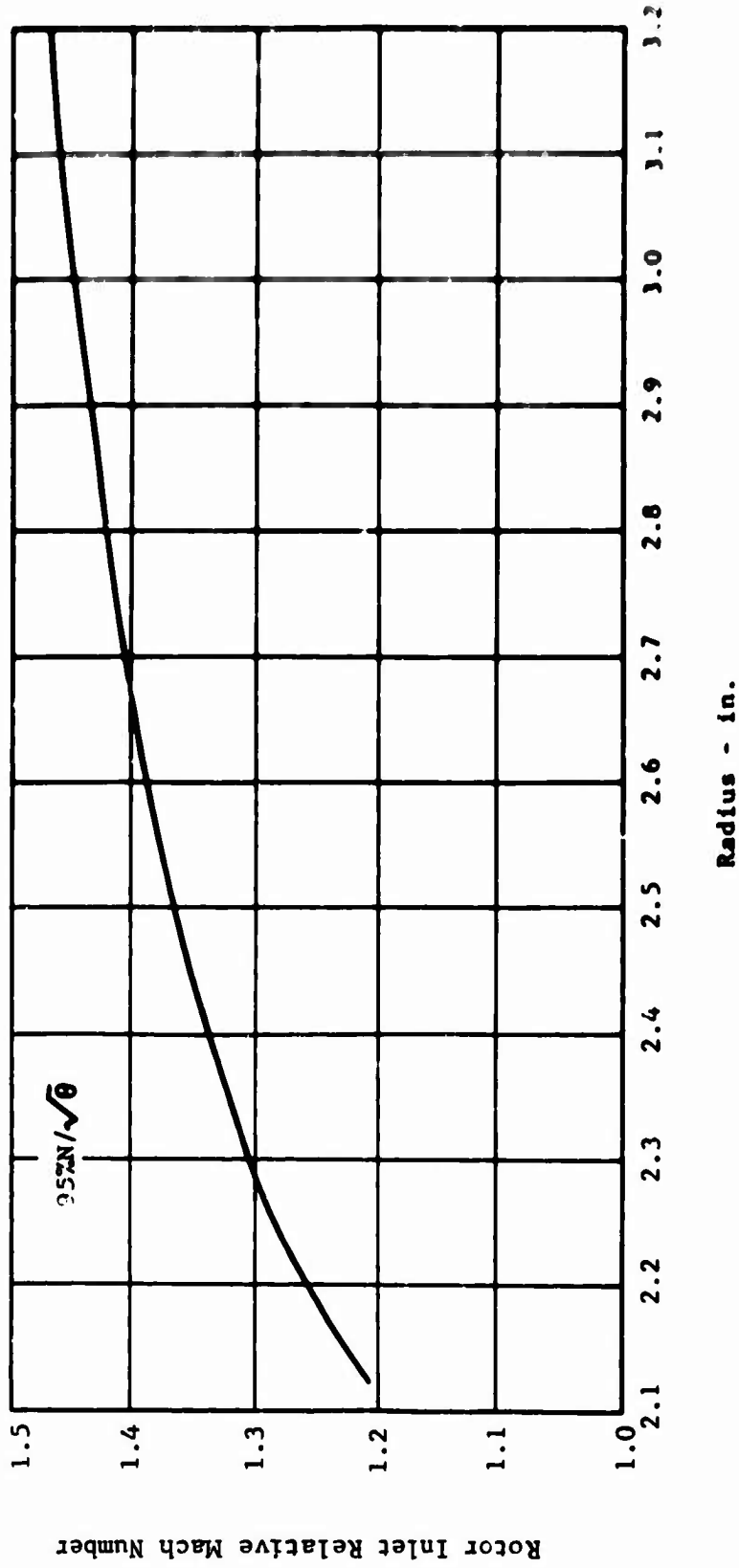


Figure 34. Rotor Relative Inlet Mach Number, Build 3.

2.8:1 Supersonic Compressor Performance Design IGV Setting

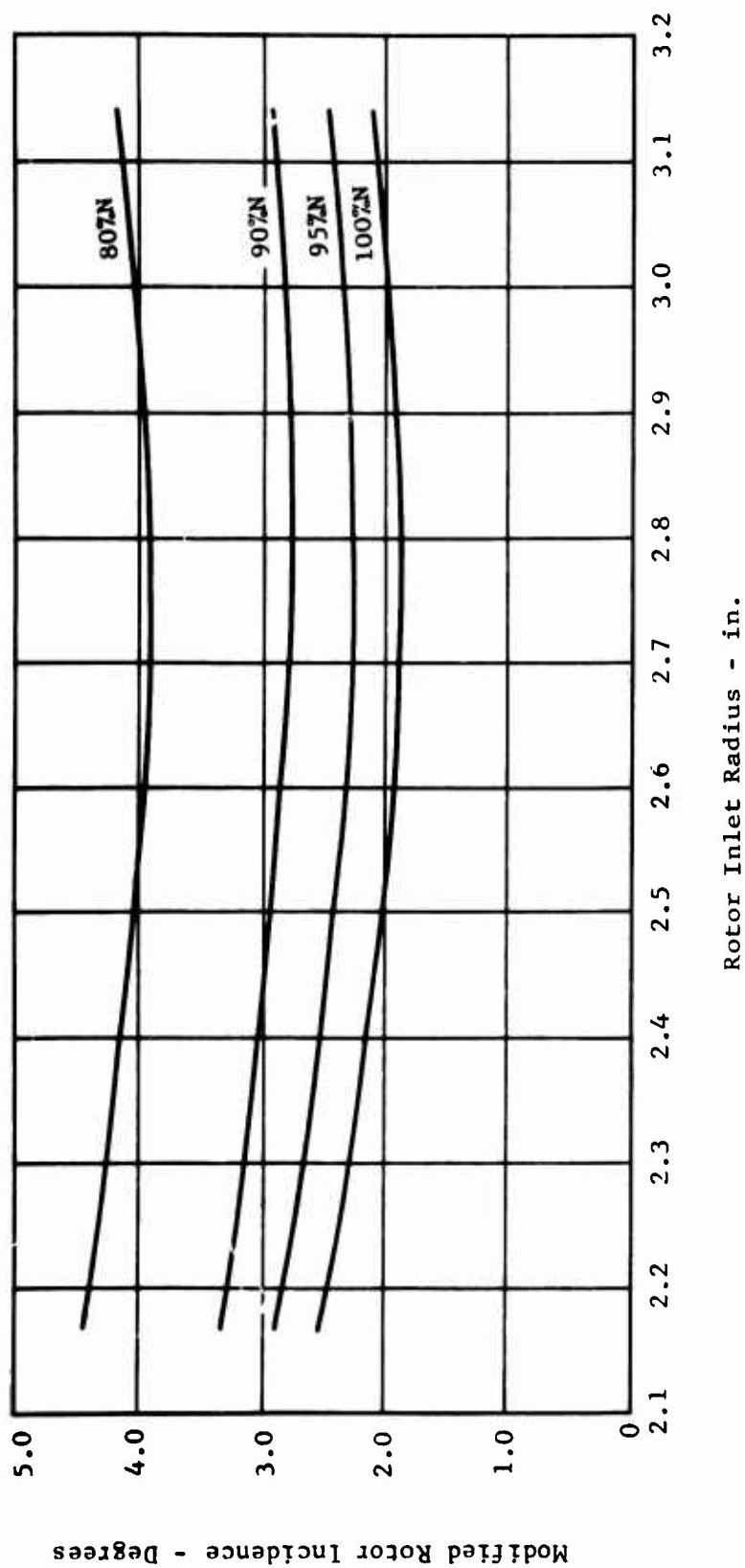


Figure 35. Modified Rotor Incidence Angle Versus Radius, Build 3.

tip does not change significantly with speed, but the level of incidence does. Figure 36 presents the variation of rotor incidence with speed.

Rotor Exit Conditions and Deviation

The rotor exit total pressure and temperature profiles at the 100 percent speed peak pressure ratio point for build 3 (design inlet guide vane setting) are presented in Figure 37. These profiles are based on the fixed probe data since valid total pressure traverse data could not be obtained at this point. The temperature trend agrees closely with the design case. The absolute temperature level cannot be compared directly with the design case since the experimental inlet temperature is 15.7 degrees Rankine lower than standard. The total pressure profile indicates a somewhat higher hub pressure, but a lower tip pressure, than design. The experimental barometer was .09 inch of mercury below standard; therefore, measured performance is slightly more favorable than the direct comparison indicates. The tip total pressure, however, is clearly deficient compared to the design; this is attributed primarily to the higher tip clearance and cut-back blades in build 3.

The rotor exit absolute tangential flow angles (α_4) for the 100 percent speed peak pressure ratio point are presented in Figure 38. Both the measured traverse probe data and the results of the data analysis computer run are compared to the design case. The exit flow angles are not too sensitive to local back-pressure effects, and the traverse probe angle data are considered to be valid. The traverse data and the computer results are in good agreement, since a maximum difference of 4.0 degrees and an average difference of 2.0 degrees are indicated. The air angles measured in the rotor testing are approximately 3.5 to 6.5 degrees below the design angles, but some increase in angle will accompany the expected increase in performance in the stage tests. The leading-edge wedge angle of the exit stator is 6 degrees; and even though the average incidence angle indicated by the measured air angles is 5 degrees below the design incidence of +3 degrees, a positive flow incidence to the compression surface is still indicated. On this basis, the exit guide vane design is expected to provide acceptable performance over the possible range of incidence angles and leaves some margin for improved rotor performance. The rotor exit deviation angle data are presented in Figure 39. The measured mean exit metal angles are also presented in this figure. The deviation angles are based on the relative air angles from the data analysis program. The mean metal angles are within 0.8 degree of the design values at the hub and mean blade sections, but the mean angle at the tip is 1.3 degrees low. The data indicate a deviation angle which ranges from 0.5 to 3.0 degrees compared to design values from 4.8 to 6.0 degrees. Figure 40 indicates that the average rotor relative exit air angle at peak pressure ratio remained relatively constant with speed.

Vector Diagrams

Figures 41 through 44 present the vector diagrams for builds 2 and 3. The vector diagrams of the 100 percent speed peak pressure ratio data point for

2.8:1 Supersonic
Rotor Test Build 3
Design IGV Setting

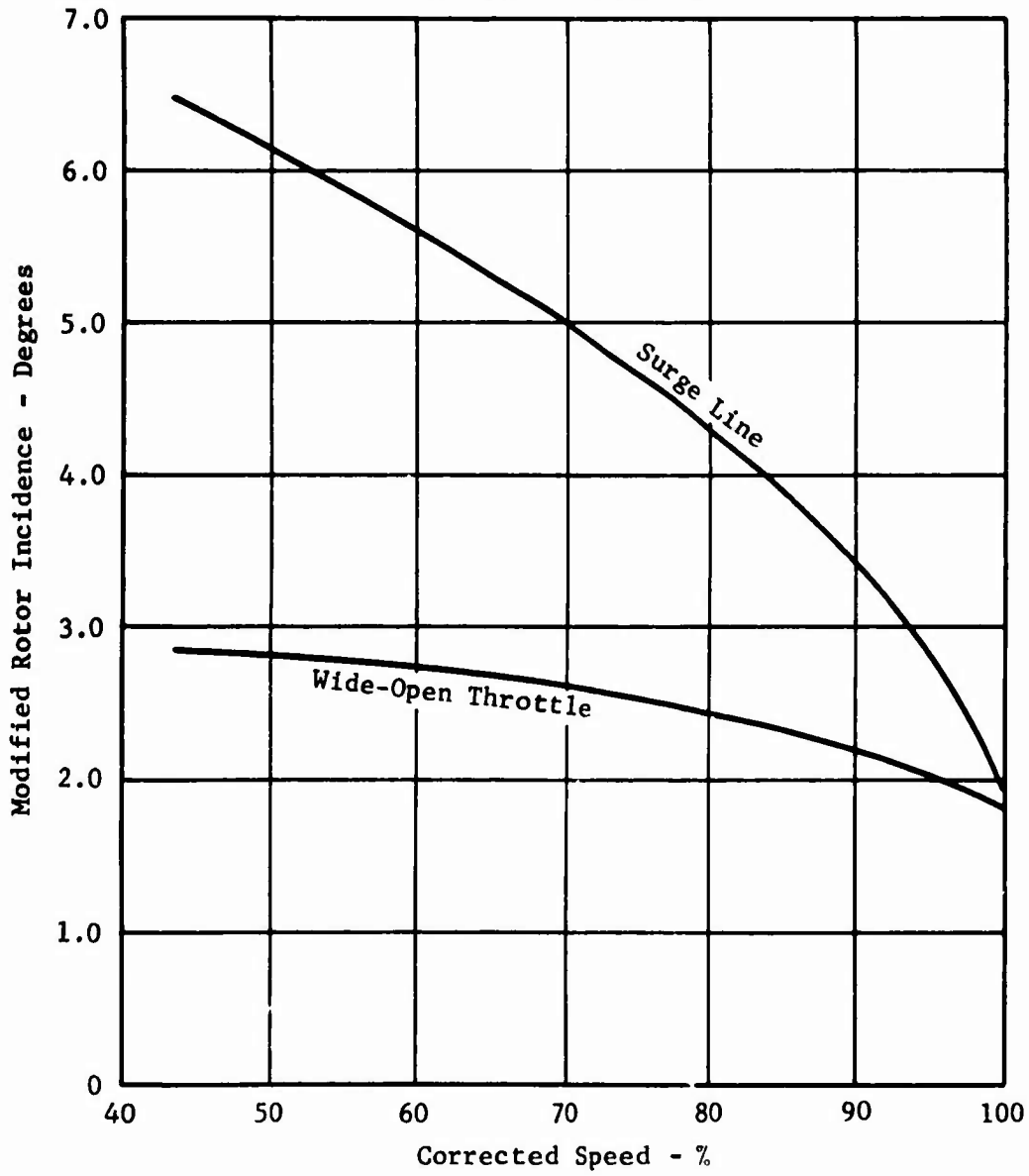


Figure 36. Variation of Modified Rotor Incidence With Speed.

2.8:1 Supersonic Compressor Rotor Test
 Design IGV Setting
 $100\%N/\sqrt{\theta}$
 $(W\sqrt{\theta})/B = 4.006$
 Pressure Ratio = 2.775

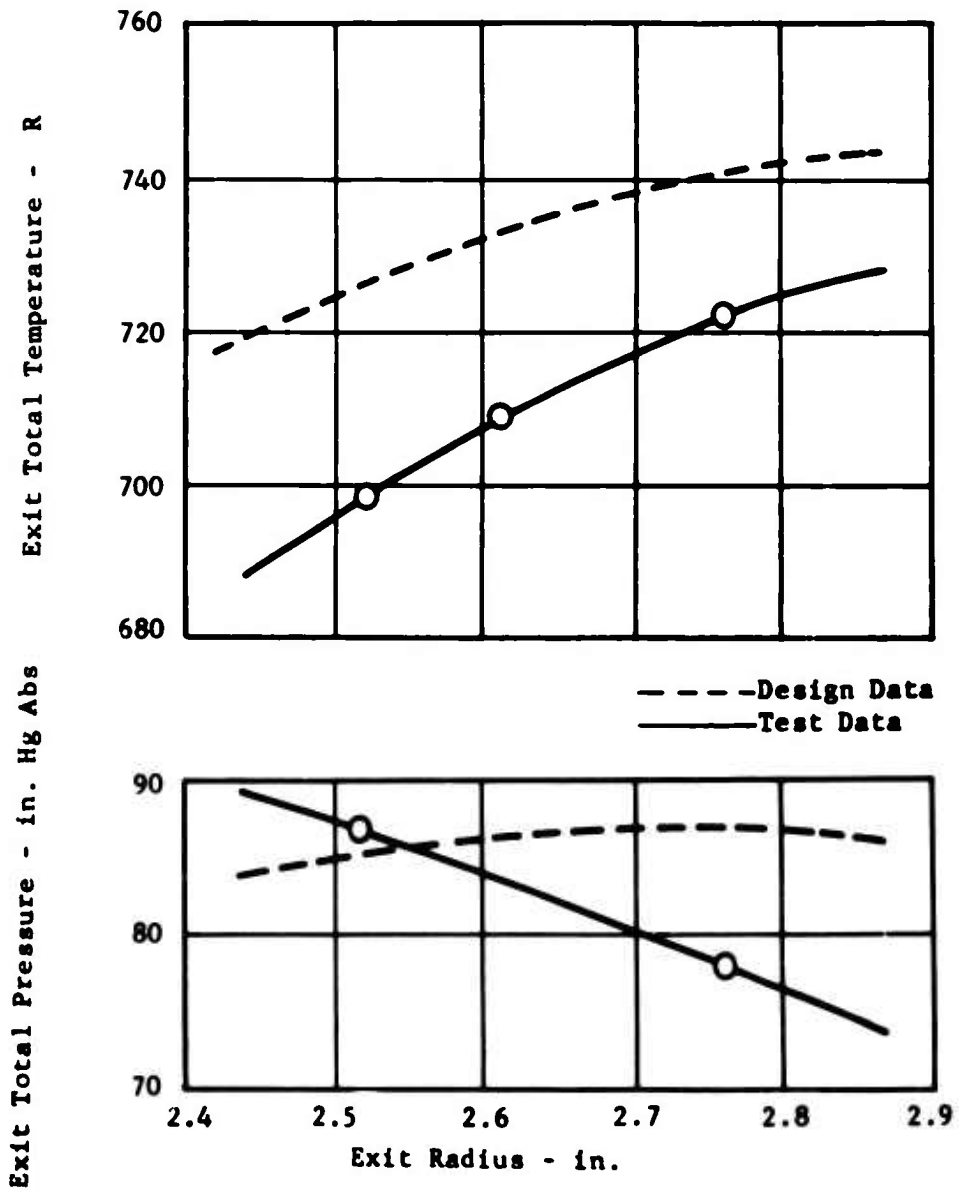


Figure 37. Build 3 Total Pressure and Temperature Profiles at Rotor Exit.

2.8:1 Supersonic Compressor Rotor Test

100%N/ $\sqrt{\theta}$

Peak Pressure Ratio

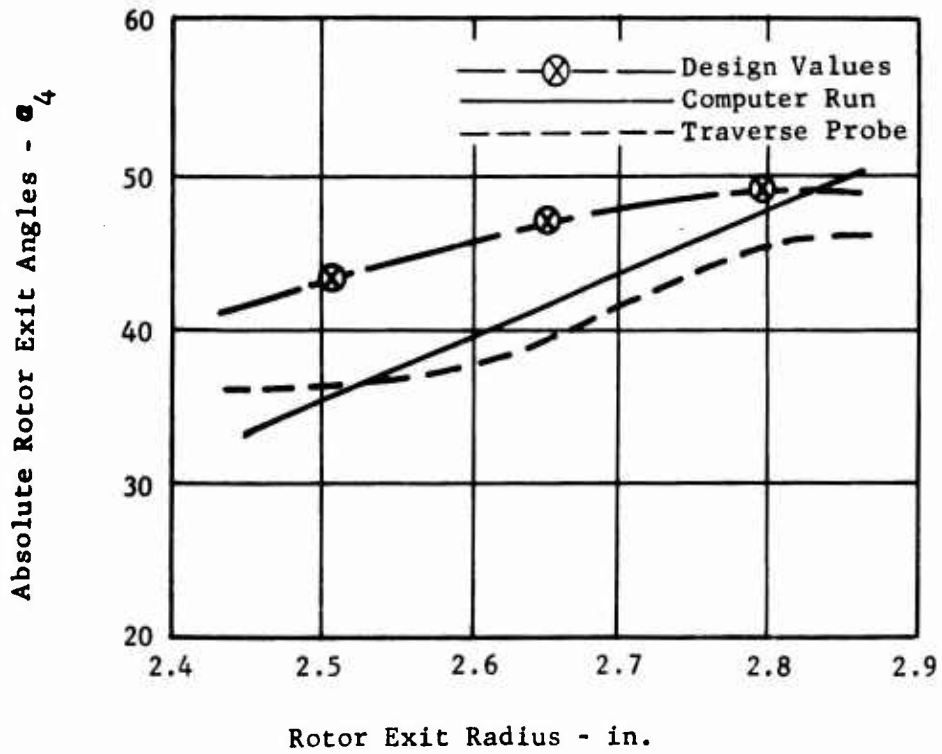


Figure 38. Build 3 Rotor Exit Absolute Flow Angles.

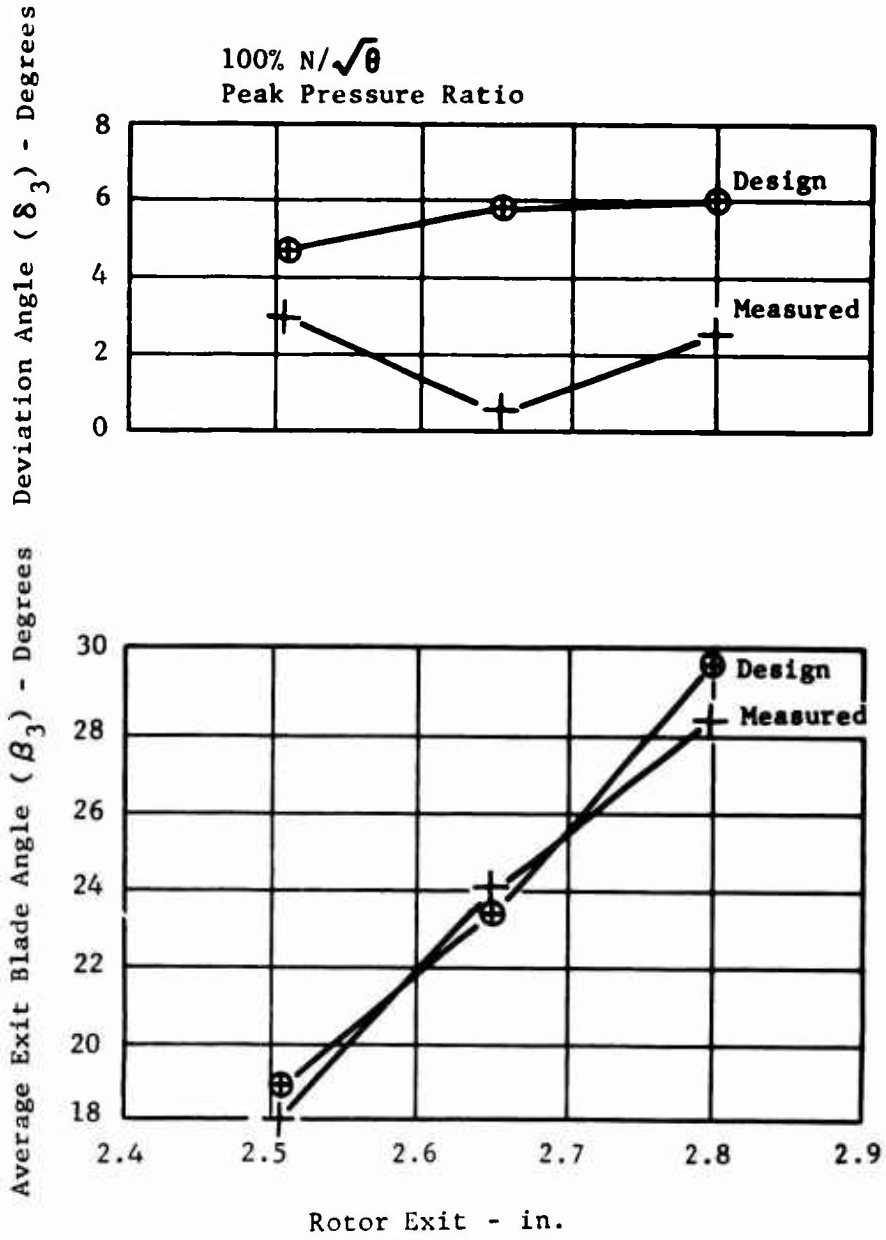


Figure 39. Build 3 Rotor Exit Deviation Angles.

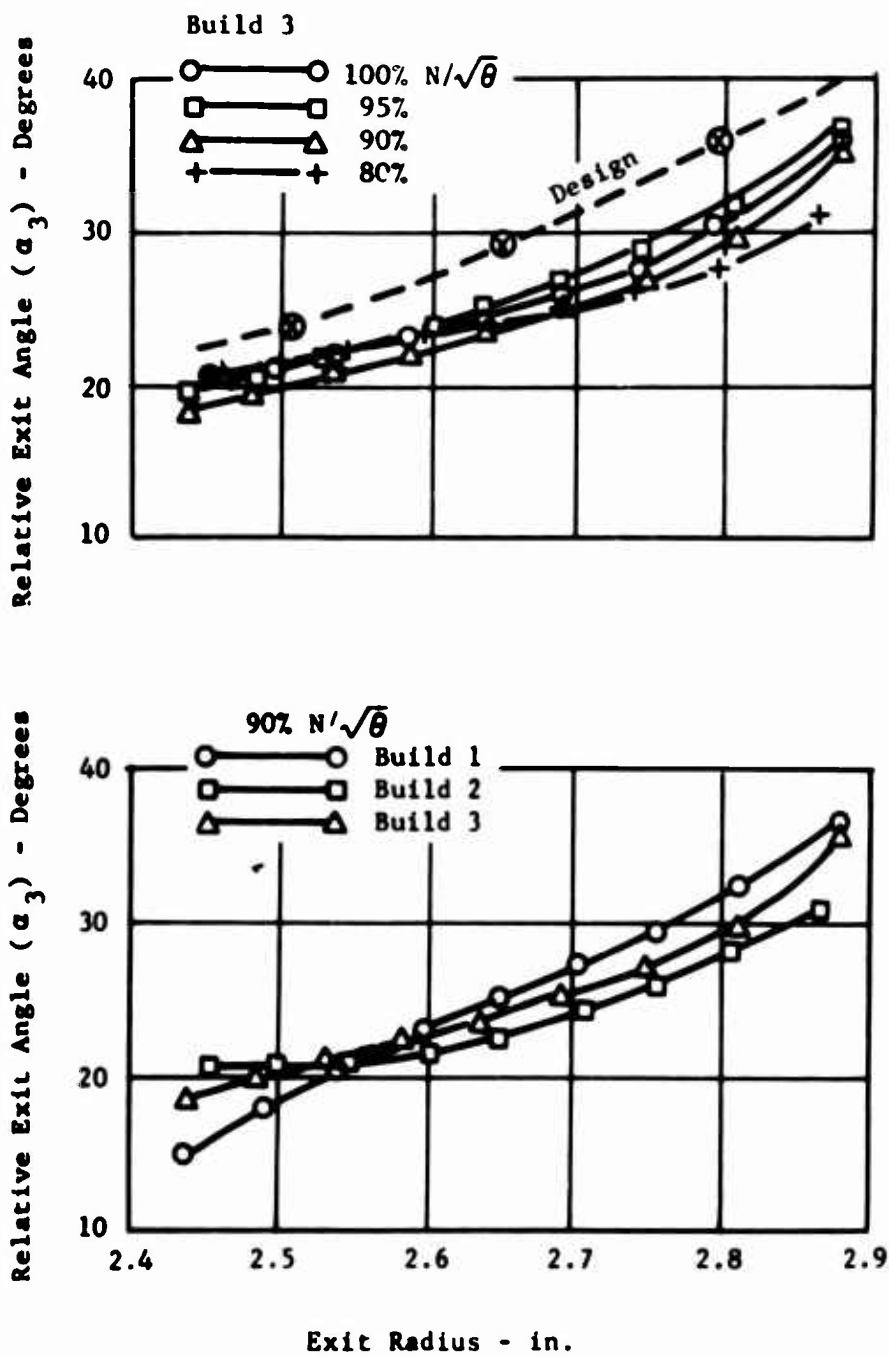


Figure 40. Effects of Speed and Build Configuration on Relative Exit Angle.

$$90\%N/\sqrt{\theta}$$

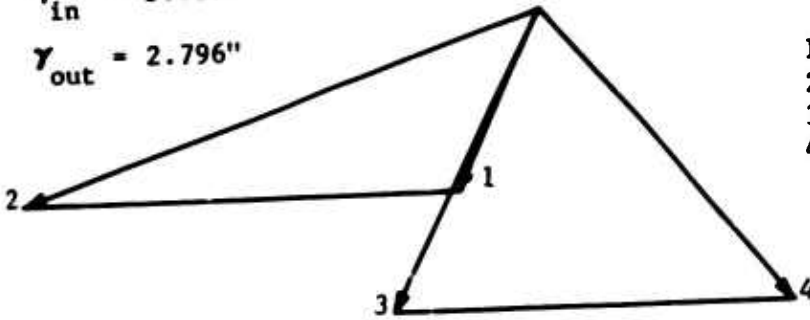
$$(W\sqrt{\theta})/8$$

$$\text{Pressure Ratio} = 2.31$$

Tip Stream Tube

$$Y_{in} = 3.017''$$

$$Y_{out} = 2.796''$$

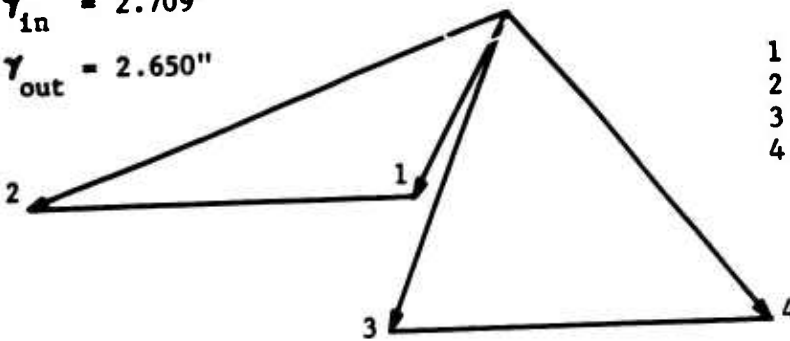


	V	α	M
1	528	26.4	.495
2	1488	71.5	1.396
3	890	28.0	.757
4	1035	40.6	.880

Mid Stream Tube

$$Y_{in} = 2.709''$$

$$Y_{out} = 2.650''$$

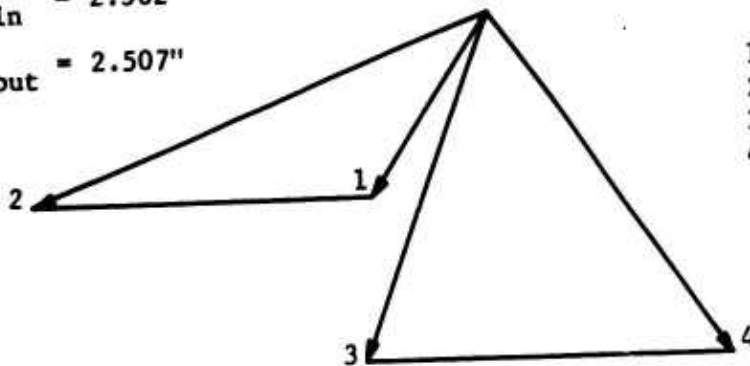


	V	α	M
1	547	29.6	.514
2	1409	70.3	1.324
3	904	22.7	.776
4	1079	39.4	.927

Hub Stream Tube

$$Y_{in} = 2.362''$$

$$Y_{out} = 2.507''$$



	V	α	M
1	564	34.4	.531
2	1324	69.4	1.246
3	969	20.8	.845
4	1104	35.0	.964

Figure 41. Build 2 Vector Diagrams for 90 Percent Speed.

$$100\%N/\sqrt{\theta}$$

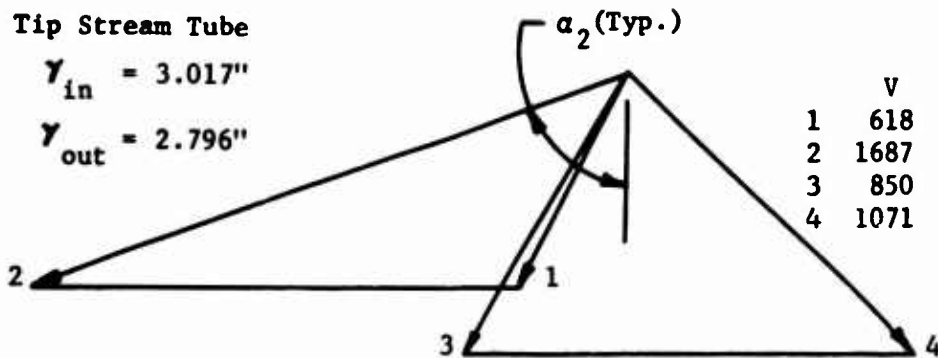
$$(W\sqrt{\theta})/8 = 4.006 \text{ lb/sec}$$

$$\text{Pressure Ratio} = 2.775$$

Tip Stream Tube

$$r_{in} = 3.017''$$

$$r_{out} = 2.796''$$

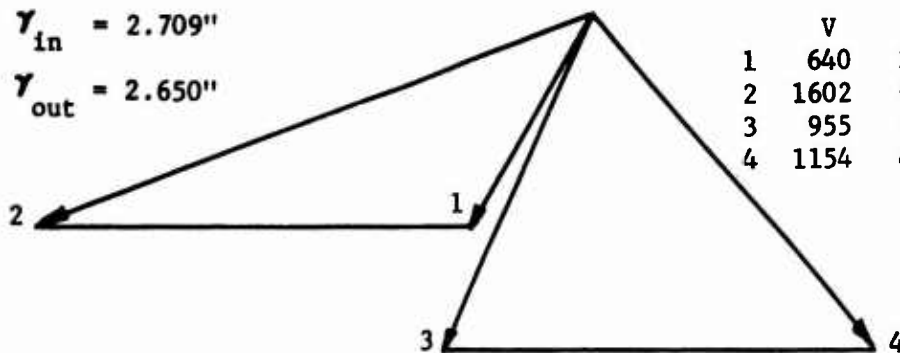


	V	α	M
1	618	26.9	.580
2	1687	71.0	1.586
3	850	30.9	.691
4	1071	47.1	.871

Mid Stream Tube

$$r_{in} = 2.709''$$

$$r_{out} = 2.650''$$

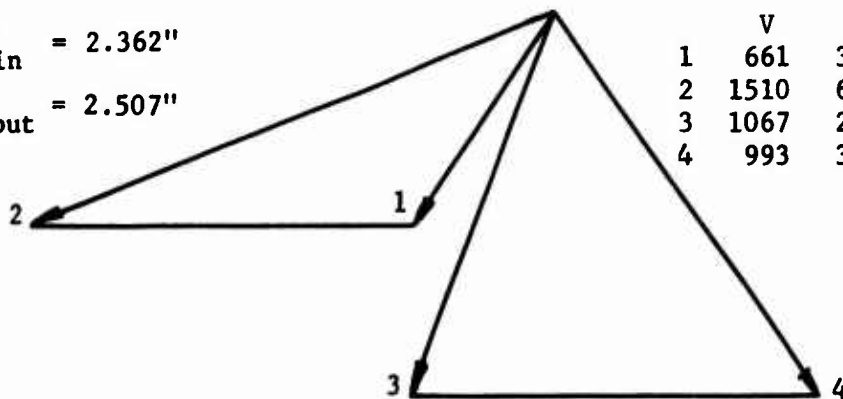


	V	α	M
1	640	30.1	.602
2	1602	69.8	1.508
3	955	24.5	.794
4	1154	41.2	.960

Hub Stream Tube

$$r_{in} = 2.362''$$

$$r_{out} = 2.507''$$



	V	α	M
1	661	34.9	.624
2	1510	69.0	1.425
3	1067	21.4	.909
4	993	35.4	1.037

Figure 42. Build 3 Vector Diagrams for 100 Percent Speed.

$$957N/\sqrt{\theta}$$

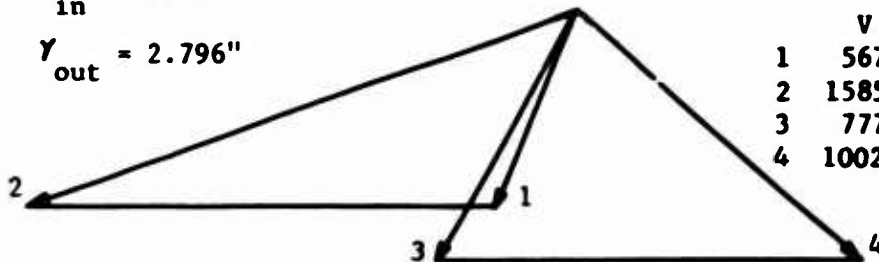
$$(W\sqrt{g})/8 = 3.799 \text{ lb/sec}$$

$$\text{Pressure Ratio} = 2.539$$

Tip Stream Tube

$$\gamma_{in} = 3.017''$$

$$\gamma_{out} = 2.796''$$

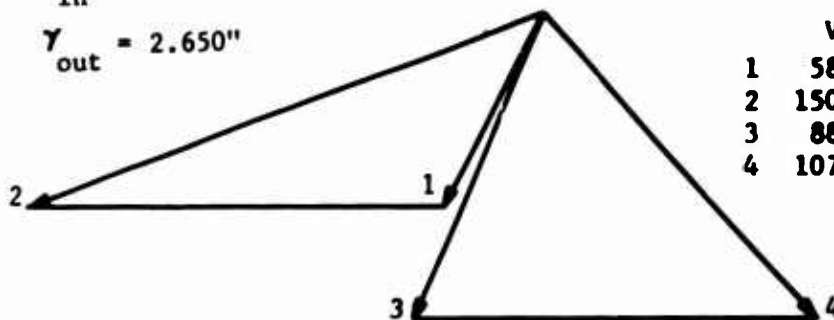


	v	a	M
1	567	26.6	.530
2	1585	71.3	1.446
3	777	31.4	.638
4	1002	48.6	.823

Mid Stream Tube

$$\gamma_{in} = 2.709''$$

$$\gamma_{out} = 2.650''$$

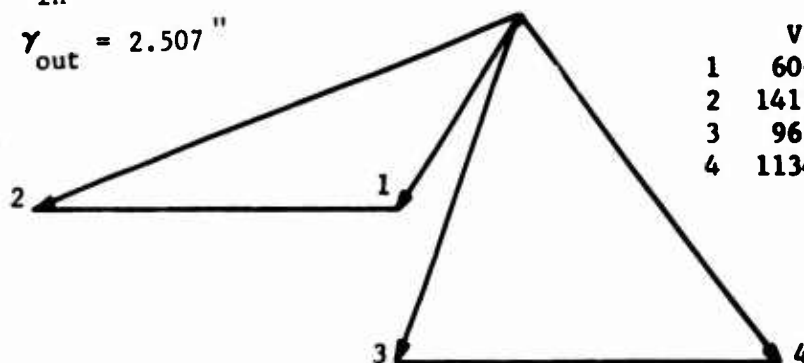


	v	a	M
1	586	29.8	.549
2	1500	70.2	1.405
3	882	25.2	.739
4	1075	42.1	.901

Hub Stream Tube

$$\gamma_{in} = 2.362''$$

$$\gamma_{out} = 2.507''$$



	v	a	M
1	606	34.6	.568
2	1412	69.3	1.325
3	967	21.1	.825
4	1134	37.4	.968

Figure 43. Build 3 Vector Diagrams for 95 Percent Speed.

$$90\%N/\sqrt{\theta}$$

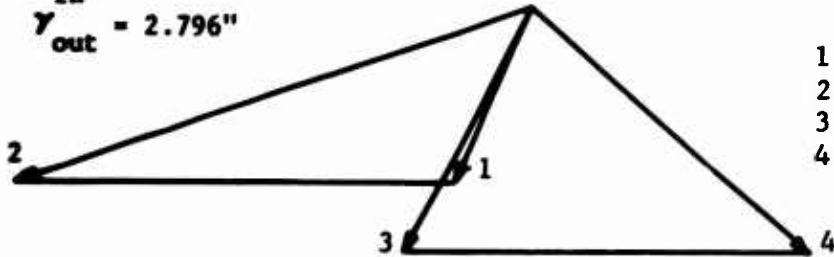
$$(W\sqrt{\theta})/8 = 3.551 \text{ lb/sec}$$

$$\text{Pressure Ratio} = 2.28$$

Tip Stream Tube

$$\gamma_{in} = 3.017''$$

$$\gamma_{out} = 2.796''$$

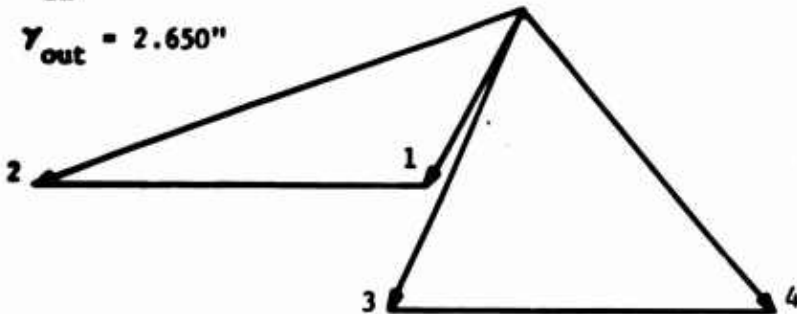


	V	α	M
1	515	26.3	.480
2	1481	71.8	1.381
3	735	29.0	.612
4	978	48.9	.814

Mid Stream Tube

$$\gamma_{in} = 2.709''$$

$$\gamma_{out} = 2.650''$$

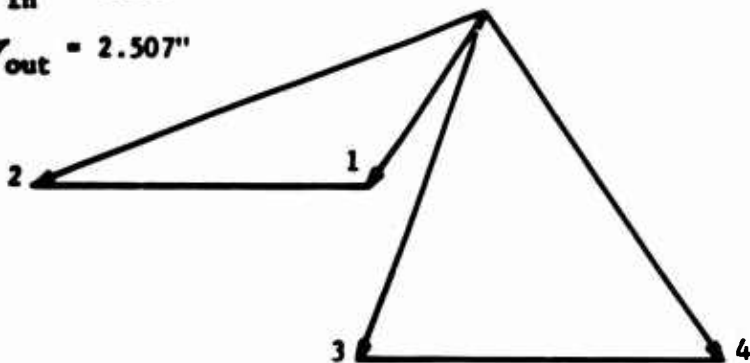


	V	α	M
1	532	29.5	.497
2	1400	70.7	1.307
3	859	23.9	.731
4	1044	41.2	.888

Hub Stream Tube

$$\gamma_{in} = 2.362''$$

$$\gamma_{out} = 2.507''$$



	V	α	M
1	549	34.4	.514
2	453	69.8	1.229
3	944	20.2	.818
4	1101	36.4	.954

Figure 44. Build 3 Vector Diagrams for 90 Percent Speed.

build 3 are presented in Figure 42. The inlet vectors for this point are in good agreement with the design case. The exit vectors indicate higher exit Mach numbers than design for both the absolute and relative legs (vectors 4 and 3, respectively). These higher Mach numbers reflect a lower static pressure rise than the design value. It is suspected that the circumferential variation in back-pressure level caused a premature stall which prevented achievement of the design static pressure rise during the rotor testing. The hub absolute Mach number is indicated as slightly above sonic, but the relative vector is subsonic. The excessively high hub Mach number is also considered to be related to the nonuniform back-pressure level.

Figures 45, 46, and 47 present the vector diagrams for builds 4 and 5 (inlet guide vane settings of 6 degrees closed and 8 degrees open, respectively).

Rotor Passage Recovery

Figure 48 compares the rotor passage recovery from the build 3, 100 percent speed peak pressure ratio point with the design Mach number recovery. The average recovery meets the design recovery, but it is higher at the hub and lower at the tip than predicted. The predicted design recoveries included adjustment factors of 1.01 at the hub streamtube and 0.99 at the tip streamtube which accounted for the effects of the boundary layer being centrifuged to the tip and the tip clearance losses. The resulting data indicate that a more extreme variation in these factors from hub to tip exists. The data establish a hub streamtube factor of 1.09 and a tip streamtube factor of 0.89. A higher tip streamtube factor such as 0.91 is justified as a design criterion since the tip clearance for build 3 was higher than required.

6° Closed IGV Setting

100%N/√θ

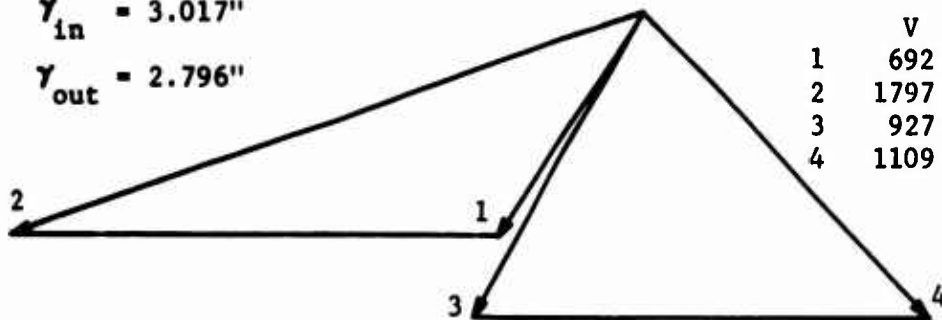
$(W\sqrt{\theta})/\theta = 4.021 \text{ lb/sec}$

Pressure Ratio = 2.782

Tip Stream Tube

$\gamma_{in} = 3.017''$

$\gamma_{out} = 2.796''$

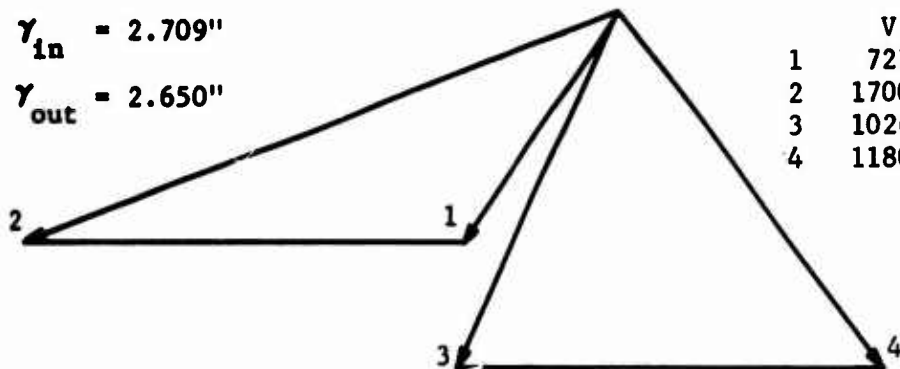


	V	α	M
1	692	33.0	.650
2	1797	71.2	1.689
3	927	30.0	.742
4	1109	43.6	.888

Mid Stream Tube

$\gamma_{in} = 2.709''$

$\gamma_{out} = 2.650''$

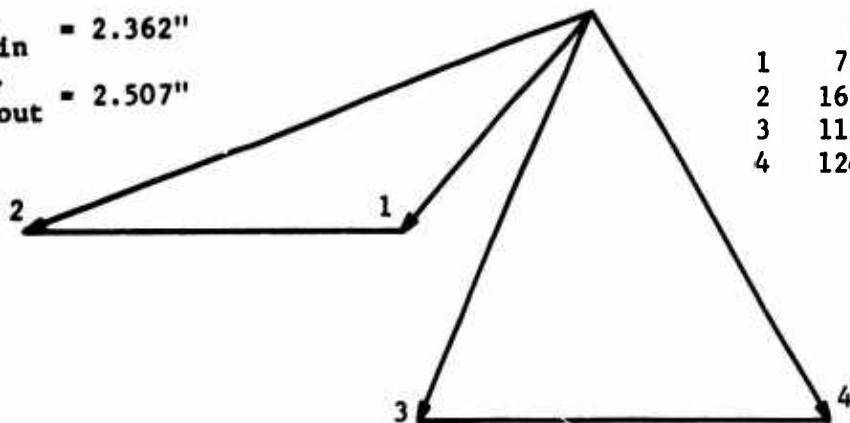


	V	α	M
1	721	33.9	.680
2	1700	69.4	1.604
3	1026	25.1	.843
4	1180	38.1	.971

Hub Stream Tube

$\gamma_{in} = 2.362''$

$\gamma_{out} = 2.507''$



	V	α	M
1	754	41.0	.714
2	1633	69.6	1.547
3	1158	23.1	.975
4	1246	31.3	1.050

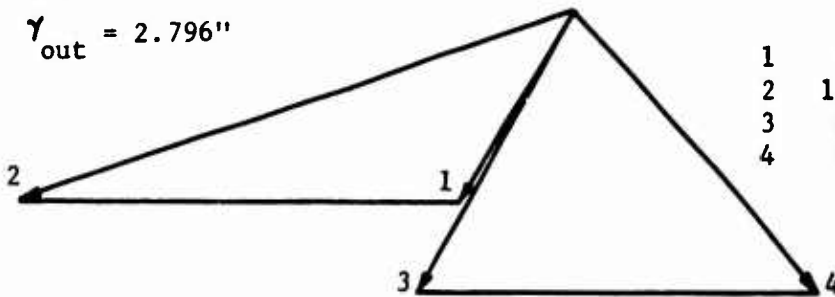
Figure 45. Build 4 Vector Diagrams for 100 Percent Speed.

6° Closed IGV Setting
 90%N/ $\sqrt{\theta}$
 $(W\sqrt{\theta})/8 = 3.694$ lb/sec
 Pressure Ratio = 2.396

Tip Stream Tube

$\gamma_{in} = 3.017''$

$\gamma_{out} = 2.796''$

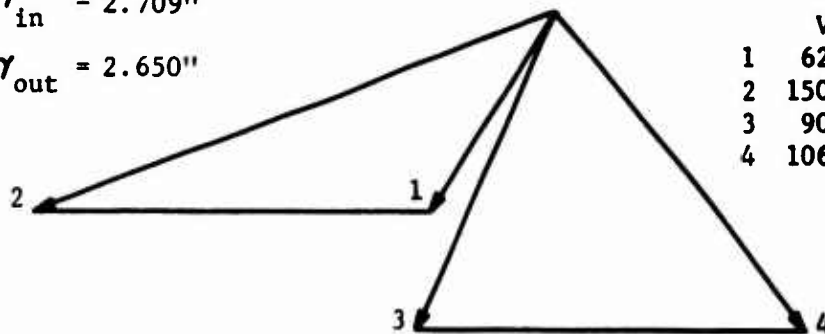


	V	α	M
1	595	32.5	.554
2	1591	71.6	1.480
3	864	31.1	.711
4	988	41.6	.814

Mid Stream Tube

$\gamma_{in} = 2.709''$

$\gamma_{out} = 2.650''$

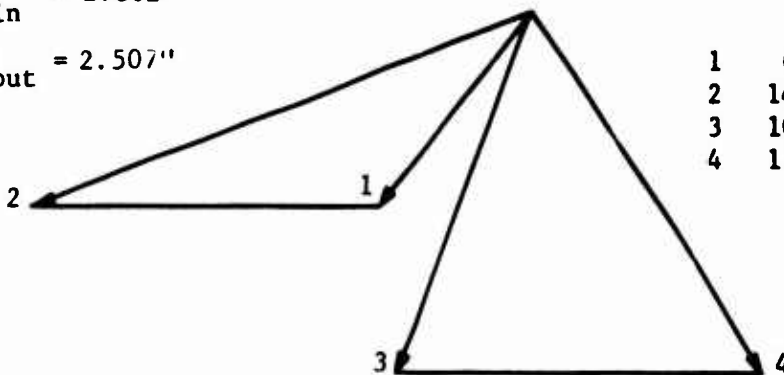


	V	α	M
1	620	33.4	.578
2	1501	69.9	1.400
3	906	24.3	.758
4	1065	39.2	.891

Hub Stream Tube

$\gamma_{in} = 2.362''$

$\gamma_{out} = 2.507''$



	V	α	M
1	647	40.4	.605
2	1438	70.0	1.345
3	1016	21.6	.867
4	1128	33.1	.963

Figure 46. Build 4 Vector Diagrams for 90 Percent Speed.

8° Open IGV Setting

$90\%N/\sqrt{\theta}$

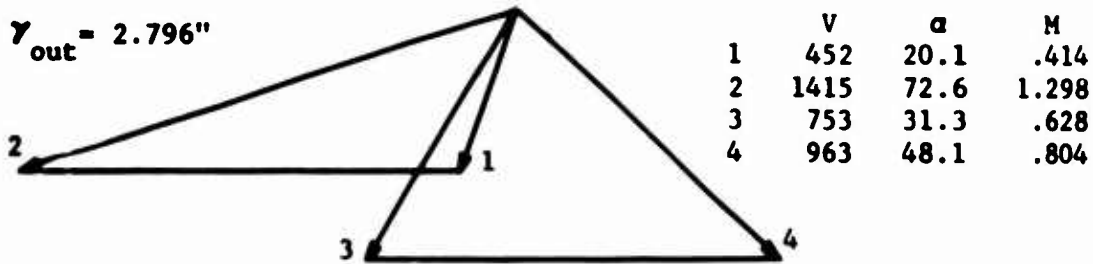
$(W\sqrt{\theta})/8 = 3.36 \text{ lb/sec}$

Pressure Ratio = 2.178

Tip Stream Tube

$r_{in} = 3.017''$

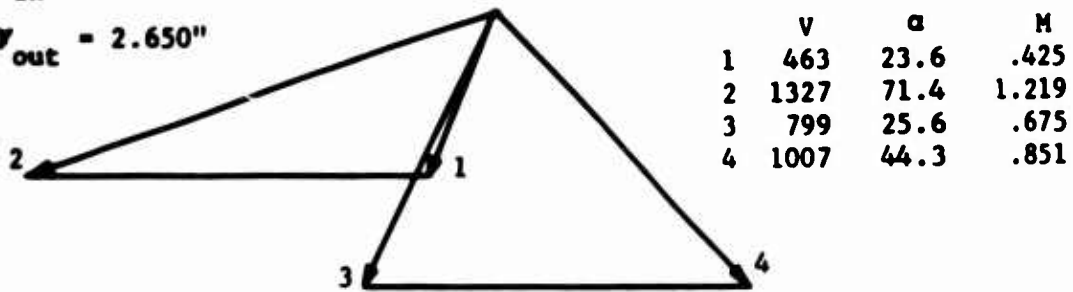
$r_{out} = 2.796''$



Mid Stream Tube

$r_{in} = 2.709''$

$r_{out} = 2.650''$



Hub Stream Tube

$r_{in} = 2.362''$

$r_{out} = 2.507''$

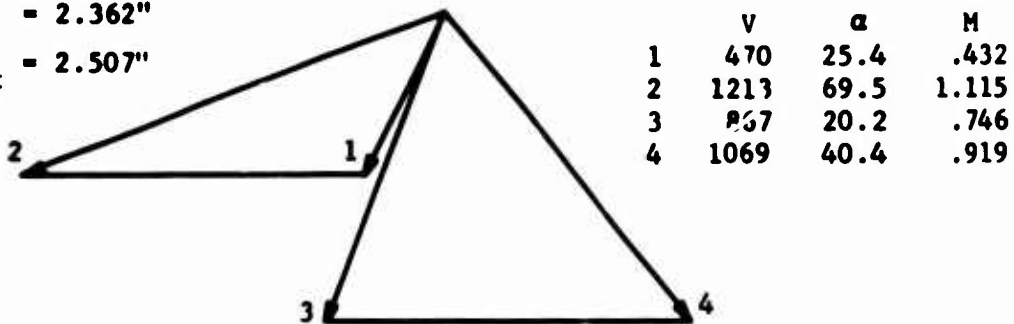


Figure 47. Build 5 Vector Diagrams for 90 Percent Speed.

2.8:1 Supersonic Compressor Rotor Test

Design IGV Setting

- — — — — Build 1
- - - - - Build 2
- — — — — Build 3

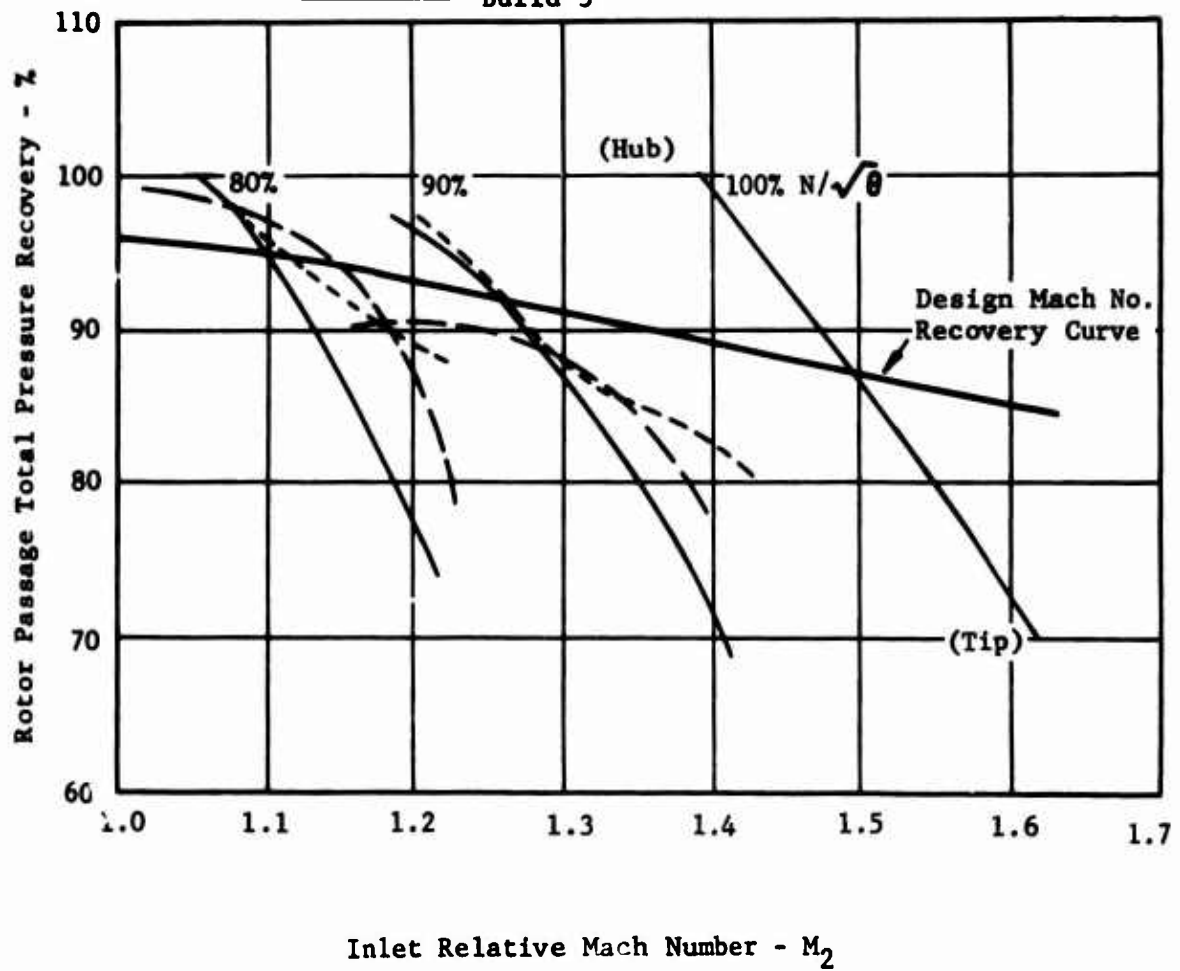


Figure 48. Rotor Passage Total Pressure Recovery.

CONCLUSIONS

The analysis of the test results for the rotor development phase led to the following conclusions:

1. The inlet guide vane and rotor blade design tested in builds 2 and 3 can meet the rotor performance goals when tested with a static tip clearance of .009 to .012 inch under uniform circumferential back-pressure conditions.
2. The demonstrated rotor performance approaches closely the performance goals, and further optimization would be accomplished best in the Phase III stage development tests. The circumferential variation in back-pressure level and the influence of the traversing probe on the local back-pressure level are conditions associated with the rotor testing which prevent a complete performance evaluation.
3. A modified incidence angle of 2.3° has been established as the design criterion for this compressor rotor.
4. The rotor passage recovery data confirm the design Mach number recovery curve.
5. The data indicate that hub and tip streamtube recovery factors of 1.09 and 0.91 respectively should be used for design purposes instead of the 1.01 and 0.99 used in the initial design.
6. The exit stator design should be based on the design rotor exit absolute flow angles. The measured rotor exit flow angles are an average of 5 degrees and a maximum of 6.5 degrees below the design values. These measured angles do not represent any significant negative incidence to the compression surface of the design stator angles and provide some margin for increases in rotor exit angles which will accompany expected increases in rotor performance.

APPENDIX I

PHASE II TEST PLAN

OBJECTIVE

The objective of the rotor development program is to evaluate the combined inlet guide vanes and rotor performance of the 2.8:1 single-stage supersonic compressor design through experimental testing, data analysis, and design modifications. The performance goals for the inlet guide vanes and rotor are:

Pressure Ratio	2.89:1
Adiabatic Efficiency	85.2%
Weight Flow	4.0 lb/sec
Design Speed	50,700 rpm

APPROACH

The inlet guide vane performance for this compressor has been established independently of the rotor by a flow test program using an external air supply. These data will be used in the analysis of the combined inlet guide vane and rotor data.

The first step in the program will be to develop a compressor map between 40 and 100 percent speed by obtaining experimental data for the initial design configuration with the inlet guide vanes at their design setting. Compressor maps will also be developed between 70 and 100 percent speed for two other inlet guide vane settings. Complete temperature and pressure data will be recorded during the testing.

The data points in the 90 to 100 percent speed range, which represent peak pressure ratio and peak efficiency, will be analyzed to establish vector diagrams that satisfy the experimental data. The experimental vector diagrams will be compared to the design conditions to pinpoint deficient areas.

Based on the results of the data analysis, design modifications will be established. These modifications will be incorporated in the compressor hardware by machining, blade bending, and similar means.

An experimental map for the modified configuration will be developed at the optimum guide vane setting, and the cycle will be repeated. At least two compressor builds are estimated for this series.

A redesign is planned after the first series of tests to correct deficiencies which require modifications beyond the limits of reworking the existing hardware. It is expected that the key design modifications will be established in the first test series.

A second test series will be conducted with the redesigned component or components in the same manner as the first test series. Three builds

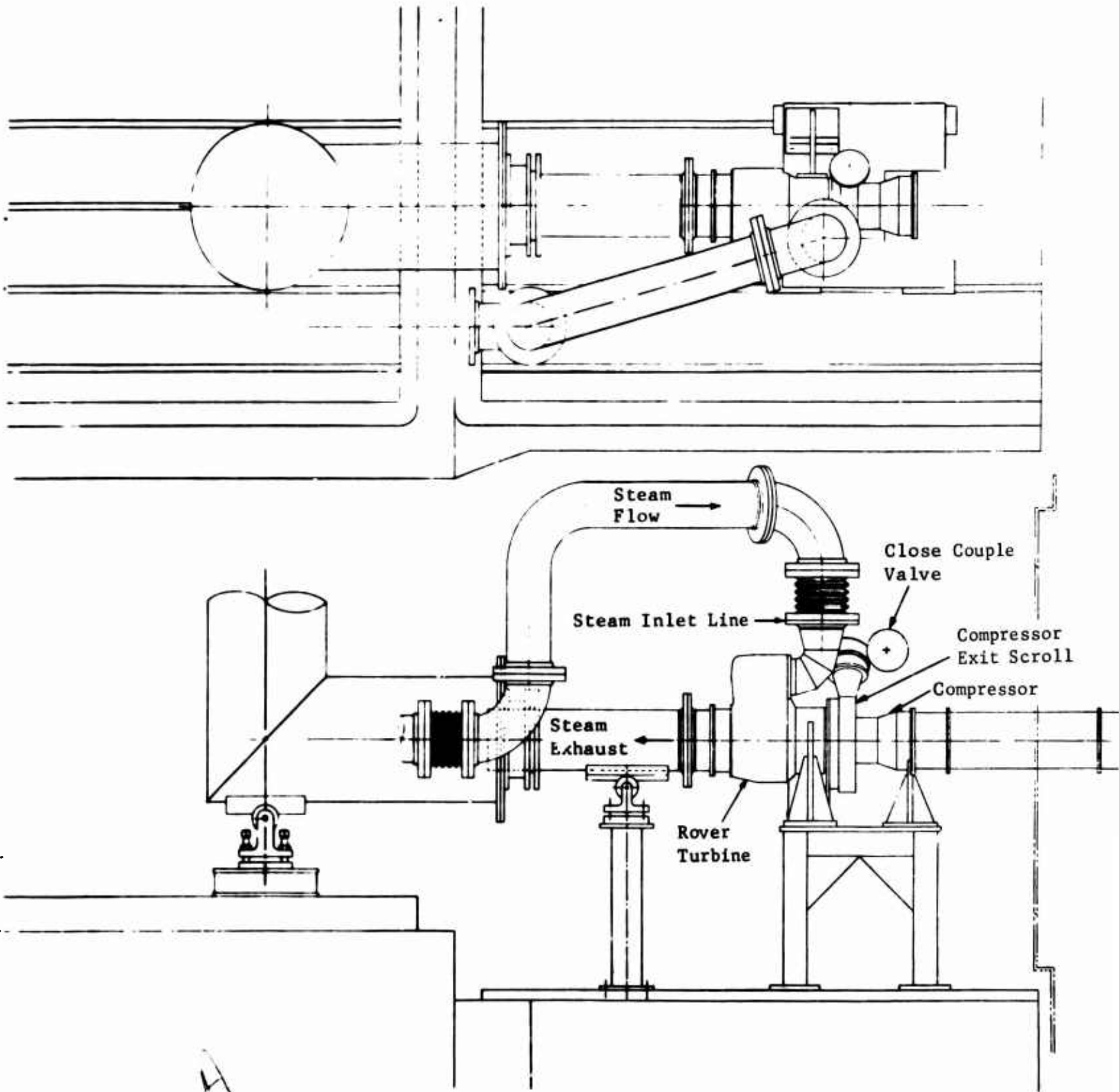
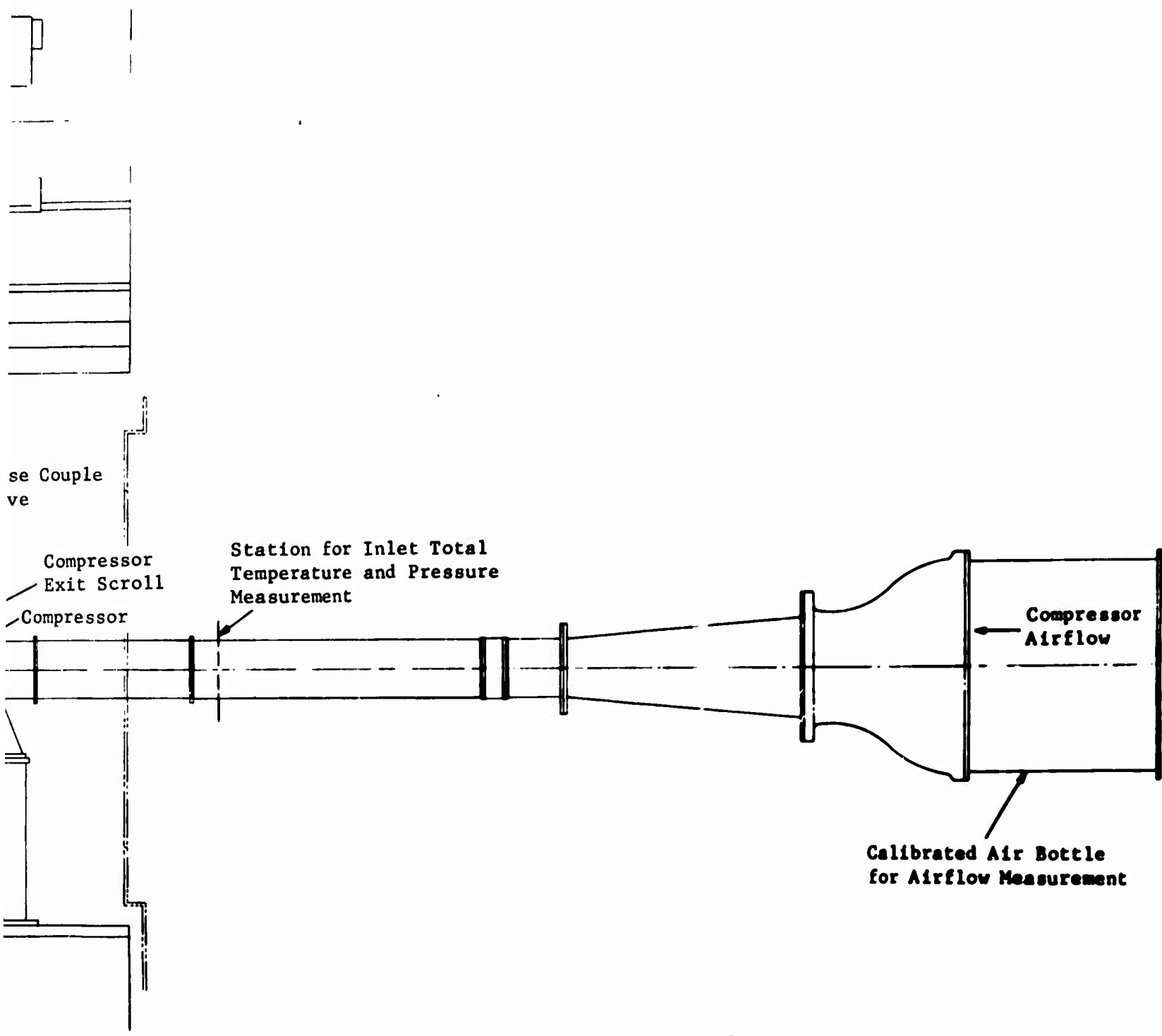


Figure 49. Compressor Test Rig Installation.



se Couple
ve

Compressor
Exit Scroll
Compressor

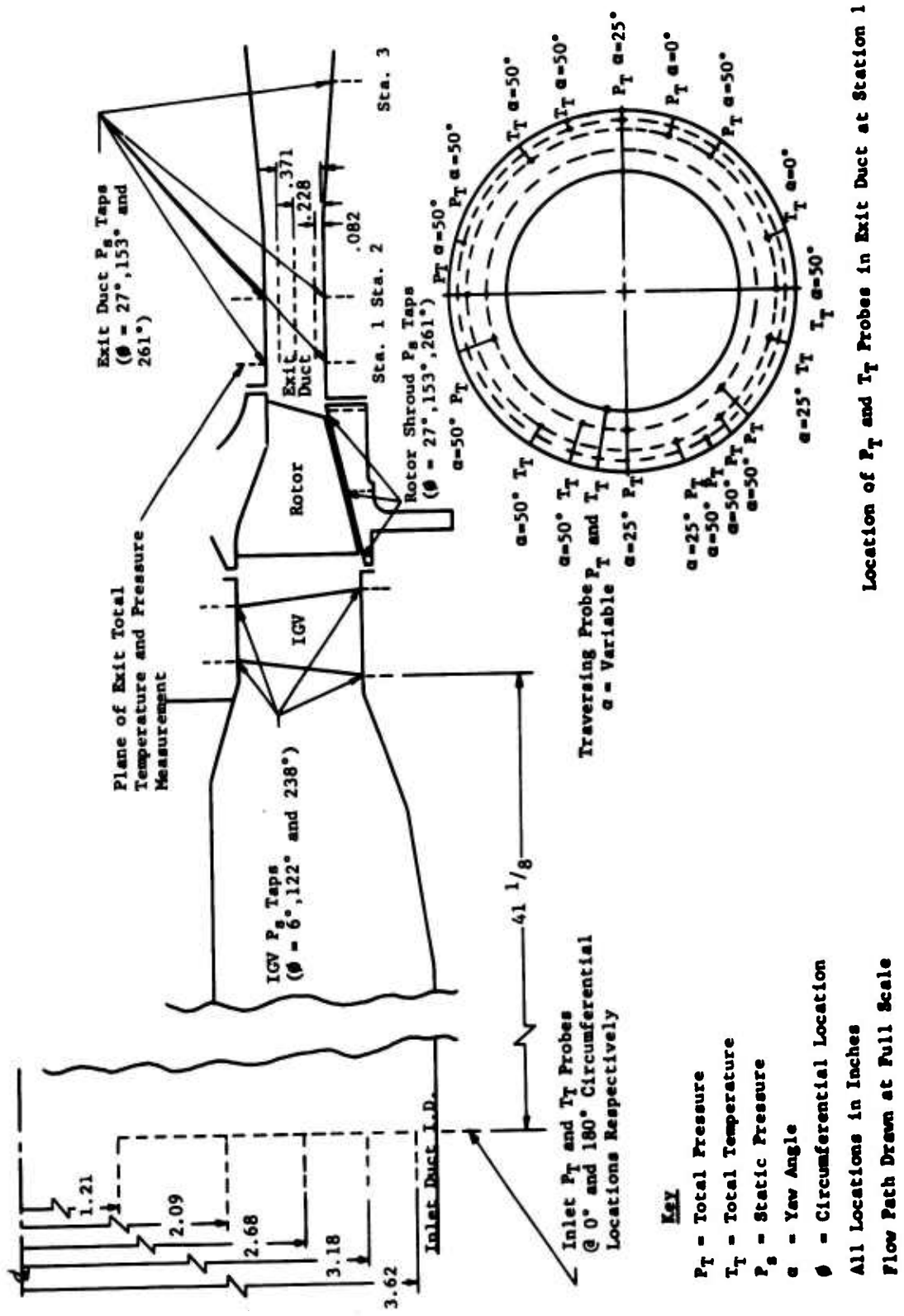
Station for Inlet Total
Temperature and Pressure
Measurement

Compressor
Airflow

Calibrated Air Bottle
for Airflow Measurement

R

BLANK PAGE



Location of P_T and T_T Probes in Exit Duct at Station 1

Figure 50. Schematic of Rotor Test Pressure and Temperature Instrumentation.

are estimated for the second series in which final hardware modifications will be made. A complete compressor map will be developed between 40 and 100 percent for the final configuration.

TEST CONFIGURATION

Compressor

- a. The compressor build will include the inlet guide vanes and the 2.8:1 pressure ratio rotor but no exit stators or interconnecting duct. The compressor will be mounted to and powered by the steam-driven Rover turbine on test stand WX25R (see Figures 49 and 50).
- b. The inlet guide vanes will be set in the zero position. (design setting) initially, but repositioning may be required as indicated by the test results.
- c. The rotor blade clearance will be set at .010 inch for the initial build. This setting is expected to result in a .002- to .003-inch running clearance with the abradable shroud surface. Interference of the rotor tips and the abradable shroud is not planned for the first build. The self-grinding feature of the rotor tip and shroud will be included in subsequent builds after the vibrational characteristics of the compressor have proven to be satisfactory. This should insure tracking in to a minimum running clearance.
- d. An external air supply will be used to pressurize the cavity between the front oil seal and the rotor labyrinth seal. This pressurization serves to balance the axial forces on the rotor to minimize bearing loads and to provide a pressure differential across the oil seal to eliminate oil leakage.

Test Equipment

- a. **Air Inlet System** - The air inlet system consists of an air filter, a calibrated air bottle, a convergent adapter, and approximately 7 feet of straight ducting.
- b. **Exit Air System** - The compressor exit scroll is connected to a close-coupled valve with a divergent adapter. The exhaust air from the close-coupled valve is ducted and dumped into the vertical stack of the steam exhaust system.
- c. **Turbine Thrust Balance System** - Pressurized air is supplied to the downstream side of the turbine balance piston to reduce the thrust load on the bearing. An automatic system maintains the air pressure equal to the steam pressure at the exit of the turbine stator.
- d. **Oil System** - Oil is supplied from a pump to three inlet points on the compressor and turbine at a pressure of 30 psi. The inlet points feed (1) the compressor front bearing, (2) the compressor

rear main bearing and turbine front main bearing and (3) the turbine rear main bearing. The oil from the compressor front main bearing collects in the compressor sump, while the remaining oil collects in the turbine sump. The return oil from both sumps is scavenged with a common pump.

INSTRUMENTATION

Compressor Speed

A magnetic pickup is set to sense six lobes on the front compressor shaft nut. The signal is fed into an rpm meter for direct rpm readout. The signal is also fed into an oscilloscope, and the rpm is periodically checked against a known frequency calibration signal.

Compressor Airflow

The pressure differential across a standard calibrated air bottle is measured on an inclinometer to determine the compressor airflow. The air bottle is located at the entrance of the compressor inlet air system.

Compressor Pressures

The compressor pressures to be measured include fixed total pressure probes, a traversing yaw probe, and static pressure taps. All of the pressures except those from the traversing probe are recorded on manometer banks, which are photographed. The data from the traversing probe are recorded on X-Y plotters. The locations and ranges of all pressures are detailed in Table III.

- a. Inlet Total Pressure - The inlet total pressure is measured by a five-element total pressure rake located in the inlet ducting upstream of the compressor. The probe elements are located at the centers of equal areas along the zero-degree radial position from the duct centerline to the ID.
- b. Rotor Exit Total Pressure - The rotor exit total pressure is measured with an array of fixed total probes and a traversing yaw probe. These measurements are made at an axial station which represents the leading-edge plane of the exit stators.

The fixed total probes are positioned at yaw angles of 0°, 25°, and 50° to cover the exit flow angle variation expected between wide-open throttle and the surge line and at three radii which represent the hub, mean, and tip streamtubes. These fixed total probes are distributed uniformly at various circumferential locations.

The traversing yaw probe senses and automatically aligns the probe along the flow yaw angle and is capable of a continuous traverse from the tip to the hub of the annular passage. During a traverse,

TABLE III. ROTOR TEST INSTRUMENTATION

Instrumentation	Location			Operating Range	Quick Look Board
	Axial	Circumf.	Radial		
1 Pitot, $\alpha = 50^\circ$	Exit Duct Station 1 (Leading Edge) (Exit Stator)	225°, 342°	0.371" from Flow Path OD	0 to 60 in. Hg gage	
1 Pitot, $\alpha = 0^\circ$	Exit Duct Station 1 (Leading Edge) (Exit Stator)	108°	0.228" from Flow Path OD	0 to 60 in. Hg gage	1 pressure
1 Pitot, $\alpha = 25^\circ$	Exit Duct Station 1 (Leading Edge) (Exit Stator)	252°	0.228" from Flow Path OD	0 to 60 in. Hg gage	1 pressure
1 Pitot, $\alpha = 25^\circ$	Exit Duct Station 1 (Leading Edge) (Exit Stator)	90°	0.082" from Flow Path OD	0 to 60 in. Hg gage	
1 Pitot, $\alpha = 25^\circ$	Exit Duct Station 1 (Leading Edge) (Exit Stator)	270°	0.371" from Flow Path OD	0 to 60 in. Hg gage	
3 Total ic Thermo $\alpha = 50^\circ$	Exit Duct Station 1 (Leading Edge) (Exit Stator)	54°, 180°, 306°	0.228" from Flow Path OD	50° to 500°F	
1 Total ic Thermo $\alpha = 50^\circ$	Exit Duct Station 1 (Leading Edge) (Exit Stator)	72°	0.082" from Flow Path OD	50° to 500°F	
1 Total ic Thermo $\alpha = 50^\circ$	Exit Duct Station 1 (Leading Edge) (Exit Stator)	288°	0.371" from Flow Path OD	50° to 500°F	
1 Total ic Thermo $\alpha = 0^\circ$	Exit Duct Station 1 (Leading Edge) (Exit Stator)	162°	0.228" from Flow Path OD	50° to 500°F	
1 Total ic Thermo $\alpha = 25^\circ$	Exit Duct Station 1 (Leading Edge) (Exit Stator)	198°	0.228" from Flow Path OD	50° to 500°F	
Traversing Probe (Total Pressure) (Total Temperature) (Yaw Angle)	Exit Duct Station 1 (Leading Edge) (Exit Stator)	279°	variable	0 to 60 in Hg gage 50° to 500°F 0 to 70°F	

TABLE III. - CONTINUED

Instrumentation	Axial	Location Circumf.	Radial	Operating Range	Quick Look Board
5 Inlet Totals (Pressures, Temperatures)	Inlet Duct	0°, 180°	1.21", 2.09", 2.68", 3.18", 3.62"	-60 to 0 in. Hg gage	
Static Pressure in Labyrinth Cav.				-60 to 0 in. Hg gage	
3 Statics	Leading Edge IGW	6°, 122°, 238°	Flow Path OD	-60 to 0 in. Hg gage	
3 Statics	Leading Edge IGW	6°, 122°, 238°	Flow Path ID	-60 to 0 in. Hg gage	
3 Statics	Trailing Edge IGW	6°, 122°, 238°	Flow Path OD	-60 to 0 in. Hg gage	1 pressure
3 Statics	Trailing Edge IGW	6°, 122°, 238°	Flow Path ID	-60 to 0 in. Hg gage	
3 Statics	Leading Edge-Rotor	40°, 166°, 274°	Flow Path OD	-60 to 0 in. Hg gage	
3 Statics	Mid Chord Rotor	27°, 153°, 261°	Flow Path OD	0 to 60 in. Hg gage	
3 Statics	Trailing Edge-Rotor	14°, 140°, 248°	Flow Path OD	0 to 60 in. Hg gage	1 pressure
3 Statics	Leading Edge Exit Stator	27°, 153°, 261°	Flow Path OD	0 to 60 in. Hg gage	
3 Statics	Exit Duct Station 1 (Leading Edge) (Exit Stator)	27°, 153°, 261°	Flow Path ID	0 to 60 in. Hg gage	
3 Statics	Exit Duct Station 2 (0.49" Aft) (of Station 1)	27°, 153°, 261°	Flow Path OD	0 to 60 in. Hg gage	
3 Statics	Exit Duct Station 3 (2.14" Aft) (of Station 1)	27°, 153°, 261°	Flow Path OD	0 to 60 in. Hg gage	
3 Pitot, $\alpha = 50^\circ$	Exit Duct Station 1 (Leading Edge) (Exit Stator)	0°, 126°, 234°	0.228" from Flow Path OD	0 to 60 in. Hg gage	1 pressure
1 Pitot, $\alpha = 50^\circ$	Exit Duct Station 1 (Leading Edge) (Exit Stator)	18°, 243°	0.082" from Flow Path OD	0 to 60 in. Hg gage	

the total pressure, yaw angle, and total temperature are recorded on X-Y plotters as a function of radius.

- c. Static Pressures - Static pressure taps are located on the OD and ID of the flow path in the inlet section and at the leading and trailing-edges of each of the blade rows. Static taps are also located at the leading edge, mid-chord, and trailing-edge of the rotor shroud. These pressures are measured at each of three equally spaced circumferential locations.

Compressor Temperatures

The compressor temperature instrumentation includes fixed total temperature probes and a traversing total temperature probe. The fixed probe total temperatures are read out from a multiple selector Brown recorder, and the traversing probe temperature is recorded on an X-Y plotter. The detailed locations of the thermocouples are presented in Table III.

- a. Inlet Total Temperature - The inlet temperature is measured by a five-element total temperature IC thermocouple rake which is located and spaced the same as the inlet total pressure rake.
- b. Rotor Exit Total Temperature - The rotor exit total temperature is measured with an array of fixed total temperature thermocouples and a total temperature thermocouple on the traversing yaw probe. These measurements are made at an axial station which represents the leading edge of the exit stators.

The yaw angles and streamtube locations of the thermocouples are the same as those described for the rotor exit total pressures. A switch-box arrangement permits recording of the exit temperature rise with respect to the inlet temperature.

The traversing thermocouple is a part of the same traversing yaw probe described for the total pressure.

Vibration

Vibration pickups are located so as to record the vertical and horizontal vibrations at the front compressor support, turbine front support, and turbine rear support. The vibrations are recorded in units of acceleration (g's) since the displacement values are less than 0.1 mil.

Oil Temperature and Pressure

The oil temperature is recorded at the inlet and outlet of the compressor rig, and the temperature rise is monitored as an indication of satisfactory bearing operation. The oil inlet pressure is recorded to insure adequate oil flow.

Steam Pressure

The steam pressure is recorded upstream of the control valve and at the inlet steam jacket for the turbine.

Blade Stresses

Provisions have been made to incorporate strain gauges on the compressor rotor blades. A slip ring assembly is available, and an alternate design for incorporating this assembly in the compressor rig has been made. The final decision as to whether this instrumentation is necessary will depend on the results of the rotor static natural frequency calibration and the subsequent final review of the flutter analysis.

PRETEST INSPECTIONS

Dimensional Inspections

Dimensional inspection of the hardware is performed prior to and during assembly to establish and check critical dimensions, clearances, and air-foil geometry.

Blade Natural Frequencies

The static natural vibrational frequency of the blades is measured by exciting the blades and calibrating their natural frequency against a known frequency on an oscilloscope. A microphone is used to sense the blade frequency. The result is compared to the predicted value, and the blade flutter analysis is reviewed.

Rotor Balancing

The compressor and turbine rotors and shaft assemblies are balanced to within .001-.003 ounce-inches at 2500 rpm prior to assembly.

Magnaflux

The compressor rotor is given a Magnaflux inspection prior to assembly.

Test Procedures

Table IV presents the scheduled test points. The normal test procedure is as follows:

1. All subsystems (such as the oil system and the balance air systems) are started and checked for proper operation prior to opening the steam control valve and starting the compressor.
2. The steam control valve is activated and the compressor speed is brought slowly up to the first test speed with the close-coupled valve for the compressor air system in the wide-open position

TABLE IV. SCHEDULED TEST POINTS FOR ROTOR TEST

% Speed	$(W\sqrt{\theta})/8$	P/P
40	Wide-open throttle	
		2.0
		1.5
		1.2
		Surge point
60	Wide-open throttle	
		2.7
		2.5
		Surge point
		Wide-open throttle
80	Wide-open throttle	
		3.5
		3.4
		Surge point
		Wide-open throttle
90	Wide-open throttle	1.80
		2.0
		2.2
		Surge point
		2.32
100	Wide-open throttle	2.08
		2.3
		2.6
		2.8
		Surge point
		2.90

The above points are estimated based on predicted performance and are intended as a guide. Deviation from predicted performance may require adjustment of the data points to be run.

(maximum airflow). The vibration meter is monitored continuously throughout the test.

3. The inlet temperature is noted after it has stabilized, and the speed is then adjusted to the desired corrected speed ($N/\sqrt{\theta}$).
4. After all instruments are stabilized, a complete set of data is recorded, including a photograph of the manometer banks and full traverse from tip to hub with the traversing yaw probe.
5. A constant speed line is developed by closing the close-coupled valve while maintaining speed, until the next scheduled reduced weight flow is attained. Step 4 is then repeated. Four to five test points are planned for each speed line. The final test point on a given speed line is obtained by closing the close-coupled valve until compressor surge is audible. The weight flow at which surge is first detected is noted, and the close-coupled valve is opened until a weight flow slightly above surge is attained. This point is then taken as the last data point on the speed line.
6. The close-coupled valve is set wide open, and the compressor is then accelerated to the next highest speed. The process is repeated for each of the scheduled speed lines up to 100 percent speed. In the range of 90 to 100 percent speed, where the speed lines are expected to exhibit almost constant weight flow, the constant speed line is developed by closing the close-coupled valve to meet prescribed increments of increased pressure ratio rather than increments of reduced weight flow.

DATA PRESENTATION

Compressor Map

The standard compressor map in which the adiabatic efficiency and total-to-total pressure ratio are plotted against corrected weight flow for each of the corrected speed lines will be generated and compared to the predicted map. The predicted stage map is presented in Figure 51. This map will be based on the average compressor inlet conditions and the average rotor exit conditions (measured at the inlet station for the exit stator design). The corrected conditions and efficiency are computed as follows:

$$\text{Corrected weight flow} = (W_a \sqrt{\theta}) / \delta$$

Where W_a = actual measured airflow in pounds per second

$$\sqrt{\theta} = \sqrt{\frac{T_{\text{inlet}}}{T_{\text{reference}}}}$$

T_{inlet} = average total temperature at the compressor inlet ($^{\circ}\text{R}$)

$T_{\text{reference}} = 519^{\circ}\text{R}$

$$\delta = \frac{P_{t \text{ inlet}}}{P_{t \text{ reference}}}$$

$P_{t \text{ inlet}}$ = average total pressure at compressor inlet (inch mercury absolute)

$P_{t \text{ reference}} = 29.92$ inch mercury absolute

$$\text{Corrected speed} = N / \sqrt{\theta}$$

Where N = actual measured speed in revolutions per minute

$$\sqrt{\theta} = \text{same as above}$$

$$\text{Percent speed} = \frac{(N / \sqrt{\theta} \text{ measured})}{(N / \sqrt{\theta} \text{ design})} \times 100$$

Where $(N / \sqrt{\theta}) \text{ measured} = \text{same as above}$

$(N / \sqrt{\theta}) \text{ design} = 50,700$ rpm

$$\text{Pressure ratio} = P_{T_4} / P_{T_0}$$

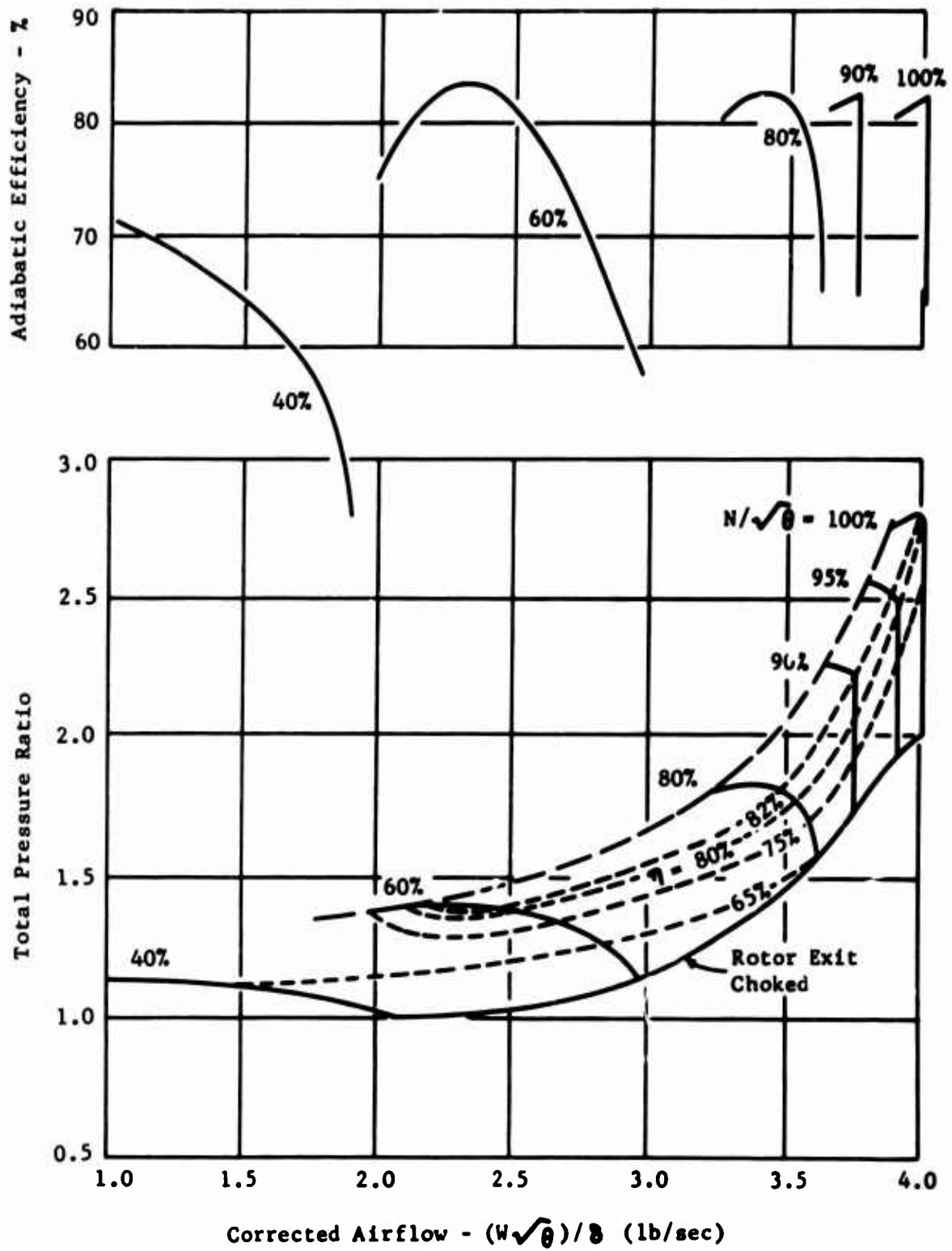


Figure 51. 2.8:1 Supersonic Compressor Predicted Stage Map.

Where P_{T_4} = total pressure integrated from hub to tip of the absolute velocity vector leaving the rotor

P_{T_0} = integrated total pressure at the compressor inlet

$$\text{Adiabatic efficiency} = \frac{\Delta H'}{\Delta H} \times 100$$

Where $\Delta H'$ = isentropic enthalpy rise for the measured pressure ratio (Btu/lb)

ΔH = actual enthalpy rise based on the average measured total temperatures at the compressor inlet (T_{inlet}) and the total temperature of the absolute rotor exit velocity vector integrated from hub to tip (Btu/lb)

Rotor Exit Conditions

The following rotor exit parameters will be presented as a function of radius from hub to tip:

- Total pressure
- Total temperature
- Absolute Mach number
- Absolute flow angle with respect to axial

Vector Diagrams

The velocity vector diagrams representing the rotor inlet and outlet conditions will be presented for three streamtube positions and will be compared to the design vector diagrams.

DATA ANALYSIS

A data analysis computer program will be used to construct the streamline paths, mass flow weighted pressure ratio, efficiency and vector diagrams which satisfy the test results. The inputs for this program are the measured inlet and outlet radial profiles of total pressure and total temperature, the measured weight flow, and the compressor geometry. The program computes a solution which satisfies these inputs and radial equilibrium for both tangential velocities and meridional streamline curvature. In addition to the parameters discussed above, numerous other parameters are calculated by the program such as streamtube diffusion factors, loss coefficients, and incidence and deviation angles.

The data analysis will be run for key test points such as peak pressure ratios and peak efficiencies in the 90 to 100 percent speed range and for any other points which may give some insight to deficiencies in the design. In each case, adjustments will be made to the program inputs until the solution best satisfies all of the measured data (e.g., static pressures and total temperature and pressure profiles). This solution will then be

used to analyze deficient areas and to determine which modifications will improve the performance. The compressor design techniques and empirical data will also be reevaluated based on these results.

APPENDIX II

PHASE III TEST PLAN

OBJECTIVE

The objective of the stage development program is to evaluate the complete stage performance of the 2.8:1 single-stage supersonic compressor design through experimental testing, data analysis, and design modifications. The compressor stage consists of the inlet, inlet guide vanes, rotor, exit stators, and interconnecting duct which matches the inlet of the proposed second-stage centrifugal compressor. The stage performance goals are:

Pressure Ratio	2.8:1
Adiabatic Efficiency	82.2%
Weight Flow	4.0 lb/sec
Design Speed	50,700 rpm

The compressor rotor developed under Phase II of this program will be utilized in the stage testing.

APPROACH

The inlet guide vane performance for this compressor was established independent of the rotor by a flow test program using an external air supply. The combined inlet guide vane and rotor performance is being developed under Phase II of the program. This development involves experimental performance evaluation and rotor modification necessary to meet the design performance goals. Sufficient experimental data will be established on the finalized rotor configuration to provide the following combined inlet guide vane and rotor performance:

1. Compressor map between 40 and 100 percent speed at the optimum inlet guide vane setting.
2. Compressor maps between 70 and 100 percent at two other guide vane settings.
3. Rotor exit temperature, pressure, and flow angle radial traverse profiles at key performance points (peak pressure ratio, peak efficiency, etc.).

The design of the exit stators and interconnecting duct will be finalized based on the results of the Phase II test.

Testing of the complete compressor stage with the inlet guide vanes at design setting will be the initial step in the Phase III test program. Two builds are estimated for this series of tests. A compressor map will be developed between 40 and 100 percent speed for this configuration. Compressor maps for other inlet guide vane settings will be developed between 70 and 100 percent speed. Complete pressure and temperature data will be recorded during the testing.

The data points in the 90 to 100 percent speed range, which represent peak pressure ratio and peak efficiency, will be analyzed to establish vector diagrams that satisfy the experimental data. The experimental vector diagrams will be compared to the design conditions and previously measured inlet guide vane and rotor performance to pinpoint deficient areas.

An advanced inlet guide vane will be designed, fabricated and substituted for the NACA 65 series guide vanes. The stage test will be repeated as described above to evaluate the performance with the new guide vanes.

Based on the results of the data analysis, design modifications will be established. Where possible, these modifications will be incorporated in the compressor hardware by machining, blade bending, and similar means. Redesign and new procurement are planned in the event that the required modifications are beyond the limits of reworking the existing hardware. A second series of tests will be conducted and the data analyzed to evaluate the redesigned component or components in the same manner as the first test series. Two builds are estimated for this series.

An experimental map will be developed between 40 and 100 percent speed for the optimum stage configuration. Compressor maps for other inlet guide vane settings will be developed between 70 and 100 percent speed. Radial temperature and pressure profiles will be established at the exit plane of the interconnecting duct for key performance points.

TEST CONFIGURATION

Compressor

- a. The compressor build will include the inlet guide vanes, the 2.8:1 pressure ratio rotor, the exit stators, and the interconnecting duct. The compressor will be mounted to and powered by the steam-driven Rover turbine on test stand WX25R (see Figures 49 and 52).
- b. The inlet guide vanes will be set in the zero position (design setting) initially, but repositioning may be required as indicated by the test results.
- c. The rotor blade tip clearance will be set at the optimum value based on the Phase II test results. A rotor shroud with an abradable surface is tentatively planned for this testing, pending the final results of its application in the Phase II testing.
- d. An external air supply will be used to pressurize the cavity between the front oil seal and the rotor labyrinth seal. This pressurization serves to balance the axial forces on the rotor to minimize bearing loads and to provide a pressure differential across the oil seal to eliminate oil leakage.

Test Equipment

- a. Air Inlet System - The air inlet system consists of an air filter, a calibrated air bottle, a convergent adapter, and approximately 7 feet of straight ducting.
- b. Exit Air System - The compressor exit scroll is connected to a close-coupled valve with a divergent adapter. The exhaust air from the close-coupled valve is ducted and dumped into the vertical stack of the steam exhaust system.
- c. Turbine Thrust Balance System - Pressurized air is supplied to the downstream side of the turbine balance piston to reduce the thrust load on the bearing. An automatic system maintains the air pressure equal to the stream pressure at the exit of the turbine stator.
- d. Oil System - Oil is supplied from a pump to three inlet points on the compressor and turbine at a pressure of 300 psi. The inlet points feed (1) the compressor front bearing, (2) the compressor rear main bearing and turbine front main bearing, (3) and the turbine rear main bearing. The oil from the compressor front main bearing collects in the compressor sump, while the remaining oil collects in the turbine sump. The return oil from both sumps is scavenged with a common pump.

INSTRUMENTATION

Compressor Speed

A magnetic pickup is set to sense 12 lobes on the front compressor shaft nut. The signal is fed into an eput meter for direct rpm readout. The signal is also fed into an oscilloscope, and the rpm is periodically checked against a known frequency calibration signal.

Compressor Airflow

The pressure differential across a standard calibrated air bottle is measured on an inclinometer to determine the compressor airflow. The air bottle is located at the entrance of the compressor inlet air system.

Compressor Pressures

The compressor pressures to be measured include fixed total pressure probes, a traversing yaw probe, and static pressure taps. All of the pressures, except those from the traversing probe, are recorded on manometer banks, which are photographed. The data from the traversing probe are recorded on X-Y plotters. The locations and ranges of all pressures are detailed in Table V.

- a. Inlet Total Pressure - The inlet total pressure is measured by a five-element total pressure rake located in the inlet ducting

upstream of the compressor. The probe elements are located at the centers of equal areas along the zero-degree radial position from the duct centerline to the ID.

- b. **Stage Exit Total Pressure** - The stage exit total pressure is measured with an array of fixed total probes and traversing yaw probes. These measurements are made at an axial station which represents the exit plane of the exit stators and interconnecting duct.

The fixed total probes are positioned at yaw angles of 0° , $+20^\circ$, and -20° to cover the possible exit flow angle variation and at three radii which represent the hub, mean, and tip stream tubes. These fixed total probes are distributed uniformly at various circumferential locations.

The traversing yaw probe senses and automatically aligns the probe along the flow yaw angle and is capable of a continuous traverse from the tip to the hub of the annular passage. During a traverse, the total pressure, yaw angle, and total temperature are recorded on X-Y plotters as a function of radius. Both radial and circumferential traverses will be made.

- c. **Static Pressures** - Static pressure taps are located on the OD and ID of the flow path in the inlet section, at the leading and trailing edges of each of the blade rows, and at the exit plane of the interconnecting duct. Static taps are also located at the leading-edge, mid-chord, and trailing-edge of the rotor shroud. These pressures are measured at each of three equally spaced circumferential locations.

Compressor Temperatures

The compressor temperature instrumentation includes fixed total temperature probes and a traversing total temperature probe. The fixed probe total temperatures are read out from a multiple selector Brown recorder while the traversing probe temperature is recorded on an X-Y plotter. The detailed locations of the thermocouples are presented in Table V.

- a. **Inlet Total Temperature** - The inlet temperature is measured by a five-element total temperature IC thermocouple rake which is located and spaced the same as the inlet total pressure rake.
- b. **Stage Exit Total Temperature** - The stage exit total temperature is measured with an array of fixed total temperature thermocouples and a total temperature thermocouple on the traversing yaw probe. These measurements are made at an axial station which represents the exit plane of the interconnecting duct.

The yaw angles and streamtube locations of the thermocouples are the same as those described for the rotor exit total pressures. A switchbox arrangement permits recording of the exit temperature

TABLE V. STAGE TEST INSTRUMENTATION

Instrumentation	Axial	Location Circumf.	Radial	Operating Range	Quick Look Board
5 Inlet Totals (Pressures, Temperatures)	Inlet Duct	0°, 180°	1.21", 2.09" 2.68", 3.18", 3.62"	-60 to 0 in. Hg gage	
Static Pressure in Labyrinth Cav				-60 to 0 in. Hg gage	
3 Statics	Leading Edge IGV	6°, 122°, 238°	Flow Path OD	-60 to 0 in. Hg gage	
3 Statics	Leading Edge IGV	6°, 122°, 238°	Flow Path ID	-60 to 0 in. Hg gage	
3 Statics	Trailing Edge IGV	6°, 122°, 238°	Flow Path OD	-60 to 0 in. Hg gage	1 pressure
3 Statics	Trailing Edge IGV	6°, 122°, 238°	Flow Path I ID	-60 to 0 in. Hg gage	
3 Statics	Leading Edge-Rotor	40°, 166°, 274°	Flow Path OD	-60 to 0 in. Hg gage	
3 Statics	Mid Chord Rotor	27°, 153°, 261°	Flow Path OD	0 to 60 in. Hg gage	
3 Statics	Trailing Edge- Rotor	14°, 140°, 248°	Flow Path OD	0 to 60 in. Hg gage	1 pressure
3 Statics	Leading Edge Exit Stator	27°, 153°, 261°	Flow Path OD	0 to 60 in. Hg gage	
3 Statics	Leading Edge Exit Stator	27°, 153°, 261°	Flow Path ID	0 to 60 in. Hg gage	
3 Statics	Trailing Edge Exit Stator	27°, 153°, 261°	Flow Path OD	0 to 60 in. Hg gage	
3 Statics	Trailing Edge Exit Stator	27°, 153°, 261°	Flow Path ID	0 to 60 in. Hg gage	
3 Statics	Stage Exit Plane	27°, 153°, 261°	Flow Path OD	0 to 60 in. Hg gage	
3 Statics	Stage Exit Plane	27°, 153°, 261°	Flow Path ID	0 to 60 in. Hg gage	
3 Pitot, $\alpha = 0^\circ$	Stage Exit Plane	0°, 126°, 234°	0.384" from Flow Path OD	0 to 60 in. Hg. gage	1 pressure
2 Pitot, $\alpha = 0^\circ$	Stage Exit Plane	18, 243°	0.120" from Flow Path OD	0 to 60 in. Hg. gage	1 pressure
2 Pitot, $\alpha = 0^\circ$	Stage Exit Plane	225°, 343°	0.693" from Flow Path OD	0 to 60 in. Hg. gage	1 pressure
1 Pitot, $\alpha = +20^\circ$	Stage Exit Plane	108°	0.384" from Flow Path OD	0 to 60 in. Hg. gage	
1 Pitot, $\alpha = -20^\circ$	Stage Exit Plane	90°	0.384" from Flow Path OD	0 to 60 in. Hg. gage	1 Pressure
1 Pitot, $\alpha = +20^\circ$	Stage Exit Plane	252°	0.120" from Flow Path OD	0 to 60 in. Hg. gage	1 pressure
1 Pitot, $\alpha = -20^\circ$	Stage Exit Plane	270°	0.120" from Flow Path OD	0 to 60 in. Hg. gage	
1 Pitot, $\alpha = +20^\circ$	Stage Exit Plane	351°	0.693" from Flow Path OD	0 to 60 in. Hg. gage	
1 Pitot, $\alpha = -20^\circ$	Stage Exit Plane	333°	0.693" from Flow Path OD	0 to 60 in. Hg. gage	
3 Total ic Thermo $\alpha = 0^\circ$	Stage Exit Plane	22°, 180°, 306°	0.384" from Flow Path OD	50° to 500°F	
1 Total ic Thermo $\alpha = 0^\circ$	Stage Exit Plane	122°	0.693" from Flow Path OD	50° to 500°F	
1 Total ic Thermo $\alpha = 0^\circ$	Stage Exit Plane	288°	0.120" from Flow Path OD	50° to 500°F	
Traversing Probe (Total Pressure) (Total Temperature) (Yaw Angle)	Stage Exit Plane	279°	Variable	0 to 60 in. Hg. gage 50° to 500°F 30° to -30°	
Traversing Probe (Total Pressure) (Total Temperature) (Yaw Angle)	Stage Exit Plane	152°	Variable	0 to 60 in. Hg. gage 50° to 500°F +30° to -30°	
Traversing Probe Variable (Total Pressure) (Total Temperature) (Pitch Angle)	Stage Exit Plane	Variable 200°-242°	0.384" from Flow Path OD	0 to 60 in. Hg. gage 50° to 500°F +30° to -30°	

both as an absolute value and as a temperature rise with respect to the inlet temperature.

The traversing thermocouple is a part of the same traversing yaw probe described for the total pressure.

Vibration

Vibration pickups are located so as to record the vertical and horizontal vibrations at the front compressor support, turbine front support, and turbine rear support. The vibrations are recorded in units of acceleration (g's) since the displacement values are less than 0.1 mil.

Oil Temperatures and Pressures and Flow Rate

The oil temperature is recorded at the inlet and outlet of the compressor rig, and the temperature rise is monitored as an indication of satisfactory bearing operation. The oil flow rates to each of the three rig supply lines are monitored continuously. The pressure differential of calibrated orifices is measured to indicate the flow rates.

Steam Pressure

The steam pressure is recorded upstream of the control valve and at the inlet steam jacket for the turbine.

Blade Stresses

Provisions have been made to incorporate strain gauges on the compressor rotor blades. A slip ring assembly is available, and an alternate design for incorporating this assembly in the compressor rig has been made. Strain gauges were not included in initial Phase II testing and are not planned for the Phase III testing unless flutter problems are encountered in Phase II.

PRETEST INSPECTIONS

Dimensional Inspection

Dimensional inspection of the hardware is performed prior to and during assembly to establish and check critical dimensions, clearances, and airfoil geometry.

Blade Natural Frequencies

The static natural vibrational frequency of the blades is measured by exciting the blades and calibrating their natural frequency against a known frequency on an oscilloscope. A microphone is used to sense the blade frequency. The result is compared to the predicted value and the blade flutter analysis is reviewed.

Rotor Balancing

The compressor and turbine rotors and shaft assemblies are balanced to within .001-.003 ounce-inches at 2500 rpm prior to assembly.

Magnaflux

The compressor rotor is given a Magnaflux inspection prior to assembly.

TEST PROCEDURES

Table VI presents the scheduled test points. The normal test procedure is as follows:

1. All subsystems (such as the oil system and the balance air systems) are started and checked for proper operation prior to opening the steam control valve and starting the compressor.
2. The steam control valve is activated and the compressor speed is brought slowly up to the first test speed with the close-coupled valve for the compressor air system in the wide-open position (maximum airflow). The vibration meter is monitored continuously through the test.
3. The inlet temperature is noted after it has stabilized, and the speed is then adjusted to the desired corrected speed ($N/\sqrt{\theta}$).
4. After all instruments are stabilized, a complete set of data is recorded, including a photograph of the manometer banks and full traverse from tip to hub with the traversing yaw probe.
5. A constant speed line is developed by closing the close-coupled valve while maintaining speed, until the next scheduled reduced weight flow is attained. Step 4 is then repeated. Four to five test points are planned for each speed line. The final test point on a given speed line is obtained by closing the close-coupled valve until compressor surge is audible. The weight flow at which surge is first detected is noted, and the close-coupled valve is opened until a weight flow slightly above surge is attained. This point is then taken as the last data point on the speed line.
6. The close-coupled valve is set wide open, and the compressor is then accelerated to the next highest speed. The process is repeated for each of the scheduled speed lines up to 100 percent speed. In the range of 90 to 100 percent speed, where the speed lines are expected to exhibit almost constant weight flow, the constant speed line is developed by closing the close-coupled valve to meet prescribed increments of increased pressure ratio rather than increments of reduced weight flow.

TABLE VI. SCHEDULED STAGE TEST POINTS

% Speed	$(W\sqrt{\theta})/8$	P/P
40	Wide-open Throttle	
	2.0	
	1.5	
	1.2	
	Surge Point	
60	Wide-open Throttle	
	2.7	
	2.5	
	Surge Point	
80	Wide-open Throttle	
	3.5	
	3.4	
90	Wide-open Throttle	1.80
		2.0
		2.2
	Surge Point	2.32
100	Wide-open Throttle	2.08
		2.3
		2.6
		2.8
	Surge Point	2.90

The above points are estimated based on predicted performance and are intended as a guide. Deviation from predicted performance may require adjusting the data points to be run.

DATA PRESENTATION

Compressor Map

The standard compressor map in which the adiabatic efficiency and total-to-total pressure ratio are plotted against corrected weight flow for each of the corrected speed lines will be generated and compared to the predicted map. The predicted stage map is presented on Figure 13. This map will be based on the average compressor inlet conditions and the average stage exit conditions (measured at the exit plane of the interconnecting duct). The corrected conditions and efficiency are computed as follows:

$$\text{Corrected weight flow} = (W_a \sqrt{\theta}) / \delta$$

Where W_a = actual measured airflow in pounds per second

$$\sqrt{\theta} = \sqrt{\frac{T_{\text{inlet}}}{T_{\text{reference}}}}$$

T_{inlet} = average total temperature at the compressor inlet ($^{\circ}\text{R}$)

$$T_{\text{reference}} = 519^{\circ}\text{R}$$

$$\delta = \frac{P_{t \text{ inlet}}}{P_{t \text{ reference}}}$$

$P_{t \text{ inlet}}$ = average inlet total pressure inch mercury absolute

$$P_{t \text{ reference}} = 29.92 \text{ inch mercury absolute}$$

$$\text{Corrected speed} = N / \sqrt{\theta}$$

Where N = actual measured speed in revolutions per minute

$$\sqrt{\theta} = \text{same as above}$$

$$\text{Percent speed} = \frac{(N / \sqrt{\theta} \text{ measured})}{(N / \sqrt{\theta} \text{ design})} \times 100$$

Where $(N / \sqrt{\theta}) \text{ measured}$ = same as above

$$(N / \sqrt{\theta}) \text{ design} = 50,700 \text{ rpm}$$

$$\text{Pressure ratio} = \frac{P_{T_5}}{P_{T_0}}$$

Where P_{T_5} = total pressure integrated from hub to tip of the velocity vector leaving the stage exit plane

P_{T_0} = integrated total pressure at the compressor inlet

$$\text{Adiabatic efficiency} = \frac{\Delta H'}{\Delta H} \times 100$$

Where $\Delta H'$ = isentropic enthalpy rise for the measured pressure ratio (BTU/lb)

ΔH = actual enthalpy rise based on the average measured total temperatures at the compressor inlet (T_{inlet}) and the total temperature of the stage exit velocity vector integrated from hub to tip (BTU/lb)

Stage Exit Conditions

The following stage exit parameters will be presented as a function of radius from hub to tip:

- Total pressure
- Total temperature
- Mach number
- Flow angle with respect to axial

The circumferential pressure profile spanning two exit stator blades at the interconnecting duct exit plane will also be presented.

Vector Diagrams

The velocity vector diagrams representing the inlet and outlet conditions for the inlet guide vanes, rotor, and exit stator will be presented for three streamtube positions and will be compared to the design vector diagrams.

DATA ANALYSIS

A data analysis computer program will be used to construct the streamline paths mass flow weighted pressure ratio, efficiency and vector diagrams which satisfy the test results. The inputs for this program are the measured inlet and outlet radial profiles of total pressure and total temperature, the measured weight flow, and the compressor geometry. The program computes a solution which satisfied these inputs and radial equilibrium for both tangential velocities and meridional streamline curvature. In addition to the parameters discussed above, numerous other parameters are calculated by the program, such as streamtube diffusion factors, loss coefficients, and incidence and deviation angles.

The data analysis will be run for key test points such as peak pressure ratios and peak efficiencies in the 90 to 100 percent speed range and for any other points which may give some insight to deficiencies on the design. In each case, adjustments will be made to the program inputs until the

solution best satisfies all of the measured data (e.g., static pressures and total temperature and pressure profiles). This solution will then be used to analyze deficient areas and to determine which modifications will improve the performance. The compressor design techniques and empirical data will also be reevaluated based on these results.

DISTRIBUTION

US Army Materiel Command	4
US Army Aviation Systems Command	6
Chief of R&D, DA	2
US Army R&D Group (Europe)	2
US Army Aviation Materiel Laboratories	18
US Army Mobility Equipment R&D Center	1
US Army Limited War Laboratory	1
US Army Ballistic Research Laboratories	1
Army Aeronautical Research Laboratory, Ames Research Center	1
US Army Research Office-Durham	1
US Army Materiel Systems Analysis Agency	1
US Army Test and Evaluation Command	1
US Army Combat Developments Command, Fort Belvoir	2
US Army Combat Developments Command Experimentation Command	1
US Army Tank-Automotive Command	2
US Army Aviation Systems Test Activity, Edwards AFB	2
Air Force Aero Propulsion Laboratory, Wright-Patterson AFB	1
Air Force Flight Dynamics Laboratory, Wright-Patterson AFB	1
Systems Engineering Group, Wright-Patterson AFB	2
Naval Air Systems Command, DN	15
Office of Naval Research	1
Commandant of the Marine Corps	1
Marine Corps Liaison Officer, US Army Transportation School	1
Lewis Research Center, NASA	1
Ames Research Center, NASA	2
Langley Research Center, NASA	1
NASA Scientific and Technical Information Facility	2
NAFEC Library (FAA)	2
US Naval Air Station, Norfolk	1
Federal Aviation Administration, Washington, DC	2
US Government Printing Office	1
Defense Documentation Center	20

Unclassified
Security Classification

DOCUMENT CONTROL DATA - R & D		
<i>(Security classification of title, body of abstract and indexing annotations must be entered when the report must be classified)</i>		
1. ORIGINATING ACTIVITY (Corporate author) Curtiss-Wright Corporation Wood-Ridge, New Jersey 07075		2. REPORT SECURITY CLASSIFICATION Unclassified
3. REPORT TITLE Single Stage Axial Compressor Component Development for Small Gas Turbine Engines Volume II - Rotor Development		
4. DESCRIPTIVE NOTES (Type of report and inclusive dates) Final Report Volume II May 1966 to May 1967		
5. AUTHOR(S) (First name, middle initial, last name) Charles H. Muller, Leslie R. Cox		
6. REPORT DATE May 1969	7a. TOTAL NO. OF PAGES 113	7b. NO. OF FIGS 1
8a. CONTRACT OR GRANT NO. DA44-177-AMC-392(T)	8b. ORIGINATOR'S REPORT NUMBER USAWLABS Technical Report 68-908	
9. PROJECT NO. Task 1G162203D14413	10. DTIC REPORT NUMBER (Any other number that may be assigned this report) Curtiss-Wright 68-050-233.F	
11. DISTRIBUTION STATEMENT This document is subject to special export controls and each transmittal to foreign governments or foreign nationals may be made only with prior approval of US Army Aviation Materiel Laboratories, Fort Eustis, Virginia 23604.		
11. SUPPLEMENTARY NOTES Volume II of a 3-volume report	12. DISTRIBUTION STATEMENT U.S. Army Aviation Materiel Laboratories Fort Eustis, Virginia	
13. ABSTRACT This report describes the development of the rotor for the 2.8:1 single stage super-sonic axial compressor design. The rotor performance was evaluated through experimental testing with the inlet guide vanes but without the exit stator. The experimental results are analyzed and compared to the design data and criteria. Although a circumferential flow distortion at the rotor exit prevented a very accurate assessment of the performance potential, the data provided ample evidence that the rotor performance goals could be met with uniform exit conditions. The presence of the exit stator during the stage development tests in the subsequent phase was expected to reduce the flow distortion at the rotor exit to near uniform conditions.		

DD FORM 1 NOV 68 1473

REPLACES DD FORM 1473, 1 JAN 64, WHICH IS OBSOLETE FOR ARMY USE.

Unclassified
Security Classification

1375-00

Unclassified
Security Classification

14. KEY WORDS	LINK A		LINK B		LINK C	
	ROLE	WT	ROLE	WT	ROLE	WT
Compressor Research and Development Supersonic Compressors Small Gas Turbine Technology						

Unclassified
Security Classification